THE UNIVERSITY
of EDINBURGH

Effects of Glucocorticoids in Macrophages

Alasdair Jubb

Presented for the degree Doctor of Philosophy

University of Edinburgh

2015

PhD – The University of Edinburgh – 2015

Declaration

Unless explicitly stated otherwise the work presented here is my own. The work has not been submitted for any other degree or qualification.

…….. Date ……

Alasdair Jubb

Contents

Acknowledgements **9**
Abstract **11**
Figures **13**
Tables **15**
Abbreviations ..... **ii**
Published, presented and submitted work from this thesis ..... **i**
Chapter 1: Introduction **1**
1.1 Glucocorticoids 1
1.1.1 Discovery, use and problems 1
1.1.2 Towards a mechanism for glucocorticoid action 6
1.1.3 The role of GR dimerization and the 'dissociated' glucocorticoid 10
1.2 Chromatin and the control of gene expression 11
1.2.1 Chromatin 11
1.2.2 Long range control of gene regulation 12
1.2.3 GC effects on chromatin 25
1.3 Macrophages 26
1.3.1 Overview and relevance 26
1.3.2 Macrophage response to GC 27
1.4 Models, conservation and divergence 29
1.5 Summary 31
1.6 Thesis aims 31
Chapter 2: Methods **33**
2.1 Laboratory procedures 33
2.1.1 Ethics 33
2.1.2 Cell culture 33
2.1.3 RNA extraction and processing 34
2.1.4 Chromatin Immunoprecipitation 34
2.1.5 Single cell RT-qPCR 37
2.1.6 3D DNA FISH 37
2.2 Data Analysis 40

2.2.1 Expression data....41
2.2.2 Single cell PCR....41
2.2.3 Promoter Analysis....41
2.2.4 Comparison to GWAS results and inflammatory genes....42
2.2.5 Functional Annotation....42
2.2.6 ChIP-sequencing....42
2.2.7 Interspecies and evolutionary analysis....43
2.2.8 Analysis of 3D FISH data....44
Chapter 3: The transcriptional response of macrophages to glucocorticoids....45
3.1 Introduction....45
3.2 The response of mouse bone marrow derived macrophages to dexamethasone....46
3.3 The response of human monocyte derived macrophages to dexamethasone 51
3.4 The expression response is different and is not linked to promoter variation 54
3.5 Targets of glucocorticoids in human macrophages enrich for risk variants for inflammatory disease....61
3.6 Discussion....63
3.7 Summary....65
Chapter 4: Glucocorticoid receptor binding in macrophages....67
4.1 Introduction....67
4.2 GR binding in Mouse Bone Marrow Derived Macrophages....68
4.3 GR binding in Human Monocyte Derived Macrophages....76
4.4 Glucocorticoid receptor binding is associated with induced, not repressed genes....80
4.5 Inter-species differences of glucocorticoid receptor binding are associated with sequence changes that lead to motif loss....82
4.6 Discussion....91
4.7 Summary....95
Chapter 5: Dynamic regulation of chromatin structure in macrophages by glucocorticoids....97
5.1 Introduction....97
5.2 GR binding is associated with rapid and prolonged chromatin decompaction 98
5.3 Rapid chromatin decompaction of *Fkbp5* locus does not depend on transcription....105

5.4 GR binds rapidly at enhancers in the *Fkbp5* locus 108
5.5 Rapid decompaction may be a feature of GR bound loci 112
5.6 Discussion 115
5.7 Summary 117
Chapter 6: Conclusions and future work 119
6.1 Conclusions 119
6.1.1 The genome wide response to GC in macrophages 119
6.1.2 GC effects on chromatin organisation in macrophages 119
6.2 Future work 120
6.2.1 Enhancer turnover and variability 120
6.2.2 Kinetics of the macrophage response to GC and mechanisms of repression 123
6.2.3 GC driven chromatin dynamics 123
6.3 Summary 127
References 129
Appendix 1 149
Appendix 2 155

Acknowledgements

Thanks must first go to the directors of the Edinburgh Clinical Academic Track Brian Walker and John Iredale and the Wellcome Trust/NES for giving me the post in the first place. The flexibility of the programme and advice they have given me, more recently also Andrew Jackson, has enabled me to identify and take on a much more ambitious project than I could have done otherwise.

Thanks to my supervisors David Hume and Wendy Bickmore for taking me on without any track record to speak of and helping me put together a worthwhile project. Both were and continue to be incredibly supportive of my attempts to scale what remains at times a pretty precipitous learning curve.

There is no way I could have done any of this without the teaching and support provided by the Bickmore and Hume and wider Maclab group members. Thankfully there are plenty of them to spread the load, some are named below but thanks are due to all. From the Bickmoreans Rob Illingworth has to get first mention due to the sheer amount of time I spent bending his ear about ChIP. Rob Young added welcome and necessary computational and enhancer expertise and Shelagh Boyle enabled all things FISH related. Thanks are due to all : Hazel, Pradeep ‘should be fine’ MM, Liz, Gillian (GD), Sehrish, Iain, Nezha, Pierre, Celine, Leisha, Jess and Andrew as well as the wider E3 community for the unfailingly entertaining environment. Paul and Matt for helping me out in imaging at HGU. At Roslin thanks must go to the core of the lab Clare, Kristen, Lindsay, Anna, and Gemma; to those who helped me get going Kyle Upton and Ronan Kapetanovic; to Tom Freeman for introducing me to the world of expression analysis and his lab for providing good chat and gender balance; to Malcom Fisher and latterly Sara Clohisey and Gemma Davies for blood days Maggie for the fish, Bob in imaging. Specific mention to my ECAT forerunner at Roslin, Kenny Baillie, for help, advice, and being consistently distractible by the promise of a haggis roll.

And finally, of course, thanks to Francesca and Saoirse.

Abstract

Glucocorticoids (GC) are powerful metabolic hormones with anti-inflammatory actions. Despite major side effects they remain widely prescribed therapies. GC regulates gene expression through an intracellular receptor (GR), which is a ligand activated transcription factor. Macrophages are innate immune cells and major targets of GC. Traditionally repression of pro-inflammatory genes in the context of an inflammatory stimulus has been considered the primary mode of action of GC in macrophages.

The work described in this thesis has demonstrated that GC act primarily as inducers of gene expression in primary macrophages from both mouse and man, but the set of induced genes is very different between the two species. Chromatin immunoprecipitation and sequencing (ChIP-seq) in each species using anti-GR antibodies revealed candidate enhancers in the vicinity of inducible genes that were generally not shared between mouse and man. The differences in binding were correlated with DNA sequence changes at the enhancer sites between the two species, that caused gain or loss of predicted GR receptor-binding motifs.

The mechanism of action of GC was investigated by imaging several different target loci using fluorescence in situ hybridisation in macrophage nuclei. Chromatin at specific GC responsive loci was found to decondense within minutes of exposure of macrophages to the ligand. The apparent decondensation was effect was maintained for at least 24 hours and was not prevented by inhibitors of transcription.

The general principles of the GC response were shared between species. However the divergence found underlines the caution that must be used when translating specific findings from mouse to man. Additionally, the data support a role for GR driven changes to chromatin structure in gene regulation in macrophages.

Figures

Figure 1.1 Steroidogenesis 2

Figure 1.2 The hypothalamic-pituitary-adrenal axis 3

Figure 1.3 Schematic diagram of the glucocorticoid receptor 7

Figure 1.4 Structures of cortisol and dexamethasone 8

Figure 1.5 Models of long range control of gene expression 16

Figure 1.6 Principles of chromosome conformation capture 20

Figure 1.7 Schematic overview of DNA FISH 23

Figure 3.1 Validation and thresholding of microarray data. 48

Figure 3.2 Expression response over 24h of mBMDM to 100nM dexamethasone ... 50

Figure 3.3 Expression response of hMDM to 100nM dexamethasone. 53

Figure 3.4 The expression response to dexamethasone is divergent despite promoter sequence conservation. 55

Figure 3.5 Enriched functional annotation terms for the response of macrophages to dexamethasone. 57

Figure 3.6 Motifs over-represented in the promoters of dexamethasone regulated genes. 60

Figure 3.7. Enrichment for SNPs with GWAS link to inflammatory disease near dexamethasone regulated genes. 63

Figure 4.1 Optimisation of ChIP, example of antibody screening. 69

Figure 4.2 GR binding in dexamethasone treated mBMDM 71

Figure 4.3 Characterisation of GR bound sites in mBMDM 73

Figure 4.4 GR bound sites in mBMDM overlap sites previously reported to bear marks associated with enhancers 75

Figure 4.5 Genome wide binding of glucocorticoid receptor in hMDM 78

Figure 4.6 Characterisation of GR bound sites in hMDM 79

Figure 4.7 Induced genes are associated with GR binding 81

Figure 4.8 Evolutionary outcomes for GR peaks in human. 83

Figure 4.9 GR binding sites are minimally conserved between mouse and man and this is linked to the divergent transcriptional response to GC. 85

Figure 4.10 Conserved GR binding is linked to conservation of the GRE 89

Figure 4.11 Loss of GRE motif is associated with species specific binding. 90

Figure 5.1 Location of fosmids used for 3D DNA FISH at *Fkbp5* locus 99

Figure 5.2 Location of fosmid probes used for 3D DNA FISH at *Tmod1* locus 100

Figure 5.3 Chromatin decompaction in response to glucocorticoids 102

Figure 5.4 Prolonged chromatin decompaction at *Fkbp5* locus 104

Figure 5.5 Alpha-amanitin does not block rapid decompaction at *Fkbp5* 106

Figure 5.6 Glucocorticoid receptor binding at *Fkbp5* locus 109

Figure 5.7 Characteristics of the response to dexamethasone at *Fkbp5* 111

Figure 5.8 The site and response of a dexamethasone sensitive locus on chromosome 19 113

Figure 5.9 Chromatin decompaction at a GR bound locus on mouse chromosome 19 114

Figure 6.1 Variability in expression of CCL7 in response to GC 122

Figure 6.2 Rapid chromatin decompaction occurs in RAW264.7 cells 125

Tables

Table 1.1 Side effects of glucocorticoid therapy 5

Table 2.1 Primer sequences used for expression and ChIP RT-qPCR 36

Table 2.2 Fosmid clones used for DNA FISH (co-ordinates from mm9 genome assembly). 38

Table 3.1 Transcription factors regulated by 100nM dexamethasone in mBMDM 50

Table 3.2 Transcription factors regulated by 100nM dexamethasone in hMDM. 53

Table 3.3 Intersection between dexamethasone regulated genes in hMDM and reported GWAS hits for inflammatory disease 61

Table 3.4 Weak GWAS hits regulated by GC in hMDM 62

Table 4.1 Conserved GR bound sites 87

Abbreviations

3C	Chromatin conformation capture
ACTB	Beta actin
ACTH	adrencorticotrophic hormone
ADORA3	adenosine A3 receptor
Ama	alpha-amanitin (toxin)
AMP	adenosine monophosphate
AP-1	activator protein 1
ARG2	arginase2
ATP	adenosine triphosphate
BAC	bacterial artificial chromosome
bio	biotin
Brg1	Brahma related gene 1 (Smarca4)
Brm	Brahma
C1QB	complement
CBP	CREB binding protein
CEPB	C/CAAT enhancer binding protein
CHD	chromodomain helicase DNA binding
ChIP	Chromatin immunoprecipitation
COMPASS	complex of proteins associated with Set1
CREB	cyclic AMP response element binding protein
CRH	corticotrophin releasing hormone
CRISPR	clustered regularly interspaced palindromic repeats
CSF1	colony stimulating factor 1
CTCF	CCCTC binding factor
Cyp2s1	cytochrome P450, family 2, subfamily S, polypeptide 1
Dex	dexamethasone
dig	digoxygenin
DNA	deoxyribonucleic acid
DUSP1	dual specificity phophatase 1
EDTA	ethylenediaminetetraacetic acid
Egr2	Early growth response 2
ENCODE	encyclopedia of DNA elements
ETS	E26 transformation specific (family of trasncription factors)
F13a1	coagulation factor XIII, A1 polypeptide
FAIRE	formaldehyde assisted identification of regulatory elements
FISH	Fluoresence in situ hybridization
FK506	tacrolimus
FKBP4	FK506 binding protein 52
FKBP5	FK506 binding protein 51

FOS	Finkel-Biskis-Jinkins murine osteosarcoma viral oncogene homologue
GAPDH	glyceraldehyde 3-phosphate dehydrogenase
GC	glucocorticoids
GERP	genome evolutionary restraint profile
GMCSF	granulocyte macrophage colony stimulating factor
GO	Gene ontology
GR	glucocorticoid receptor
GRE	glucocorticoid response element
GTE	glucose tris EDTA
GWAS	Genome wide association study
h	hour
H3K27ac	Histone 3 lysine 27 acetylation
H3K4me1/2/3	histone 3 lysine 4 mono / di / tri methylation
H4K16ac	histone 4 lysine 16 acetylation
HAT	histone acetyl transferase
HDAC	histone deacetylase
Hif1b	hypoxia inducible factor B
hMDM	human monocyte derived macrophages
HMT	histone methyl transferase
HOMER	Hypergeometric motif enrichment (now a wider suite of tools)
HSP70	heat shock protein 70kDa
HSP90	Heat shock protein 90kDa
IgG	Immunoglobulin G
IL6	Interleukin 6
ILR1	interleukin receptor 1
ILR2	interleukin receptor 2
INO80	inositol requiring 80
IRF4	interferon regulatory factor 4
ISWI	imitation switch
Jdp2	Jun dimerisation protein 2
kb	kilobases
KEGG	Kyoto encyclopedia of genes and genomes
KLF4	Krueppel like factor 4
Klf9	Krueppel like factor 9
LCR	locus control region
LDB1	LIM domain binding protein 1
LINE	long interpsersed nuclear element
LPS	bacterial lipopolysaccharide
MAP3K6	mitogen activated protein kinase kinase kinase 6
mBMDM	mouse bone marrow derived macorphages
MMP19	matrix metalloproteinase 19
MMTV	mouse mammary tumour virus

MR	mineralocorticoid receptor
Ms****	membrane spanning****
MT2	metallothionein 2
NCoR	nuclear receptor corepressor
nGRE	negative glucocorticoid response element
nM	nanomolar
NP-40	Tergitol-type NP-40, **nonyl**phenoxypolyethoxylethanol
NR3C1	glucocorticoid receptor
p23	prostaglandin E synthase 3(cytosolic), *PTGES3*
p300	E1A binding protein p300
PDK4	pyruvate dehydrogenase kinase, isozyme 4
PDLIM4	PDZ and LIM domain 4
PER1	Period homologue 1
PIK3IP1	phosphoinositide-3-kinase interacting protein 1
PLAU	urokinase
Polr2a	RNA polymerase subunit 1, Rpb1
PU.1	spleen focus forming virus proviral integration oncogene, SPI1
RAB15	RAB15, member RAS oncogene family
Rad21	Rad21 homologue
Rgs2	regulator of G-protein signaling 2
RNA	ribonucleic cid
RNAPII	RNA polymerase II
Rpb1	RNA polymerase subunit 1, Polr2a
RT-qPCR	Real time quantitative polymerase chain reaction
RXR	retinoic acid receptor
SDC4	syndecan 4
SDS	sodium dodecyl sulphate
SEM	standard error of the mean
seq	next generation sequencing
SGK1	serum/glucocorticoid regulated kinase 1
SINE	short interspersed nuclear element
SLE	systemic lupus erythematosis
Smarca4	SWI/SNF related matrix associated, actin dependent, regulator of chromatin, subfamily a, member 4
SMRT	silencing mediator of retinoic acid and thyroid hormone receptor
SPI1	spleen focus forming virus proviral integration oncogene, PU.1
SSC	saline sodium citrate (Sodium chloride 150mM, sodium citrate 15mM)
SWI/SNF	Switch/Sucrose non fermentable
SWI/SNF	switching defective / sucrose non fermenting
TAD	topology associated domain

TALE	transcription activator like effector
TIFAB	TRAF-interacting protein with forkhead-associated domain, family member B
TLR4	Toll like receptor 4
Tmod1	tropomodulin 1
TNFAIP3	tumour necrosis factor, alpha-induced protein 3
TNFα	tumour necrosis factor alpha
Tris	tris(hydroxymethyl)aminomethane
TSC22D3	Glucocorticoid inducible leucine zipper
TSS	transcription start site
TTS	transcription termination site
UCSC	University of California Santa Cruz
um	micrometres
ZBTB16	zinc finger and BTB domain containing 16

Published, presented and submitted work from this thesis

Abstract and oral presentation at Anaesthesia Research Society winter meeting:

> Effects of glucocorticoids in macrophages. AW Jubb, WA Bickmore, DA Hume May 2013, *BJA,* Vol: 110 Pages: 866-867

Poster EMBL Transcription and Chromatin meeting 2014:

> Dynamic chromatin remodeling at glucocorticoid sensitive loci. AW Jubb, DA Hume, WA Bickmore.

Poster UK Academy of Medical Sciences Spring Meeting 2015:

> Divergent enhancers are linked to differential transcriptional activation in mouse and human macrophages. AW Jubb, RS Young, WA Bickmore, DA Hume.

Submitted manuscript:

> Divergent enhancers are linked to differential transcriptional activation in mouse and human macrophages. AW Jubb, RS Young, WA Bickmore, DA Hume. *Genome Biology*

Chapter 1: Introduction

1.1 Glucocorticoids

1.1.1 Discovery, use and problems

Glucocorticoids (GC) are powerful metabolic hormones with anti-inflammatory actions. First isolated and brought to clinical use over 60 years ago (Hench PS, Slocumb CH, Polley HF, 1950), they produce dramatic alleviation of inflammation in the majority of cases. Their therapeutic impact combined with the efficiency with which they can be produced ensures that they remain the most widely prescribed anti-inflammatory therapies (Fardet et al., 2011; van Staa et al., 2000).

GC are synthesised in, and secreted from, the zona fasciculata of the adrenal gland from a cholesterol precursor (Figure 1.1). Plasma GC levels fluctuate in a diurnal rhythm and are integrated with the autonomic nervous system such that release from the adrenals also occurs in response to stress. GC form the efferent limb of the hypothalamic-pituitary-adrenal (HPA) axis, a classical hormone feedback loop (Figure 1.2) (Nicolaides et al., 2015). Pro-inflammatory cytokines stimulate the HPA (Silverman and Sternberg, 2012) and dysregulation of this axis is linked to increased morbidity and mortality in humans with severe illness (Annane et al., 2000, 2009; Boonen et al., 2013).

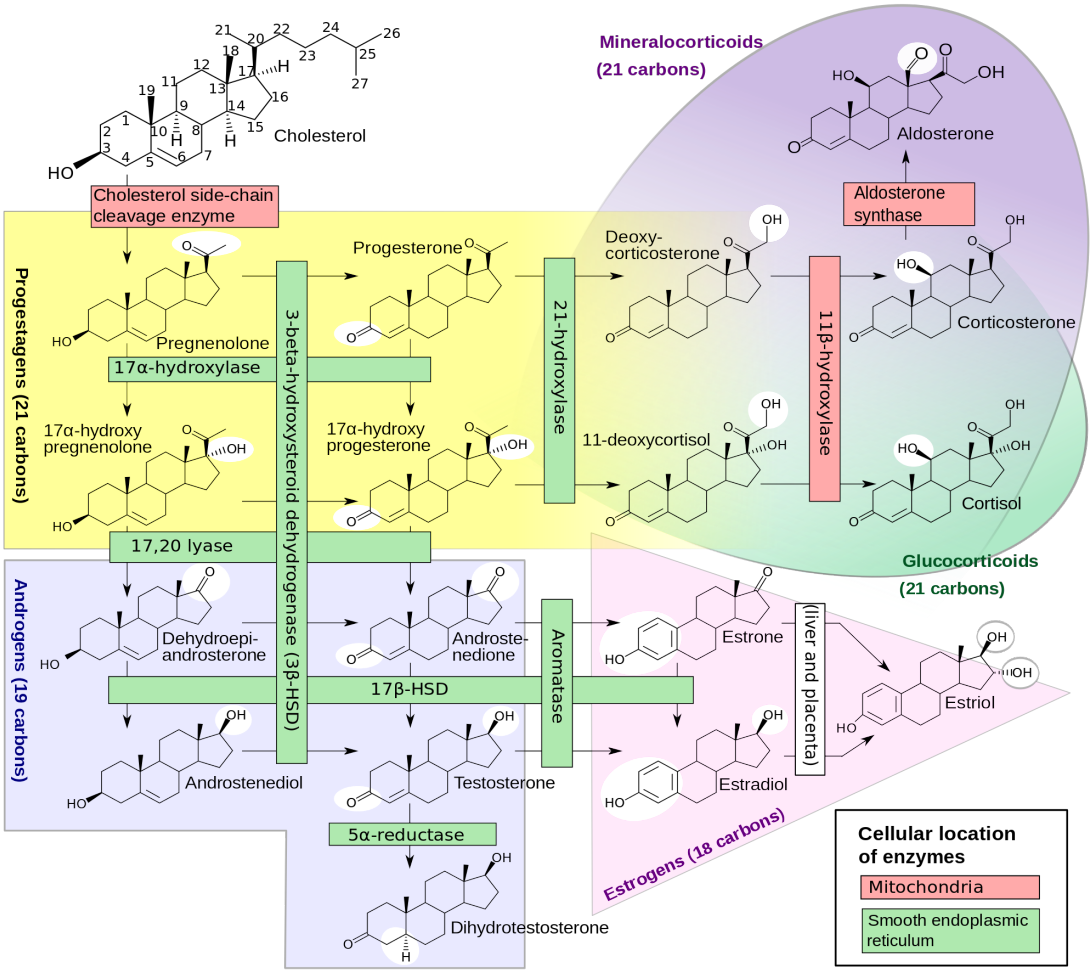

Figure 1.1 Steroidogenesis

An overview of steroidogenesis showing the steps in production of GC from cholesterol. Also shown are the pathways that produce the related mineralocorticoids, estrogens and androgens. White highlights indicate changed moieties after each reaction. Image is in the public domain (Häggström, 2014).

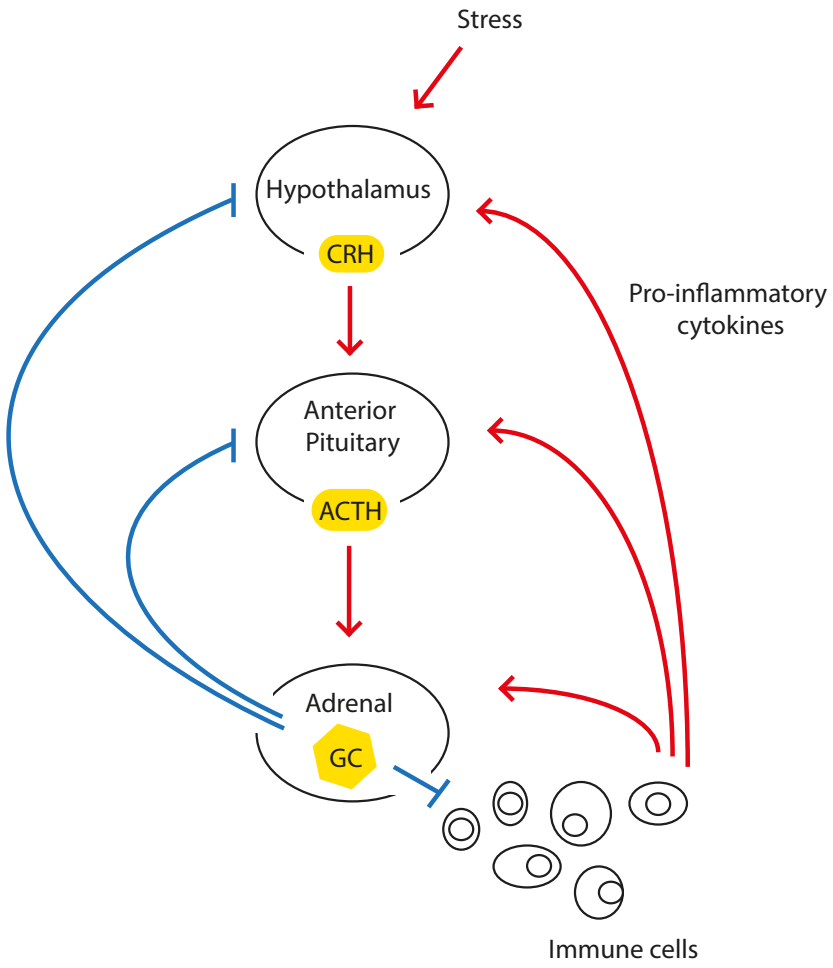

Figure 1.2 The hypothalamic-pituitary-adrenal axis

Schematic diagram illustrating pathways resulting in secretion and feedback control of GC through the HPA axis. CRH = corticotrophin releasing hormone, ACTH = adrenocorticotrophic hormone, GC = glucocorticoids, predominantly cortisol in man. Pro-inflammatory cytokines include for example Tumour Necrosis Factor alpha (TNFα), Interleukin 6 (IL6).

Physiological GC have wide ranging effects, which act to maintain homeostasis, for example in intermediary metabolism, fluid balance, bone metabolism, psychology, development and the cell cycle (Nicolaides et al., 2015).When exogenous GC are given as therapy it necessarily follows that they can

produce a litany of side effects (Table 1.1) making their longevity in the clinic all the more remarkable. The corollary of their many functions is that they have clinical efficacy in many situations that are not primarily inflammatory, from analgesia and anti-emesis to anti-cancer chemotherapy. Despite extensive investigation of the actions of GC, it remains the case that an alternative with equivalent efficacy but reduced side effects has not yet been developed. It may be argued that this is in part because our knowledge of the mechanisms by which GC act remains incomplete.

Table 1.1 Side effects of glucocorticoid therapy

Eye	increased risk of cataracts increased risk of glaucoma
Central nervous system	mood disorders psychosis memory impairment increased risk of stroke
Cardiovascular	atherosclerosis hypertension heart failure ischaemic heart disease
Gastrointestinal	gastritis ulcers
Immune	immunosuppression neutrophilia
Metabolic	fat redistribution (truncal obesity) insulin resistance raised fasting glucose
Renal	fluid retention
Genito-urinary	menstrual irregularity
Musculoskeletal	osteoporosis avascular necrosis growth impairment in children muscle weakness
Skin	thinning purpura raised incidence of skin cancers striae hypertrichosis

1.1.2 Towards a mechanism for glucocorticoid action

Highly lipid soluble (Figure 1.1,Figure 1.4) GC diffuse freely into cells. Intracellular levels of active GC are regulated by 11β-hydroxysteroid dehydrogenase enzymes and these can modulate inflammation (Chapman et al., 2006; Hadoke et al., 2013). Inside the cell GC act via an intracellular receptor (GR), which has the general structure common to receptors for other steroidal hormones such as androgens and progesterone (Oakley and Cidlowski, 2011) (Figure 1.3). GR is produced from a single gene in all species examined (Lu and Cidlowski, 2004) and has two main two isoforms GRα and GRβ produced by alternate splicing (Hollenberg et al., 1985; Oakley and Cidlowski, 2011), the major difference being that GRα binds ligand and induces expression of GC sensitive reporter genes whilst GRβ does neither (Lu and Cidlowski, 2004). It has become clear that GRβ is likely to have a role in regulating GC sensitivity (Gross and Cidlowski, 2008), but it does not respond directly to GC, rather it acts indirectly in balance with GRα. This thesis is focused on relatively acute responses to GC therefore the abbreviation GR is used to mean GRα unless stated otherwise.

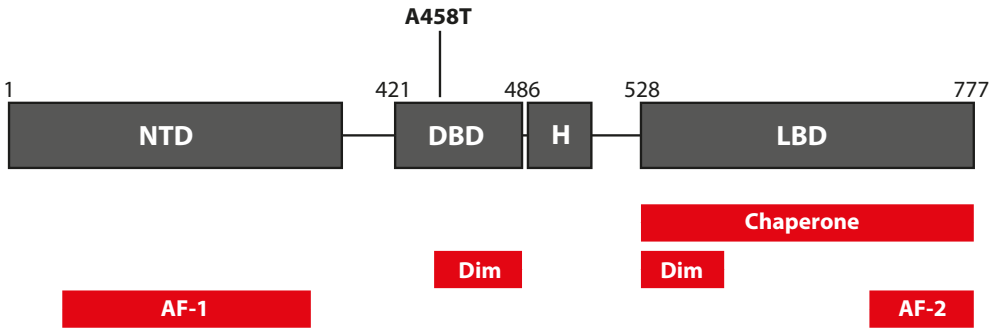

Figure 1.3 Schematic diagram of the glucocorticoid receptor

The main domains of the glucocorticoid receptor are shown in grey. Red bars indicate regions with identified roles. The position of the mutant A458T is given, (see text). NTD = N-terminal domain, DBD = DNA binding domain, H = hinge region, LBD = ligand binding domain. AF-1 and AF-2 = Activator Function 1 & 2 involved in interactions with other factors. Dim = dimerization. Chaperone = domain interacts with GR chaperone proteins such as HSP90. Small figures represent the amino acid position.

In the non-stimulated state GR is held in the cytoplasm bound to a chaperone complex, which is involved in receptor maturation and modulates ligand affinity. Components of the chaperone complex include heat shock proteins (40, 70 and 90), p23 and the immunophilins FKBP5 or FKBP4 (Oakley and Cidlowski, 2011; Vandevyver et al., 2012). Ligand binding results in conformational changes in GR and a switch from FKBP5 to FKBP4 binding. FKBP4 interacts actively with the cytoskeleton, via the ATP utilising motor protein dynein, increases the affinity of GR for GC and is necessary for efficient GR signalling (Wochnik et al., 2005). Conversely, high levels of FKBP5 reduce the binding affinity of GR for GC and have been associated with the glucocorticoid resistance observed in some new world primates (Denny et al., 2000). Binding of GC also exposes nuclear localisation signals and the receptor, assisted by the chaperone complex, translocates rapidly to

the nucleus (Vandevyver et al., 2012). FKBP4 and FKBP5 can modulate the interaction of GR with both ligand, other chaperones and active transport along the cytoskeleton and thus can regulate GC sensitivity at several levels (Jääskeläinen et al., 2011; Vandevyver et al., 2012).

Many modifications of natural GC have produced molecules with differing pharmacology. For example, the widely-studied synthetic glucocorticoid, dexamethasone is modified at 3 positions and has higher binding affinity for GR and minimal affinity for mineralocorticoid receptor (Figure 1.4).

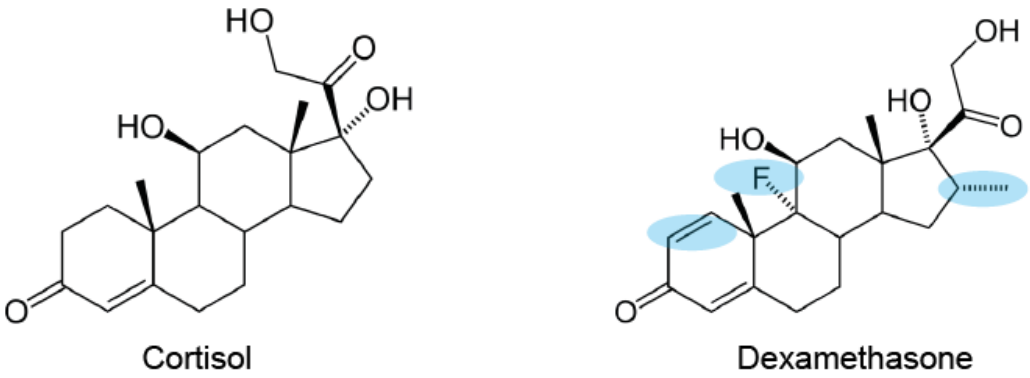

Figure 1.4 Structures of cortisol and dexamethasone

Comparison of the 2D structures of cortisol, the major GC in humans and the commonly used synthetic GC dexamethasone. Differences are highlighted in blue, these lead to higher affinity for GR but minimal affinity for mineralocorticoid receptor (MR).

Nuclear GR can bind directly to DNA, classically as a homo-dimer (Nixon et al., 2013) recognising a Glucocorticoid Responsive Element (GRE). The GRE was identified initially from study of the promoter region of the tyrosine amino transferase gene and forms an inverted repeat of 6 base pairs, separated by a 3 base pair spacer (AGAACAnnnTGTTCT) (Strahle et al., 1987). Studies of genome wide

GR binding have shown that the consensus GRE motif is not always strictly required and substantial degeneracy may be tolerated (John et al., 2011; Reddy et al., 2009).

GR also acts indirectly by binding other transcription factors such as NFκB and AP-1 (Ratman et al., 2013; Uhlenhaut et al., 2013) as well as by recruiting coregulators, for example GRIP1 (Lonard and O'Malley, 2012; Rogatsky et al., 2002). Direct GR-DNA binding has been reported to occur at distal regulatory elements (enhancers), closer to induced than to repressed genes (Reddy et al., 2009). Binding is dynamic, with visualized occupancy times in the order of seconds (McNally et al., 2000; Voss et al., 2011) with equally dynamic effects on downstream transcription (Stavreva et al., 2009). Ligand and DNA binding events allosterically modulate the action of GR (Meijsing et al., 2009; Watson et al., 2013). The favoured model of gene repression by GR is interaction with other factors as described above – termed 'transrepression'. An alternative mode of gene repression by GR has also been described via negative GR response elements (nGRE). The nGRE has the form CTCC(n)0-2GGAGA, where (n)0-2 indicates flexibility in spacing (Hudson et al., 2013; Surjit et al., 2011) and is thus distinct from the consensus GR binding elements (GRE). Binding at nGRE is monomeric on opposite DNA strands(Hudson et al., 2013). Repression is mediated by recruitment of co-repressors nuclear receptor compressor (NCoR) and silencing mediator of retinoic acid and thyroid hormone receptor (SMRT) and histone deacetylases (Surjit et al., 2011).

Non genomic mechanisms such as non specific membrane interactions and cytosolic or membrane GR may have a role in the response to GC (Stahn and Buttgereit, 2008). This thesis is concerned with the genomic effects therefore the non-genomic actions will not be explored further here.

1.1.3 The role of GR dimerization and the 'dissociated' glucocorticoid

The ideal anti-inflammatory agent acting via GR would dissociate the anti-inflammatory and metabolic effects and thereby eliminate the side effects listed in Table 1.1. In theory, some effects of GR could be retained in a receptor that did not bind directly to DNA, but bound instead to other transcription factors (Ratman et al., 2013). A GR mutant thought to be dimerization incompetent and hence unable to bind canonical GRE, A458T (human, equivalent to A465T mouse, A477T rat) (GR^{dim}) (Figure 1.3) has been identified, in which gene induction was ablated, but restraint of a pro-inflammatory stimulus was retained (Reichardt et al., 2001). This opened the possibility of achieving the desired dissociation of GC's beneficial and deleterious effects by activating GR without inducing dimer formation. However, subsequent studies indicated that dimerization deficient mutants retain the ability to induce gene expression (Frijters et al., 2010) and demonstrated homo and hetero dimer formation between GR^{dim} and GR^{wt} (Frijters et al., 2010; Presman et al., 2014). Possible explanations for the residual stimulatory activity include monomer driven induction, atypical hetero- or head to head dimerization (Nixon et al., 2013; Schiller et al., 2014).

The equivalent rat GR dimerization mutation, A477T, led to altered DNA binding kinetics and transcriptional output when expressed in human U2OS osteosarcoma cells (Watson et al., 2013). The A477T mutant GR bound with lower affinity than wild type, which was attributed to reduced co-operativity since monomer affinities were comparable between mutant and wild type. The response to GC in cells expressing the mutant receptor was altered, with some genes more responsive, some less and some unchanged (Schiller et al., 2014; Watson et al., 2013). Genes that were less responsive to the mutant receptor were enriched for local GR binding in wild type whilst those that were more responsive to the mutant receptor were more likely to have local GR bound in the mutant condition (Schiller et al., 2014). A double mutant of GR^{dim} and a substitution in the ligand binding

domain, I634A, did appear to significantly reduce dimerization, but both gene induction and repression were still possible (Presman et al., 2014).

Based upon these published findings, it appears unlikely that a therapy that activates GR but prevents dimerization will be able to cleanly dissociate the anti-inflammatory and metabolic effects of GC. Greater understanding of the modes by which GR acts in a native context may allow fine-tuning of ligands to produce the same outcome.

1.2 Chromatin and the control of gene expression

1.2.1 Chromatin

Chromatin is the name given to the complex of DNA and protein that is present in eukaryotic nuclei. It is formed from units, called nucleosomes, of approximately 146 base pairs of DNA sequence wrapped around an octamer of histone proteins, H2A, H2B, H3 and H4 (Luger et al., 1997). Lower abundance variants of core histones are present such as H2A.Z, which is enriched in nucleosomes flanking the transcription start site and at other sites involved in gene regulation (Talbert and Henikoff, 2010). Histone proteins undergo many post-translational modifications, which are associated with gene regulation and chromatin structure. For example acetylation of histone N-terminal tails by histone acetyl transferases (HATs) is associated with transcriptional activation, via charge neutralisation and by providing docking sites for bromodomain containing transcriptional regulators factors (Lee et al., 2010). Similarly trimethylation of histone 3 at lysine 4 (H3K4me3) by histone methyl transferases (HMTs) of the COMPASS (complex of proteins associated with Set1) family, is associated with active gene promoters (Shilatifard, 2006). These marks are dynamic; acetylation can be removed by histone deacetylases (HDACs) and lysine histone methylation can be removed by demethylases. Combinations of modifications occur within a given locus

providing an additional layer of regulatory information on top of the underlying sequence (Lee et al., 2010; Smith and Shilatifard, 2010).

Nucleosomes are linked by spans of DNA with the linker histone H1 associated, which has a role in both nucleosome positioning and higher order chromatin structure. In turn this higher order structure has a regulatory effect on DNA-protein, hence transcription factor, interactions (Li and Reinberg, 2011). Although gene dense regions are enriched in open chromatin, there is not a simple relationship between density of folding and activity; many inactive genes are found in open regions and active genes from gene poor regions may be found in condensed chromatin (Gilbert et al., 2004).

Remodelling of chromatin occurs via the action of ATP-dependent remodelling complexes. In eukaryotes there are 4 classes; switching defective/sucrose non fermenting (SWI/SNF), imitation switch (ISWI), chromodomain helicase DNA binding (CHD) and inositol requiring 80 (INO80) (Clapier and Cairns, 2009). Remodellers use the energy of ATP hydrolysis to change the state of chromatin by moving, ejecting or restructuring the nucleosome and thus enable DNA replication, translation and repair (Clapier and Cairns, 2009).

1.2.2 Long range control of gene regulation

1.2.2.1 Distal elements regulate transcription and have characteristic features

Transcriptional output for a given gene is the result of integration of all regulatory influences and begins from promoter regions that overlap the transcription start site (TSS) for each gene (Lenhard et al., 2012). The pre initiation complex (PIC) docks at promoters; this contains general transcription factors and DNA dependent RNA polymerase II (RNAPII) which then transcribes the sequence. Elements distant from this core promoter region play an essential role in providing the complexity and

specificity in gene regulation that is required to form complex organisms (Levine, 2010). Control of transcription by a specific DNA sequence from a distal site was was first demonstrated using a part of an animal virus, SV40, to drive β-globin transcription (Banerji et al., 1981). The sequence of the distal site, the SV40 enhancer, consisting of two 72bp repeats, enhanced expression when placed up or downstream of the gene in either orientation (Banerji et al., 1981). It was described as an enhancer due to its positive effect on transcription and was later shown to bind multiple transcription factors such as AP-1 (Lee et al., 1987). Combinatorial binding of transcription factors is now know to be a general property of enhancers (Glass and Ogawa, 2006; Levine, 2010; Métivier et al., 2003; Villar et al., 2014).

Other features of enhancers have also now been described. These include sequence conservation (Frazer et al., 2003), binding of co-activators, conserved patterns of histone modifications, nuclease sensitivity, and bi-directional transcription.

Co-activators bind to transcription factors, but do not bind DNA or regulate transcription directly. The co-activator p300 and its paralogue CREB-binding protein (CBP) were initially identified as a binding partner for cAMP-response element binding (CREB) (Chrivia et al., 1993) but are now known to interact widely with other transcription factors, including steroid receptors(Holmqvist and Mannervik, 2013). They have acetyl-transferase activity and can acetylate histones, but also have several other domains that facilitate interactions. A combination of p300 and histone 3 lysine 4 monomethylation (H3K4me1) marks enhancers (Heintzman et al., 2007; Visel et al., 2009; Wang et al., 2005). Loss of MLL3/ MLL4 subtypes of mammalian COMPASS leads to loss of H3K4me1 predominantly at enhancers(Hu et al., 2013). The location of enhancer marks is cell type specific, reflecting transcriptional diversity between tissues (Andersson et al., 2014; Heintzman et al., 2009). Acetylation of histone 3 lysine 27 (H3K27ac) is reported to mark a proportion of active enhancers, and is a modification that can be made by p300 (Heintzman et al., 2009; Holmqvist and Mannervik, 2013), whilst acetylation of histone 4 lysine 16 (H4K16ac) is also found at enhancers in embryonic stem cells (Taylor et al., 2013).

Transcription factors that can bind DNA at sites not permissive to other transcription factor binding are described as pioneer factors. Recruitment of chromatin remodellers by pioneer factor can then result in nucleosome repositioning such that the site can bind other factors. For a given cell type the position of these sites is determined by a small repertoire of lineage specific transcription factors, for example in innate immune cells macrophages the ETS factor PU.1 is dominant (below, section 1.3) (Ghisletti and Natoli, 2013; Ghisletti et al., 2010; Heinz et al., 2010).

Enrichment for transcription factor binding and depletion of nucleosomes at regulatory sites leads to sensitivity to digestion by nucleases (Felsenfeld et al., 1996). Enhancer associated histone modifications intersect with areas of increased chromatin accessibility (Thurman et al., 2012), have RNAPII bound(De Santa et al., 2010) and display a signature of bi-directional transcription (Andersson et al., 2014). Genome wide maps of DNA elements likely to have regulatory function have now been produced across several cell types (Andersson et al., 2014; Bernstein et al., 2012; Yue et al., 2014). These maps confirm earlier genetic evidence, for example in study of the *Shh* locus (Lettice et al., 2003), that enhancers can lie upstream or downstream of their target TSS and many tens or hundreds of kb distant.

Mediator is a large (30 subunit, >1MDa) co-activator complex(Tsai et al., 2014). It interacts with RNAPII and multiple transcription factors, including GR, and is involved in the expression of a large proportion of genes (Malik and Roeder, 2010). Mediator binding can be detected at both promoters and enhancers (Kagey et al., 2010; Malik and Roeder, 2010). Clusters of enhancers, referred to as super enhancers by their descriptors, have been defined in some settings on the basis of the intensity of binding of Mediator subunits (Pott and Lieb, 2014).

1.2.2.2 Models of long range regulation

There is debate about how distant regulatory sites, such as those bound by GR, cause changes in target gene transcription (Pennacchio et al., 2013). One model, currently the most prevalent, proposes that the distant element binds activating factors and co-activators, such as Mediator (Kagey et al., 2010; Malik and Roeder, 2010). This then forms a loop to come close to its target promoter, delivering the regulatory input required (Figure 1.5A) (Bulger and Groudine, 1999; Krivega and Dean, 2012).

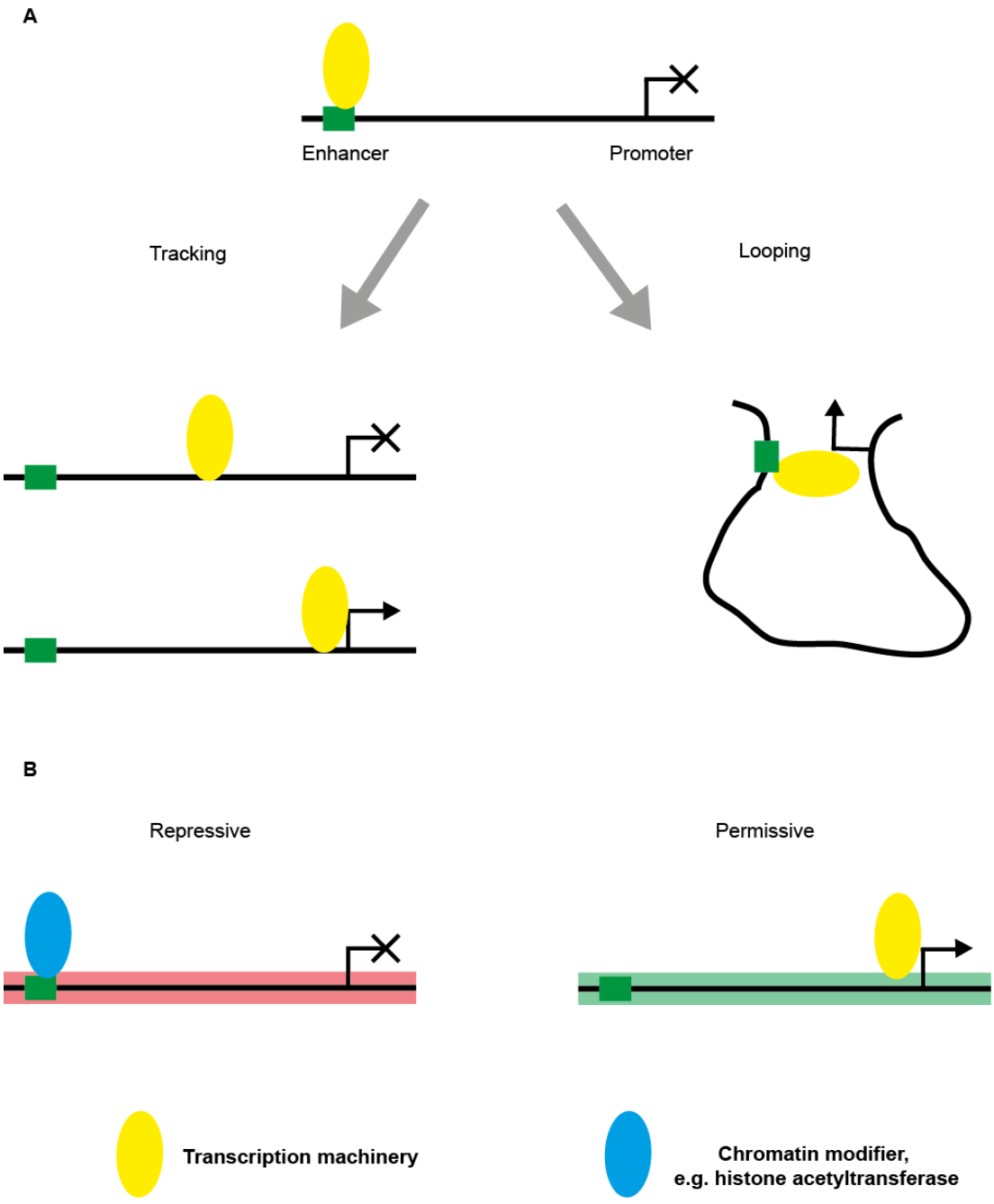

Figure 1.5 Models of long range control of gene expression

Simplified diagrams of proposed models of enhancer activity. **A** Transcription factors and the transcription machinery (yellow oval) bind to an enhancer (green rectangle). A loop may then form to the target promoter (right), bringing the factors required for gene activation to the promoter. Alternatively the transcription

machinery may run along the genome to reach the promoter and then activate the gene (left). **B** Recruitment of chromatin modifiers to an enhancer (blue oval) may induce a change to the chromatin state from repressive (left) to permissive (right) for transcription of a target gene.

The presence of loops has been inferred from results from the chromosome conformation capture (3C) family of assays. These methods are all based on formaldehyde cross-linking of cells, digestion of chromatin and re-ligation of DNA followed by reversal of cross-links to leave ligation products that enrich for genomic regions that were cross linked (Figure 1.6). These products can be analysed in various ways, from PCR to next generation sequencing, but for all interactions are inferred from an increase in detectable cross-link formation over background after formaldehyde treatment (Dekker et al., 2002; Dixon et al., 2012; Dostie et al., 2006; Lieberman-Aiden et al., 2009; Rao et al., 2014). An estimate of background can be made by digestion of a bacterial artificial chromosome (BAC) covering the region of interest, which is assumed to adopt a conformation lacking higher order structure. Interactions that are separated by non-interacting regions are then described as loops of chromatin. The critical step in these assays was thought to be proximity ligation under conditions of dilute DNA, where intra- rather than inter- molecular ligation should be favoured. However, the majority of 3C products actually come from the insoluble portion of cross-linked material that is present within intact nuclei (Gavrilov et al., 2013). Formaldehyde treatment fixes the global nuclear architecture, as measured using fluorescence microscopy, sufficiently to resist the harsh detergent treatments in 3C protocols, although there is a more homogenous structure when examined by electron microscopy (Gavrilov et al., 2013). A 3C contact reflects a combination of the tendency of two regions to cross link, their spatial proximity at the point of re-ligation and the mobility of the digested DNA ends. Hence for highly formaldehyde cross-linkable loci, such as those containing multiple lysine, tryptophan and cysteine residues in the associated proteins, a contact may be identified where the physical distance is high (Williamson et al., 2014).

Formation of a loop requires either an active or energetically favourable process, along with a mechanism for specificity. At the beta globin locus it has been shown that a loop forms from the locus control region (LCR) and is required for normal transcription. In this case it is mediated by a specific transcription factor, LDB1, forming a homo-dimer (Deng et al., 2012; Krivega et al., 2014). Dynamic higher order structures nucleated on Mediator have been proposed, via its ability to

interact with activating factors as well as other factors with roles in chromatin organisation like the cohesin complex (Kagey et al., 2010; Malik and Roeder, 2010; Phillips-Cremins et al., 2013).

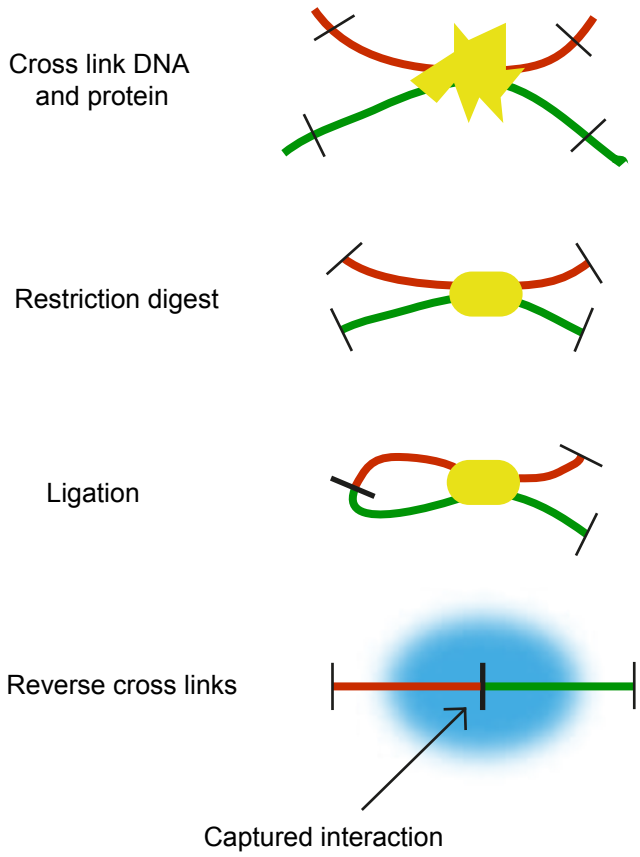

Figure 1.6 Principles of chromosome conformation capture

In chromosome conformation capture formaldehyde is used to cross link DNA and protein. This cross-linked material is then digested using a restriction enzyme. Ligation of this material prior to reversing cross-links favours formation of intra-molecular ligation products. When cross-links are reversed interactions between pieces of DNA are inferred from the frequency of their ligation products, indicated above as 'Captured interaction'. Red and green lines represent strands of DNA that are close together in the condition under study, Black lines = restriction sites that are cut by a specific restriction enzyme, Yellow = site of DNA-protein-DNA crosslinking. Blue highlights the captured interaction of interest.

Transcription factors and the transcription machinery bind to enhancers(De Santa et al., 2010). Scanning of RNAPII along the genome from enhancers to promoters is an alternative to loop formation (Figure 1.5A). Evidence of increased RNAPII in the region between the enhancer and promoter has been observed in a study of an androgen receptor responsive enhancer (Wang et al., 2005). There was no enrichment for the activating factors recruited to the enhancer and promoter in the intervening region. Hence, the observation was consistent with RNAPII scanning from enhancer to promoter rather than formation of a large chromatin conglomerate including all measured sites. How RNAPII could scan over long distances past other, non-regulated, genes is not clear.

The RNA polymerase machinery is inherently unidirectional (Duttke et al., 2015) however bidirectional transcription may often be observed (Seila et al., 2008), even at promoters. The antisense transcripts initiate from distinct sites on the reverse strand with similar sequence content to the main promoter (Duttke et al., 2015). Anti-sense transcripts are short due to an enrichment for poly-A sequence and are rapidly degraded (Ntini et al., 2013). As described above RNAPII binds to enhancers (De Santa et al., 2010) and there is bi-directional transcription (Andersson et al., 2014). Short RNA molecules, enhancer RNAs (eRNAs), that appear to be functional can be produced by enhancer transcription (Gosselin and Glass, 2014; Li et al., 2013). In macrophages targeted degradation of eRNAs from the enhancers of *Mmp9* and *Cx3cr1,* which are normally repressed by Rev-Erbs nuclear receptors, caused specific repression of the target genes (Lam et al., 2013). Expression of eRNAs adjacent to responsive genes in oestrogen sensitive cells increases after treatment with oestradiol. Interfering with eRNA expression reduces the response of the associated gene (Li et al., 2013). In the same study reduced cross-linked interactions were noted between enhancers and promoters when the eRNA was knocked down for 2 loci, *NRIP1* and *GREB1*. Mediator can interact with eRNAs that are responsive to the androgen receptor (AR) (Hsieh et al., 2014) so this may be one mechanism by which these structural effects occur. Transcription can precede and facilitate the deposition of the histone marks that are used to define enhancers (Kaikkonen et al., 2013). Conversely, enhancers can provide a locus from which domains of transcriptionally

permissive chromatin expand (Figure 1.5B) (Bulger and Groudine, 2011; Fromm et al., 2011).

1.2.2.3 Visualizing chromatin changes during gene regulation

The proximity relationship between genomic loci at the 100kb-1.5Mb scale can be assessed by DNA Fluorescence In Situ Hybridisation (DNA FISH) (Yokota et al., 1995). By this method it is possible to visualise specific sites in the genome by fluorescence microscopy, which can then be used to assess chromatin compaction (Chambeyron and Bickmore, 2004; Eskeland et al., 2010; Williamson et al., 2012; Yokota et al., 1997). Fosmid pairs flanking the locus of interest are selected and labelled. These can then be hybridized to paraformaldehyde fixed cells and their positions visualized by microscopy. The physical distance between two fosmid probes is then measured (Figure 1.7). Less compact chromatin is inferred from larger distances for the same genomic length in base pairs. For adherent cells this procedure can be done in 3 dimensions (3D) through capture and reconstruction of image stacks from cells grown on slides.

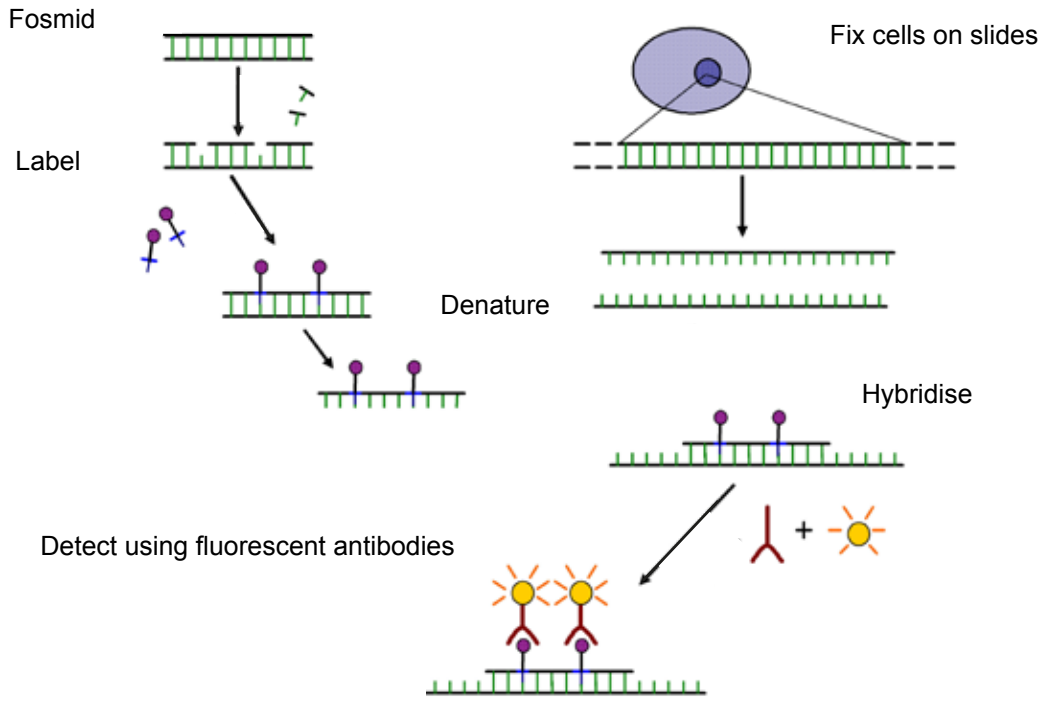

Figure 1.7 Schematic overview of DNA FISH

In DNA FISH a probe (**Fosmid**) with sequence specificity to the genomic site of interest is labelled using random cutting and infill with labelled dUTPs (purple filled circles). These may be directly linked to fluorochromes or to easily detectable haptens e.g. Biotin-dUTP (**Label**). After fixing the cells of interest on slides the labelled probe and nuclear DNA are denatured (**Denature**) then hybridised at 37° (**Hybridise**). The probes are visualised directly (for directly labelled probes), or detected, e.g. for biotin with avidin conjugated to a fluorophore, then visualized using fluorescence microscopy (**Detect**). Combining different labels allows two sites to be marked and detected simultaneously with fluorophores that have different emission spectra.

It appears that in 3D FISH key aspects of chromatin conformation are preserved (Markaki et al., 2012), but findings between 3C based and FISH based assays are not always consistent (Dostie and Bickmore, 2012; Williamson et al., 2014). For example, the Hox genes are important in patterning during mammalian development and have been studied by both FISH and 3C based techniques. When inactive, Hox loci adopt a compact state by FISH (Chambeyron and Bickmore, 2004; Eskeland et al., 2010; Morey et al., 2007) and have multiple local interactions by 3C based methods (Montavon et al., 2011; Williamson et al., 2014). Activation of Hox genes is linked to decompaction and looping out of chromosome territories (Chambeyron and Bickmore, 2004; Chambeyron et al., 2005; Morey et al., 2007; Williamson et al., 2012). Direct comparison of activation of the *Hoxd* cluster demonstrated compatible findings between the two techniques: decompaction by FISH and loss of interactions by 5C (Williamson et al., 2014). Absence of part of one repressive complex (Polycomb repressive Complex 2, PRC2) showed unfolding by FISH across *Hoxd* and was mirrored by loss of 5C interactions. By contrast loss of another repressive complex (Polycomb Repressive complex 1, PRC1) showed unfolding by FISH but the 5C contacts were maintained. This may be due to the chromatin environment and the ability of the looped out regions to form cross links on formaldehyde treatment: the mutant models have different amounts of the amino acid residues that are most readily cross linked by formaldehyde (lysine, tryptophan and cysteine) at the *Hoxd* locus (Williamson et al., 2014). As discussed above, all ligation products from 3C based assays come from insoluble cross-linked aggregates from intact nuclei that have been treated with strong detergent, therefore it is difficult to infer chromatin structure from this data (Gavrilov et al., 2013).

Interestingly, in contrast to the findings and interpretation of Williamson et al. (above), a high frequency of detected local interactions at active Hox loci captured by 5C in fibroblasts (Wang et al., 2011) and by 4C in mouse embryos (Noordermeer et al., 2011, 2014) was interpreted in a different way: they suggest that the active locus is more compact.

1.2.2.4 Topology associated domains

High throughput 'C' techniques have led to the identification of higher order structures termed topology associated domains (TADs) (Dixon et al., 2012). These are self-interacting genomic regions of approximately 900kb in size and are reported to be largely invariant between cell types and even species, hence they are perhaps less likely to change in response to stimulus. Recent work suggests that dynamic changes within TADs can be quantitatively linked to regulation of transcription, at least at loci involved in X inactivation (Giorgetti et al., 2014).

Another feature of genome organisation is DNA supercoiling. DNA supercoiling occurs when twist is induced in the helix by the passage of RNAPII (Villeponteau et al., 1984) resulting in domains of under and over wound DNA (Naughton et al., 2013). Domains of under wound DNA correlate to more open chromatin and active genes (Naughton et al., 2013) and are also remodelled by the activity of RNAPII and topoisomerase I.

1.2.3 GC effects on chromatin

Active chromatin remodelling complexes are involved in gene regulation by GR (Engel and Yamamoto, 2011; John et al., 2011; Trotter and Archer, 2007). Much of this work has derived from pioneering studies using murine cell lines that have the GC responsive Mouse Mammary Tumour Virus (MMTV) integrated in a tandem arrays containing 800-1200 GRE (Richard-Foy and Hager, 1987; Zaret and Yamamoto, 1984). The ATPase subunit of the SWI/SNF remodelling complex, Brg1, has been studied in the context of the GC response. Loading of Brg1 to the MMTV array in vitro rapidly follows GR binding (Nagaich et al., 2004) and Brg1 been shown to interact dynamically with MMTV in live cells (Johnson et al., 2008). Further, in the presence of a dominant negative form of Brg1 a subset of genes had reduced, although not ablated, response (John et al., 2011).

GR binding is largely constrained by, but also able to remodel the pattern of open chromatin measured by nuclease sensitivity (Biddie et al., 2011; Burd and Archer, 2013; John et al., 2008, 2011), if only at a minority of GR bound sites. Large scale re-organisation of chromatin was not observed in response to GC (Hakim et al., 2011). Rather, GC acts locally on the background of pre-existing nuclear architecture by increasing the frequency of pre-existing regulatory contacts (Hakim et al., 2011). At present no studies visualising the dynamics of higher order chromatin responding to GC in a primary cell context have been reported.

1.3 Macrophages

1.3.1 Overview and relevance

Macrophages are cells of the innate immune system involved in inflammation and tissue repair, as well as normal cell growth and development (Hume, 2008; Wynn et al., 2013). They differentiate from precursors under the influence of colony stimulating factors CSF1 and GMCSF. The traditional view is that macrophages derive from circulating monocytes and this is certainly the case in large measure within inflammatory lesions. However, in mice at least, there is also a role for local self-renewal of tissue macrophages seeded early in development and for proliferation of populations of tissue macrophages in response to inflammatory stimuli (Jenkins and Hume, 2014; Wynn et al., 2013). Macrophages are a substantive cell population in all tissue, and are particularly focused in areas potentially exposed to injurious stimuli and pathogens. Reflecting the pervasive nature of inflammatory processes, a role for macrophages has been posited in virtually all medical conditions (Gosselin and Glass, 2014; Wynn et al., 2013).

1.3.2 Macrophage response to GC

A feature of macrophages is their ability to detect and respond dynamically to stimuli. The most intensively studied response is that following exposure to bacterial lipopolysaccharide (LPS), a Toll-like receptor 4 agonist which generates a rapid and dramatic transcriptional response, producing a cascade of regulated genes both induced and repressed (Hume, 2012; Hume and Freeman, 2014). An initial cohort of induced genes, including for example TNF-alpha, are regulated at the level of elongation by pausing RNAPII (Hargreaves et al., 2009). Later genes are regulated by transcriptional regulation directly downstream of the TLR4 signalling cascade, through autocrine responses to cytokines produced by the initial response and in a cascade of induction or repression by induced transcription factors (Hume, 2012).

There is a growing realization that gene regulation from enhancers is critical to both specify cell type and define responses to stimuli (Andersson et al., 2014; Bernstein et al., 2012; Gosselin et al., 2014; Lavin et al., 2014; Yue et al., 2014). The enhancers involved in the LPS response have been mapped in mouse macrophages using a combination of H3K4me1 and binding p300 (section 1.2.2) (Ghisletti et al., 2010). These sites are important for directing the binding of other transcription factors(Heinz et al., 2010) and are highly enriched for binding of the lineage defining ETS transcription factor PU.1 (Barozzi et al., 2014; Natoli, 2010). A subset of inducible enhancers, sites that gain H3K4me1 after a stimulus, has also been shown for several stimuli including LPS (Ostuni et al., 2013).

Macrophages are major targets of GC. They express GR at high levels; in the mouse at relatively higher levels than in several other immune cell types (Lattin et al., 2008; Wu et al., 2009). Much of the research on therapeutic GC actions has focused on gene repression in the context of pro-inflammatory stimuli such as LPS (Chinenov et al., 2014; Ogawa et al., 2005; Uhlenhaut et al., 2013). However, immune cells such as macrophages also respond directly to GC in the absence of any other stimulus with changes in cell survival, proliferation, morphology and phagocytosis (Ehrchen et al., 2007; Galon et al., 2002; van de Garde et al., 2014;

Varga et al., 2008). GC oppose the actions of the major macrophage growth factor, CSF1 (Hume and Gordon, 1984) and can cause monocytopenia (Steer et al., 1997). Hence, there are good reasons to understand the direct actions of GC alone as a regulator of macrophage function.

Data for a single time point have been published for mouse bone marrow derived macrophages (mBMDM) responding to a high dose of dexamethasone (1uM, 16h) – a specific ligand for GR (Uhlenhaut et al., 2013). This model serum starved and removed CSF1 before treatment and showed a limited number of genes responding (32 reaching $\log_2$ fold change >1.5). Binding data for GR from chromatin immunoprecipitation followed by sequencing was also presented in this study, although the stated aim was to capture indirect interactions rather than direct GR-DNA binding. Dual cross-linking with both formaldehyde and glutaraldehyde disuccimide found ~10,000 putative GR interaction sites (Uhlenhaut et al., 2013). The interactions detected included many that contained known partner motifs, but relatively few that contain a GRE (5% at the peak centre) and hence would be likely to directly bind GR. The large number of sites and small number of genes also makes regulatory relationships difficult to discern. More recently an early responding gene set has been reported in mBMDM where they retained serum and CSF1 (100nM, 1h) (Chinenov et al., 2014). Similar to the LPS response (Hume, 2012; Raza et al., 2014), a predominance of transcription factors was observed in the early responding genes (Chinenov et al., 2014). Single time point data from human monocyte derived macrophages (hMDM) differentiated with GMCSF has been reported as part of a wider screen of the response to multiple stimuli, but no GR binding data is available (Xue et al., 2014). The characterisation of the response to GC in macrophages therefore is not yet comprehensive.

1.4 Models, conservation and divergence

Model systems necessarily underlie much scientific research. The primary model system for mammalian biology is the mouse and a great deal of understanding has been gained from its use. This success reflects the experimental tractability of the species along with moderate physiological and DNA sequence conservation with humans. However it is also clear that there are significant differences between mice and men when one examines specific details, quite apart from the obviously divergent physiological challenges.

A comparison of mouse models of inflammatory illness with the corresponding human conditions found very limited overlap in the transcriptional response (Seok et al., 2013). The are some similarities and parallels if strictly orthologous genes are considered, but these are in the minority (Takao and Miyakawa, 2014). The differences between mice and men are less surprising when one considers the divergence between macrophages of inbred mouse strains responding to inflammatory stimuli (Raza et al., 2014; Wells et al., 2003) attributable to turnover of binding sites for lineage specific and stimulus specific transcription factors between strains (Heinz et al., 2013). The differences may also contribute to costly failures in translating therapy for sepsis, severe systemic inflammation, from animal models to man (Annane et al., 2013; Kerschen et al., 2007).

As discussed above (sections 1.2.2, 1.3.2) regulatory sites that lie distant in the genome from their target promoters are now recognized as crucial in controlling gene transcription (Andersson et al., 2014; Stergachis et al., 2014; Vierstra et al., 2014; Yue et al., 2014). Variability of factor binding at these sites can be a source of phenotype diversity between species (Villar et al., 2014). This variation can accrue rapidly within species and has been fixed in the different inbred mouse strains (Stefflova et al., 2013). The pattern of use of these sites is defined by the environment in macrophages (Gosselin et al., 2014), with differentiated resident macrophages' enhancer landscapes being reprogrammed when transplanted (Lavin et al., 2014).

The cis-regulatory landscapes are quite different between mouse and man (Stergachis et al., 2014; Vierstra et al., 2014; Yue et al., 2014) and this difference is particularly concentrated in sites associated with the immune response (Vierstra et al., 2014; Yue et al., 2014). Consistent with this, comparative analysis of macrophage gene expression after an inflammatory stimulus has shown that, as described above between inbred mouse strains, innate immune responses are very different between mouse and man (Schroder et al., 2012). This inter-species divergence is likely driven by the evolutionary pressure of host pathogen interactions and is due in part to promoter sequence variation (Fairbairn et al., 2011; Schroder et al., 2012).

Given the roles of GC and macrophages in immunity, as well as the role emerging for enhancers in the response to GC, it is plausible that this response may also be divergent and that either local (Schroder et al., 2012) or distal (Heinz et al., 2013) DNA sequence changes may be involved.

1.5 Summary

The physiology and pharmacology of GC are important in human and animal health. A large body of research has begun to map the pathways by which they have their many effects. Predominantly GC act via a nuclear receptor to regulate gene expression in a complex way, which may, as our understanding develops further, provide therapeutic opportunities. Gene regulation occurs within a complex dynamic chromatin environment, which is itself responsive to GC, and involves control by distant elements.

Intimately involved in normal development, health and disease, macrophages are major targets for GC, but investigation of the response is less comprehensive than that for other stimuli such as LPS. Chromatin organisation at GC responsive loci in macrophages has not yet been examined. Study of dynamic responses to other stimuli in macrophages has shown evolutionary divergence between species and strains. If replicated in the response to GC this may be of clinical relevance.

1.6 Thesis aims

- To describe the response to GC in the most commonly used models of macrophage biology, hMDM and mBMDM using global gene expression profiling and receptor binding assays.
- To assess similarity and differences between the two systems and explore the possible origins of any differences
- To determine if there is local chromatin remodelling in response to GC in the context of primary macrophages at candidate loci and explore the mechanism.

Chapter 2: Methods

2.1 Laboratory procedures

2.1.1 Ethics

Procedures involving human volunteers were approved by the South East Scotland NHS Research Ethics Committee. All volunteers gave informed consent. Animals were cared for and managed within the Roslin Institute's guidelines for animal safety and welfare.

2.1.2 Cell culture

8-10 week male wild type C57BL/6 mice were culled by cervical dislocation. Bone marrow wash flushed from hind limbs and then cultured in RPMI supplemented with Penicillin/Streptomycin, Glutamax (Invitrogen), and 10% Foetal Calf Serum for 7 days in the presence of rhCSF-1 at 10^4U/ml. Cells were then replated at $1x10^6$ cells per ml and treated as indicated.

Human peripheral blood monocytes were isolated from blood samples by Ficoll gradient separation of buffy coats followed by MACS CD14+ve selection (Milteny). The full protocols are available on www.macrophages.com. They were then cultured as above for 7 days before being treated as indicated with dexamethasone (Sigma) 100nM or ethanol vehicle.

For DNA FISH mBMDM were differentiated as above then replated onto ethanol sterilised Superfrost (ThermoFisher) slides. Cells were left overnight to adhere before treatment as described. Where indicated transcriptional block was induced by 4 hours pre-treatment of differentiated mBMDM with 2.5mg/ml α-amanitin (Sigma). Slides were washed briefly in Phosphate Buffered Saline (160mM NaCl, 3mM KCl, 8mM Na_2HPO_4, 1mM KH_2PO_4, from tablets prepared by MRC HGU technical services (Thermo), PBS) and fixed for 10 minutes in 4% paraformaldehyde. Slides were then washed 3 times 3 minutes in PBS. Cells were permeabilised by washing in

PBS/0.5% TritonX for 5 minutes. After 2 further washes in PBS slides were air dried and stored at -80°C.

2.1.3 RNA extraction and processing

RNA was prepared using RNeasy column based extraction with on column DNase treatment (Qiagen). RNA quality was checked using a 2100 Bioanalyzer (Agilent). For RT-qPCR cDNA was prepared using SuperscriptIII (Invitrogen). Relative expression was determined using SYBR green on a LightCycler480 (Roche) compared with GAPDH as a reference. Primer sequences are given in (Table 2.1). For microarrays RNA was prepared using standard Affymetrix protocols and applied to the HT-MG430PM (mouse), or HT-U33plusPM (human) chip by Edinburgh Genomics.

For expression analysis BMDM were prepared from 3 mice, treated, extracted and applied to the arrays separately (3 x 6 arrays). Four individuals provided donations for the hMDM , which were prepared, treated and applied to the arrays separately (4x6 arrays).

2.1.4 Chromatin Immunoprecipitation

Antibodies used for chromatin immunoprecipitation of mouse GR were BuGR2 (raised against partially purified rat GR) 1μg/10^6 cells (ThermoFisher / Pierce), and normal rabbit IgG sc-2025 (Santa Cruz). For human GR ChIP we used Sigma Imprint™ anti-GR (raised against amino acids 304-428 of human GR), 1μg/10^6 cells and mouse IgG (Santa Cruz).

20ul of Protein A Dynabeads (Invitrogen) per immunoprecipitation (IP) were washed once then diluted to 200ul in block solution (1xPBS, 0.5% BSA, +2ul 0.1M PMSF). Antibody was added and rotated for 3h at 4°C.

Cells were washed gently once with PBS then cross-linked in tissue culture plates with 1% formaldehyde/RPMI at room temperature for 10 min (mouse) or 7.5min (human) and then quenched with 0.125M glycine. Cells were detached by scraping in

PBS then spun down at 400g for 5 minutes, resuspended and counted. For mBMDM 10 million cells per IP were then taken on and lysed for 15 minutes on ice in 1%SDS, 10mM EDTA, 50mMTris-HCL pH8.1 supplemented with Protease Inhibitors (Calbiochem), 1mM DTT and 0.2mM PMSF (Sigma). The solution was diluted in IP dilution buffer (0.1% Triton-X100, 2mM EDTA, 150mM NaCl, 20mM Tris-Hcl pH8.1) and sonicated using a Soniprep 150 to produce average fragment size 300-500bp. Chromatin was spun for 10min at 10,000g 4°C then supplemented with 20% Triton-X100 to 1% and Bovine Serum Albumin (BSA) (Sigma) to 50μg/ml. Input aliquots were removed and stored at -20°**.** Chromatin was then added to the antibody-bound Protein A Dynabeads (Life technologies) and rotated overnight at 4°C. Beads were washed 3 times for 10 minutes each in 1 - 1% IP dilution buffer, 2 - 1%Triton-X100/0.1%Na-deoxycholate/0.1%SDS, 50mM Hepes pH7.9, 500mM NaCl, 1mM EDTA and 3 - 0.5%Na-deoxycholate/0.5%NP-40, 20mM Tris-HCl pH 8, 1mM EDTA, 250mMLiCl. Chromatin was extracted at 37°c for 15min on a vibrating platform in 100ul extraction buffer (0.1M NaHCO3, 1%SDS). To reverse crosslinks, samples were supplemented to 300mM NaCl, treated with RNaseA (Roche) then incubated for ~8h at 65°C. Proteinase K (Genaxxon) was added and samples incubated at 55°C for 1h. DNA was purified using the MiniElute PCR purification kit (Qiagen). Real-time qPCR analysis to determined percent input bound at known GR target loci was carried out on a LightCycler 480 System using SYBR Green Master Mix (Roche). Primers used are presented in (Table 2.1). For sequencing ChIP DNA was prepared and amplified using Illumina adapters and Tru-Seq multiplex primers then sequenced using a HiSeq-2500 by Edinburgh Genomics.

For hMDM the same protocol was followed with the following differences. Material was prepared from 4 volunteers, treated, fixed for 7.5 minutes and lysed as above. It was sonicated to a fragment size of 400-600bp and the chromatin pooled, 25 million cells in total. This was split into 3 for the IP step and recombined at extraction. DNA was then isolated as above, split into 3 aliquots and blunt ended with Klenow (Roche), PNK (NEB) and T4 DNA polymerase (Roche). An overhanging A base was added using Klenow (-exo) (NEB) and Illumina adapters ligated overnight at 16^{o} C with T4 DNA ligase (NEB). The IP samples were

recombined after ligation and then split again into 7 aliquots. Libraries were amplified from each of these aliquots using Illumina Tru-seq multiplex primers and Phusion high-fidelity DNA polymerase (NEB) and the resulting material pooled and sequenced by Edinburgh Genomics on a HiSeq-2500.

Table 2.1 Primer sequences used for expression and ChIP RT-qPCR

Expression	forward	reverse
mouse		
Fkbp5	GGACCACGCTATGGTTTTGG	CTCTTTCACGATGGCAGCCT
Klf4	CGTTGACTTTGGGGCTCAGG	ACGCGAACGTGGAGAAGGAC
Wee1	CCTCGGATCCCACAAGTGCT	TGCTTCACCAGCTCCATTGC
Ypel5	GGCGCCACTGGTAGAGCATT	CCAGTGAGCATGACCCGATCT
Irf2	GCCGGTGGAACGGATGCGAA	CCGCATGCATCCAGGGGATCT
Dio2	GGGCTGCGCTGTGTCTGGAA	GGCCCCATCAGCGGTCTTCT
Ccl2	CGGCTGGAGCATCCACGTGTT	GAGTAGCAGCAGGTGAGTGGGG
Cdc42ep3	CCTCCGGGCAGAAGCTAGGA	GGGTCTTTCCGGAGAGCCAGTTA
Tlr7	TCCTCCACCAGACCTCTTGATTCCA	TCTTCCGTGTCCACATCGAAAACAC
Cdkn1c	ACTGCTGCGGCCAATGCGAA	CAGACGTTTGCGCGGGGTCT
Ednrb	AGTGCATGCGCAATGGTCCC	GGCCAGTCCTCTGCGAGCAA
F13a1	AGAGCACCCTCTCAGGAGCACA	TTATTGGGCGGGACTGCTCGC
human		
PDK4	TGCCTGTGAGACTCGCCAACA	TCCACCAAATCCATCAGGCTCTGT
CEBPD	GACAGCCTCGCTTGGACGCA	TCGTAGAAGGGCGCAGGCTC
MDM2	GGCGTGCCAAGCTTCTCTGTG	ACCTGAGTCCGATGATTCCTGCTG
BCL11A	CGCGCGACGGTGTGAAGTTA	TGGAGCTCCCAACGGGCCAT
MXD1	GGATCCGGATGGACAGCATC	GTCCGTGCTCTCCACGTCAA
EHD1	CGTTTGGCAACGCTTTCCTC	GGGGGTGTCGATGATGCTG
ADORA3	TCGCTGTGGACCGATACTTGCG	TAGAATGCACCCAGGGAGCCCA
HMGN4	CCTCGGACGGCCACGAGAC	TTCGCAGGTGGCTTGAGCAGT
CCL4	GCTGCCTTCTGCTCTCCAGC	AAAAGCAGCAGGCGGTGGGA
TLR7	GCTCTGCTCTCTTCAACCAGACCT	AGGAAACCATCTAGCCCCAAGGA
HIF1A	GCGGCGCGAACGACAAGAAA	TCGCCGAGATCTGGCTGCAT
DOCK10	GACAACGTTCCCTTGGAGCA	CCACCTCCACTGTGGGTTCTGT
DNA - ChIP	forward	reverse
mouse		
Fkbp5 +65kb	GCCAAGTTCAGCTGTGCAAT	TGCCAGCCACATTCAGAACA
Dusp1 -27kb	GGCTTTGAGCTCACTTCCTG	CTGGGTCCACTTTCCCACTA
Actb promoter	CTAGCCACGAGAGAGCGAAG	CGCGAGCACAGCTTCTTT
human		
FKBP5 +88kb	TAACCACATCAAGCGAGCTG	GCATGGTTTAGGGGTTCTTG
PER1 +500bp	CCAGGGGAAAAGGGAAGGTT	TCAGCCCACTTCGGACTAGA
ACTB promoter	AGGGCAGTTGCTCTGAAGTC	CTGCAGAAGGAGCTCTTGGA

2.1.5 Single cell RT-qPCR

This protocol uses the Cells Direct One-Step RT-PCR Kit (Invitrogen).

Cells were harvested, resuspended in PBS and sorted into wells of a 96 well plate using a FACSAria (BD Biosciences) by Roslin Institute imaging services. Three wells received 1000 cells, three 100 cells and three 10 cells for reference. The rest of the wells received a single cell. Plates were immediately snap frozen on dry ice and stored at -80.

To generate cDNA each well received: 5ul 2x reaction mix, 0.2ul Superscript III RT/Platinum *Taq* mix (with RNaseOUT Ribonuclease inhibitor), 2.5ul primer mix containing 20nM of each gene specific primer to be used in the downstream qRT-PCR assays, 1.3ul nuclease free water (Ambion). The plate was then placed in a G-Storm PCR machine and amplified using the following conditions: 50°C for 15 minutes (cell lysis and reverse transcription), 95°C for 5 minutes (inactivates superscript and activates platinum *Taq*), followed by 22 amplification cycles of 95°C for 15 seconds , 60°C for 4 minutes. The resultant cDNA was stored at -20.

2.1.6 3D DNA FISH

2.1.6.1 Bacterial culture

Genomic clones were supplied by BacPac Resources Centre at the Children's Hospital Oakland Research Institute (http://bacpac.chori.org) . Fosmid clones are listed in Table 2.2.

Bacteria from stab cultures or frozen glycerol stocks were streaked out onto LB agar to form single colonies and grown overnight at 37°C**;** cooled melted agar was supplemented with chloramphenicol 25ug/ml prior to being poured.

To prepare DNA a single colony was picked from an LB plate and used to inoculate 5ml LB broth supplemented with chloramphenicol 12.5ug/ml. Cultures were then incubated with shaking at ~300rpm (InnOva 4230 incubator, New Brunswick Scientific) at 37°C overnight with a 5:1 air to liquid ratio.

Table 2.2 Fosmid clones used for DNA FISH (co-ordinates from mm9 genome assembly).

Locus	Clone	Chromosome	Start	End
Fkbp5	WI1-1951C9	17	28621896	28660104
	WI1-980F19	17	28504480	28545426
Tmod1	WI1-2441L4	4	46121795	46162130
	WI1-552C3	4	45995494	46038724
Ms4xxx	WI1-1714F1	19	11344410	11380699
	WI1-2794B24	19	11607184	11647412

2.1.6.2 Glycerol stocks

Glycerol stocks of bacteria were prepared by adding glycerol to a concentration of 40% v/v to 1ml of an overnight culture and stored frozen at -80°C

2.1.6.3 Preparation of fosmid DNA from overnight culture

Fosmid DNA was extracted using an alkaline-lysis miniprep. Approximately 3mL of cultures were pelleted at 16,000g for 30s then resuspended in GTE buffer (50mM glucose, 25mM Tris pH8, 10mM EDTA +10mg/ml lysozyme) for 5 minutes before addition of 400ul of ice cold lysis buffer (0.2M NaOH, 1% Sodium Dodecyl Sulphate) and incubation on ice for 5 minutes. 300ul of acetate buffer (3M potassium acetate, 11.5% glacial acetic acid (v/v)) was added, and the preparation incubated on ice for a further 5 minutes. The flocculent precipitate was centrifuged at 16,000g for 5 minutes at 4°C and the clear supernatant was removed to a fresh eppendorf. Phenol:chloroform extraction was then performed by adding an equal volume of phenol-chloroform to the sample, centrifuging at 16,000g for 3 minutes, and removing the top layer. The DNA was precipitated with an equal volume of isopropanol and pelleted by centrifugation for 15 minutes at 4°C at 16,000g. The

DNA was washed with 70% ethanol, repelleted, resuspened in TE and stored at -20°C.

2.1.6.4 Labelling of fosmids

Fosmids were labelled using biotinylated dTTP or digoygenin dUTP by nick translation. 500ng to 1ug of fosmid DNA was prepared as in section 2.1.6.3 and then incubated with 2ul Nick Translation Salts(0.5M Tris pH 7.5, 0.1M $MgSO_4$, 1mM DTT, 0.5mg/ml BSA fraction V (Sigma)), 1ul 1:20 DNaseI in ice cold dH20 (Roche), 1ul T4 DNA Polymerase (Roche) 2.5ul each of dATP, dCTP, dGTP (0.5mM) and either 2.5ul biotin-16-dUTP (Roche) or 1.5ul digoxygenin-dUTP (Roche) and 1ul dTTP for biotin or digoxygenin labelling repsectively. The incubation was for 90 minutes in a 16°C waterbath. The reaction was stopped by adding 2ul 20% SDS and 3ul 0.5M EDTA and made up to 90ul with TE. It was then processed through a QuickSpin G50 sephadex column (Roche) as per manufacturers instructions.

Effective labelling was detected using streptavidin-alkaline phosphatase or anti-digoxygenin alkaline phosphatase on nitrocellulose filters prepared by soaking in 20x Saline Sodium Citrate (per litre for 20x solution, NaCl 175.3g, $Na_3C_6H_5O_7$ 88.2g, prepared by MRC HGU technical services, SSC) and then dried. Standard concentrations of biotin and dig labelled DNA were spotted onto filters alongside 4 dilutions (1:500-1:10,000) of the prepared labelled DNA. This was then cross-linked onto the filter using 1500mJ UV irradiation in a UV500 cross-linker (Hoefer). The filter was washed briefly in 0.1M Tris pH7.5 0.15M NaCl then incubated for 30minutes at 60°C in the same with Bovine Serum Albumin (Sigma) 3% (w/v). The filter was transferred to fresh buffer without BSA with the addition of 1% of the listed detectants above and incubated for 15minutes at room temperature. The filter was then washed twice in the same buffer then briefly in 0.1M Tris pH 9.5. The labelled DNA was detected using Vector Labs BCIP/NBT kit according to manufacturers instructions. Concentrations were assessed by comparison with the standards.

2.1.6.5 FISH procedure

Slides prepared as described in section 2.1.2 were treated with RNaseA at 100mg/ml for 1hour at 37°C then washed in 2xSSC and dehydrated thorugh 70%, 90% and 100% ethanol for 2 minutes each and air dried. Slides were then incubated for 5 minutes at 70°C and denatured in 70% formamide in 2xSSC, pH 7.5, for 30 minutes at 85°C. Slides were then transferred to ice cold 70% ethanol, dehydrated as previously then air dried.

80ng of labelled probe was used per slide, with 12µg Cot1 DNA (Invitrogen) and 10µg sonicated salmon sperm, resuspended in hybridization mix (50% deionised formamide(v/v), 10% dextran sulphate (v/v), 1% Tween 20(v/v) in 2xSSC) and denatured at >70°C for 5 minutes. The probes were then pre-annealed at 37°C for 15 minutes and hybridised to the prepared slides at 37°C in a humid chamber overnight.

Slides were washed for 4x3 minutes in 2xSSC at 45°C, then 0.1xSSC at 60°C, then transferred to 4xSSC/1% Tween 20. Slides were incubatd for 5 minuted in 4xSSC, 1% Marvel. Digoxygenin labelled probes were detected using FITC anti-dig Fab fragments raised in sheep(Roche) followed by FITC-conjugated anti-sheep(Vector). Biotin labelled probes were detected by Texas Red conjugated avidin(Vector), biotinylated avidin(Vector), then again by Texas Red conjugated avidin. Each incubation was for 30 minutes. Slides were washed between each incubation for 3x2 minutes in 4xSSC/1% Tween 20 at 37°C. A final wash was performed in 4xSSC/1% Tween 20 with DAPI 0.5µg/ml and slides were mounted in Vectashield.

2.1.6.6 Image capture

Images were captured using a Zeiss Axioplan 2 upright microscope with a PIFOC® collar for capture of z stacks. Acquisition and deconvolution of images was carried out using Volocity software (PerkinElmer).

2.2 Data Analysis

Microarray and sequencing data have been deposited in GEO, series GSE61881 to be made publically available on publication of the associated research manuscript.

2.2.1 Expression data

Analysis was performed using R/Bioconductor packages 'arrayQualityMetrics', 'affy' and 'limma' (Gautier et al., 2004; Kauffmann et al., 2009; Smyth, 2005). Expression values were generated using rma. Further exploratory expression analysis used unlogged expression values prefiltered for low expressed probesets as input for the graphical correlation based tool *Biolayout Express*^{3D} (Theocharidis et al., 2009). A range of correlation coefficients and MCL values was used to determine an optimal graph structure from which clusters of genes were then read. Clusters were then manually curated to remove artefacts. Genes from these lists were selected across a range of fold-changes for analysis by RT-qPCR as described above and a threshold drawn at log2 fold change where all tested genes were confirmed. To limit loss of genes with extreme profiles – and hence less likely to cluster - genes reaching $\log_2$ fold change >1.5 using a conventional analysis were also retained if the corresponding expression profile was consistent with a response across all replicates. Orthologues were identified using the HGNC Comparison of Orthology Predictions (HCOP) tool (Gray et al., 2013).

2.2.2 Single cell PCR

For each gene (*Fkbp5,* target; *Gapdh*, reference) the quantity of material present in each well of the cDNA plate was then assessed in triplicate across 3 different plates (e.g. for 2 genes and one 96 well cDNA plate this is therefore 6 x 96 well plates) using the Lightcycler 480 System and SYBR Green master mix (Roche). Wells from the cDNA plate that returned an inconsistent amplicon melting temperature or concentration. Analysis then correlated the relative amount of target vs reference for each well, normalising to the value given by material generated from 10 cells.

2.2.3 Promoter Analysis

Promoters were defined as -300, +100bp of the transcription start sites (TSS) recently described by the FANTOM5 consortium(Forrest et al., 2014). Where multiple TSSs are known, any overlaps were concatenated. Average sequence

conservation scores (phastCons) for promoter regions were extracted and enriched motifs identified using HOMER (Heinz et al., 2010).

2.2.4 Comparison to GWAS results and inflammatory genes

The GWAS catalogue (Hindorff et al., 2009) was accessed via http://www.genome.gov/gwastudies/ and manually edited to retain only hits with association to inflammatory / immune conditions (including type II diabetes, 153 unique SNPs) associations (1408 unique SNPs). The intersection of reported genes was assessed by fold change above a background distribution generated using permutation (100,000) of random gene sets. Significance of the difference was assessed using Pearson's chi-squared test. The intersection of risk SNPs and promoters was ascertained using BEDtools (Quinlan and Hall, 2010).

2.2.5 Functional Annotation

Lists of functional terms from multiple publically available databases were generated using HOMER (Heinz et al., 2010), filtered using a threshold of –log p-value 6.5, then manually curated to remove duplicate terms.

2.2.6 ChIP-sequencing

Sequencing quality was assessed with FastQC(Andrews, 2010) and sequence from adapters removed using trimmomatic (Bolger et al., 2014). Paired end reads were aligned to mm9 or hg19 by Bowtie2 (Langmead and Salzberg, 2012) using default options (-D 15 -R 2 -L 22 -i S,1,1.15). Downstream analysis was performed using HOMER(Heinz et al., 2010), including creation of bedGraph files for visualization, peak calling and annotation. Peaks were celled by comparison with the sequenced input sample for each experiment as a measure of background. For the mBMDM data after confirming congruence (86% peak overlap), data from two independent replicates were combined. Publically available sequencing data for comparisons was accessed via NCBI GEO for Uhlenlaut et al (GSE31796) and Ostuni et al. (GSE38379).

The number of observed intersections of our GR bound sites with reported sites of PU.1 binding in unstimulated mBMDM from Ostuni et al. was compared to

to the median intersection that occurred in 1,000 genome permuted GR peak locations. Significance was assessed using Pearson's chi squared test.

To compare the locations of regulated genes with GR peaks the proportion of peaks within a given genomic interval of the TSS of a regulated gene was calculated. The enrichment of regulated genes with a GR peak was calculated as the ratio of the proportion of regulated genes that contained a GR peak within a given genomic interval to the proportion of regulated genes that did not contain a GR peak within the same interval. The significance of these results was estimated by comparing them to the 95% confidence interval of 1,000 replicates of genome permuted GR peak locations. These two analyses were performed with assistance from Robert Young, MRC HGU.

2.2.7 Interspecies and evolutionary analysis

The role of species-specific GR binding was assessed by counting the number of species-specific regulated genes with a bound peak within a 1Mb window of the TSS and comparing this to the number of genes with a bound peak within 1 Mb where only the orthologues in the alternate species was regulated in our data. Where multiple orthologues were present this analysis was run 'all to all'.

Peaks were compared between species using *liftOver* provided by UCSC to get the coordinates of those peaks falling within syntenic blocks. Peaks with a greater than 25bp overlap were assigned as shared. To compare the enrichment of motifs in shared vs. aligned non-bound peaks we performed motif finding using HOMER as above, using the non-bound as background.

Insertions and deletions were called by comparison with dog (CanFam2), horse (EquCab2), cow (BosTau6) and pig (SuScr3) genomes If the sequence underlying a peak could be aligned to at least one of this species the peak was defined as being deleted, if not then it was called as a insertion. Human GR sites were assigned as deletions in mouse.

GERP scores for the locations of bound GR motifs in both human and mouse were extracted from the UCSC genome browser (Kent et al., 2002). These scores

have been calculated by running the GERP++ algorithm on the 36-way mammalian genome alignments (Davydov et al., 2010).

Analyses in this section (2.2.7) were performed following discussion with and with assistance from Robert Young, MRC HGU.

2.2.8 Analysis of 3D FISH data

Deconvolved images (section 2.1.6.6) were analysed using Volocity software (PerkinElmer). For each image stack paired-probes within nuclei were manually identified by scrolling through the layers. The software then measured the distance between the probes. Nuclei with more than two pairs of probes or poorly resolved probes were excluded. The distance distributions were then compared using an unpaired Wilcoxon rank sum test in R.

Chapter 3: The transcriptional response of macrophages to glucocorticoids

3.1 Introduction

As discussed in the introduction (Section 1.3.2), by contrast to other immune cells in the mouse, including B and T cells and classical dendritic cells, macrophages express high level of glucocortocoid receptors and are very sensitive to glucocorticoids (GC). They are a major target for the anti-inflammatory actions of GC, accordingly, there have been previous studies of the transcriptional response to GC in a number of different cellular systems. However the data generated is not sufficient to draw integrated conclusions.

In one study of mBMDM high dose (1uM) dexamethasone was used, the cells were starved of both serum and growth factor (CSF1) and the response was measured only at a single late time point (16 hours) (Uhlenhaut et al., 2013). A more recent study of mBMDM retained both serum and CSF1, but investigated only a single early time point (Chinenov et al., 2014). In humans single time point genome wide expression data for peripheral blood derived monocytes (PBMC) (Ehrchen et al., 2007), PBMC differentiated with GM-CSF and treated with high dose dexamethasone (Xue et al., 2014) or from PBMC treated with GC during differentiation (van de Garde et al., 2014) is available.

The aim of the present study was to compare and contrast the responses of mouse and human macrophages to GC under comparable conditions. Inter species comparison of macrophages is not straightforward. The most common cell culture models of primary human and mouse macrophages are peripheral blood and bone marrow respectively, but they are not directly comparable. For example there are known species differences in the response to CSF1, which produces a proatherogenic signal in human macrophages (Irvine et al., 2009). Comparison between ostensibly more similar types does not necessarily provide the solution. Mouse monocyte

derived macrophages are only available in very small numbers, severely limiting the assays possible. They may also differ from human monocyte subsets in maturation and differentiation (Ingersoll et al., 2010). Human bone marrow derived myeloid cells can be obtained but do not behave as their mouse counterparts (Hume, Stephens, Warren, & Curtin, 1985). A previous report compared the responses of hMDM and mouse BMDM to LPS (Schroder et al., 2012) . The differences in LPS-induced gene expression were clearly associated with promoter sequence variation, and the species-specific differences were confirmed in pigs, where both BMDM and MDM can be obtained readily. In this respect, pigs are more similar to man at both the genomic sequence level and in their innate immune responses (Kapetanovic et al., 2012; Schroder et al., 2012). Hence, the limitations of the cellular systems can partly be overcome if differences in transcription can be linked to differences in regulatory elements.

This chapter describes a comprehensive assessment of the response in both species using well-described and widely-used cell culture models, mBMDM and hMDM, as in the above previous comparative analysis (Schroder et al., 2012). Dexamethasone was chosen as the agonist for its high affinity for GR and relatively low affinity for the mineralocorticoid receptor (Lan et al., 1982). Global gene expression was measured using microarrays at 6 time points over 24hours after treatment with dexamethasone 100nM, to identify both initial direct targets of GC and the downstream secondary consequences.

3.2 The response of mouse bone marrow derived macrophages to dexamethasone

Primary mBMDM were treated with 100nM dexamethasone and harvested after 0, 1h, 2h, 4h, 10h, and 24h. RNA was extracted and analysed using industry standard Affymetrix expression arrays. From the raw expression data, after filtering for low-expressed and low variance probes, lists of regulated transcripts were confirmed by

RT-qPCR to produce a high confidence set of regulated transcripts (Figure 3.1 and methods). 264 induced and 102 repressed genes were identified and filtered to 160 high confidence and validated induced and 50 repressed over the full 24h time series (Figure 3.2, full list in Appendix 1). Induced genes responded with faster kinetics: 10%, 32% and 62% within 1, 2 and 4 hours respectively, compared to the repressed gene set (0%, 4% and 14% and the same time points). The robust induced gene set included several known GR targets *Dusp1* (Tchen et al., 2010)*, Tsc22d3, Fkbp5* and *Per1* (Reddy et al., 2009)). As expected from earlier studies of mBMDM (Hume and Gordon, 1984) the repressed gene list contains urokinase plasminogen activator (*Plau*) (Stacey et al., 1995). Since *Plau* is a target of sustained MAP kinase signalling (D'Alessio and Blasi, 2009), the repression may be an indirect consequence of the induction of the MAPK inhibitor *Dusp1*. Eight annotated transcription factors were amongst the induced gene set, including four (*Fos, Hivep2, Klf4, Ncoa5)* that were induced within 2 hours and that could contribute to the downstream regulatory cascade (Table 3.1). Functional annotation was not highly-informative, with enrichment for nuclear processes, apoptosis and development in the early-induced set and cell surface immune response, phagocytosis, migration and cytoskeleton amongst the late responders. This is addressed further in section 3.4. In overview, a greater number of genes increase the amount of stable mRNA in response to GC than decrease, when measured in steady state mouse macrophages. A subset of these induced genes change rapidly (before 1h).

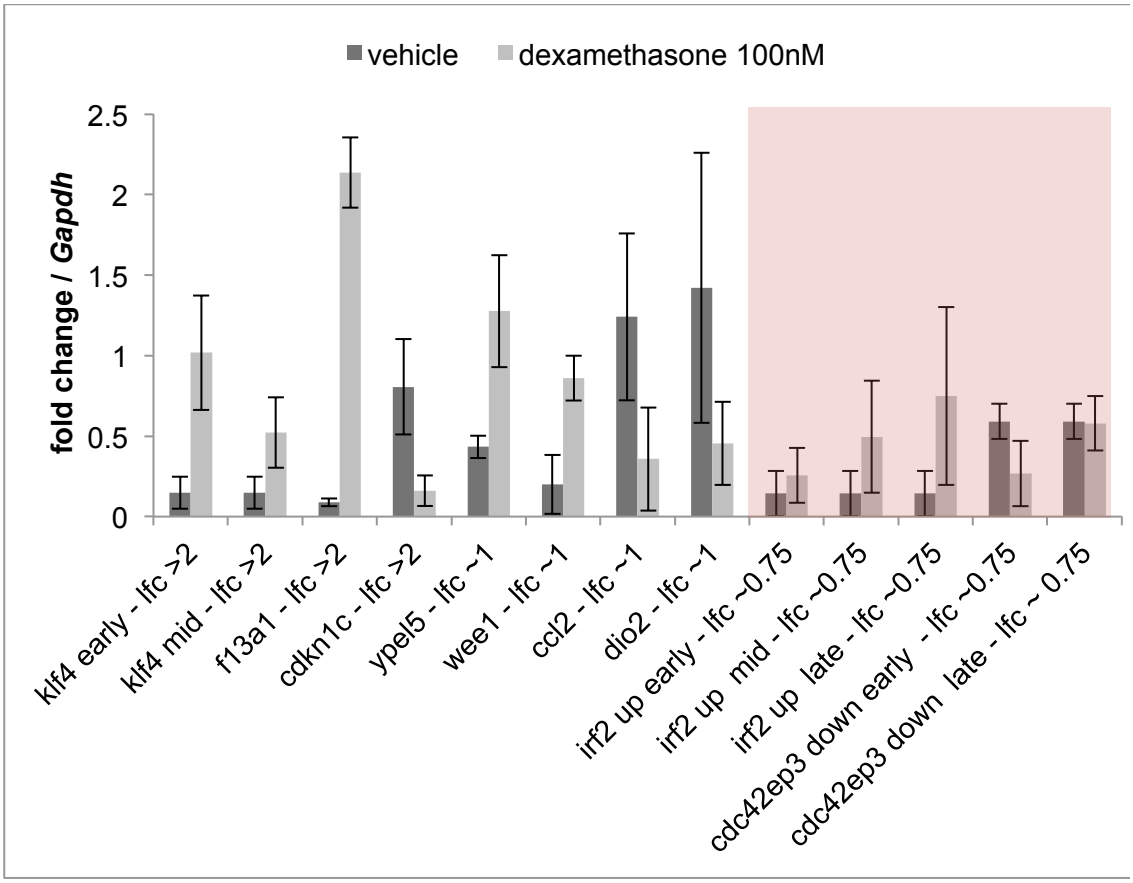

Figure 3.1 Validation and thresholding of microarray data.

From the expression arrays genes were selected to represent a range of expression levels and time points to be tested using RT-qPCR. For early, mid and late time points examples of strong (>2 log fold change in the expression microarray data) medium (~1 log fold change) and weak (~0.75 log fold change) responding genes were selected. Light red box represents the threshold value from the microarray data chosen for exclusion from downstream analysis. Error bars represent 2 x standard error of the mean for n=3 biological replicates. Lfc = $\log_2$ fold change.

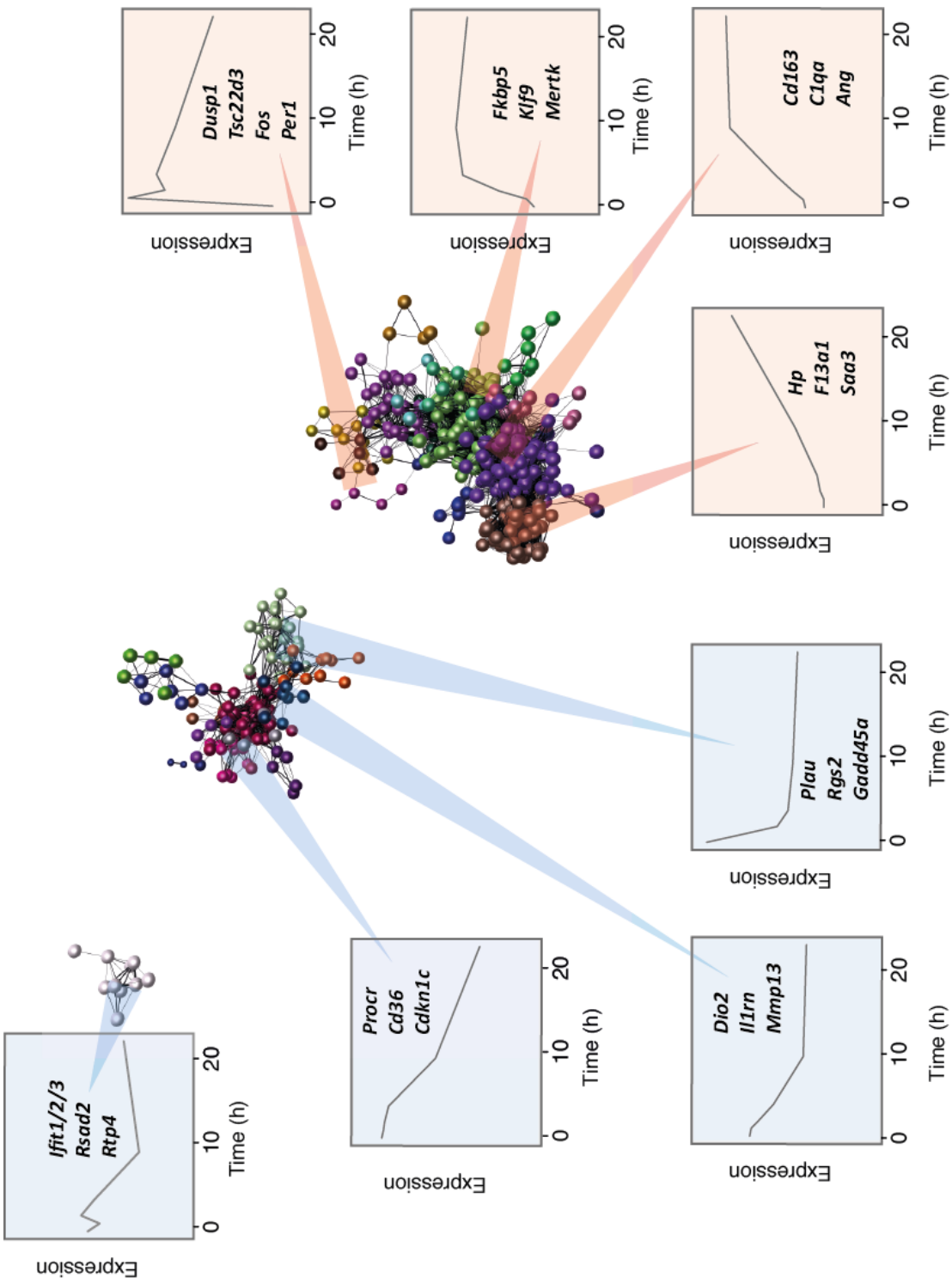
Dusp1
Tsc22d3
Fos
Per1
Fkbp5
Klf9
Mertk
Cd163
C1qa
Ang
Hp
F13a1
Saa3
Plau
Rgs2
Gadd45a
Dio2
Il1rn
Mmp13
Procr
Cd36
Cdkn1c
Ifit1/2/3
Rsad2
Rtp4
Expression
Time (h)
0
10
20

Figure 3.2 Expression response over 24h of mBMDM to 100nM dexamethasone

A Pearson correlation matrix was generated from the raw mBMDM microarray expression data, measured at 0, 1h, 2h, 4h, 10h, 24h. A graph was drawn using only those node-node relationships r>=0.89. Each node represents a probe set from the array and each edge represents a correlation. The graph was clustered using a MCL inflation value of 2.3 and each cluster assigned a different colour. Inset graphs show average expression profiles for the indicated clusters with representative gene symbols given. Light orange = induced, light blue = repressed.

Table 3.1 Transcription factors regulated by 100nM dexamethasone in mBMDM

*=Regulated by 2h

Induced
*Fos**
*Hivep2**
*Klf4**
*Ncoa5**
Jdp2
Klf9
Tcf7l2
Zbtb16
Repressed
*Egr2**

3.3 The response of human monocyte derived macrophages to dexamethasone

Microarray analysis of the response of hMDM to GC identified 225 induced and 125 repressed genes meeting the filtration threshold (Figure 3.3 and Appendix 2). As for mBMDM, the induced genes responded faster: 11, 30 and 70% changing within 1, 2 and 4 hours respectively (2, 14, and 47% for the repressed set at the same time points). Known glucocorticoid targets *DUSP1, FKBP5, PER1* & *TSC22D3* were induced by GC in the human cells, alongside the expected repression of *PLAU.* There were multiple transcription factors represented, ten induced and 4 repressed within 2h (Table 3.2).

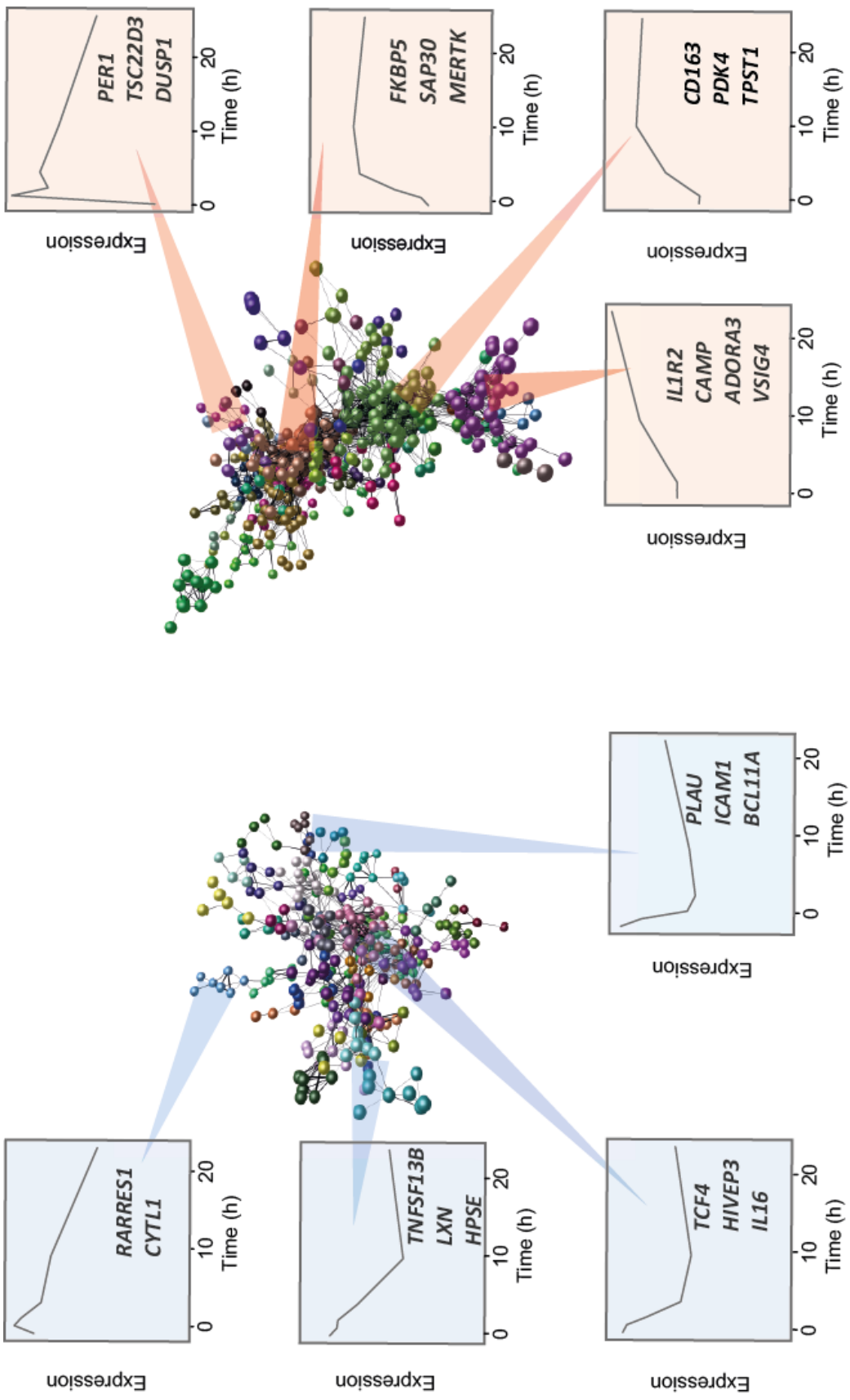
PER1
TSC22D3
DUSP1
FKBP5
SAP30
MERTK
CD163
PDK4
TPST1
IL1R2
CAMP
ADORA3
VSIG4
PLAU
ICAM1
BCL11A
RARRES1
CYTL1
TNFSF13B
LXN
HPSE
TCF4
HIVEP3
IL16
Expression
Time (h)
0
10
20

Figure 3.3 Expression response of hMDM to 100nM dexamethasone.

A Pearson correlation matrix was generated from the raw mBMDM microarray expression data, measured at 0, 1h, 2h, 4h, 10h, 24h. A graph was drawn using only those node-node relationships r>=0.91. Each node represents a probe set from the array and each edge represents a correlation. The graph was clustered using a MCL inflation value of 2.0 and each cluster assigned a different colour. Inset graphs show average expression profiles for the indicated clusters with representative gene symbols given. Light orange = induced, light blue = repressed

Table 3.2 Transcription factors regulated by 100nM dexamethasone in hMDM.

*=Regulated by 2h

Induced	Repressed
*FOS**	*CIITA**
*FOXO3**	*MXD1**
*JDP2**	*IRF1**
*KLF4**	*BCL3**
*KLF7**	*ATF5*
*KLF9**	*RELB*
*NFIL3**	*TCF7L2*
*CEBPD**	*TEF*
*MYC**	*HIVEP1*
*GADD45A**	
ELK1	
FOXO1	
HMGB2	
THRB	
ZBTB16	
OLIG1	
RUNX2	

3.4 The expression response is different and is not linked to promoter variation

Based upon the HGNC Comparison of Orthology Predictions tool (Gray et al., 2013) there were 228 mouse orthologues for 225 GC-induced hMDM genes and 131 orthologues for 125 repressed genes. The reciprocal analysis produced 157 human orthologues of 150 mBMDM induced and 55 orthologues of 50 mBMDM repressed genes. From amongst this set of robustly-regulated genes, only 33 induced and 3 repressed genes were shared by the two species (Figure 3.4A and Table 3.3). Genes regulated in the same way in both species genes were not regulated more strongly than the complete set for hMDM (median specific 1.8 vs. shared 2.0, p=0.07, Wilcoxon rank sum) although there was a slight difference in the case of mice (median 1.54 specific vs. 2.12 shared, p = 0.0009, Wilcoxon rank sum). There was also no difference in the time course of response for conserved genes; for hMDM 15/51 (29%) genes induced early are shared compared to 38/226 (17%) of all induced genes (p=0.07, Pearson's chi squared), the mBMDM equivalent figures are 9/45 (20%) and 38/160 (24%) (p=0.74, Pearson's chi squared).

Comparison of the functional categories enriched in each species showed some differences. As stated above in mBMDM functional annotation of the induced genes showed enrichment for nuclear processes, apoptosis and development in the early-induced set and cell surface immune response, phagocytosis, migration and cytoskeleton amongst the late responders. In hMDM there was substantial overlap in the terms. However, terms that were not found in mouse included adipogenesis, FOXO and insulin signalling, MAPK cascade, transcriptional misregulation in cancer and development. The immune pathways IL-10 production, NFκB, TNF, NOD-like receptor and rheumatoid arthritis were enriched in the hMDM-repressed set. Shared and differential terms are shown in Figure 3.5.

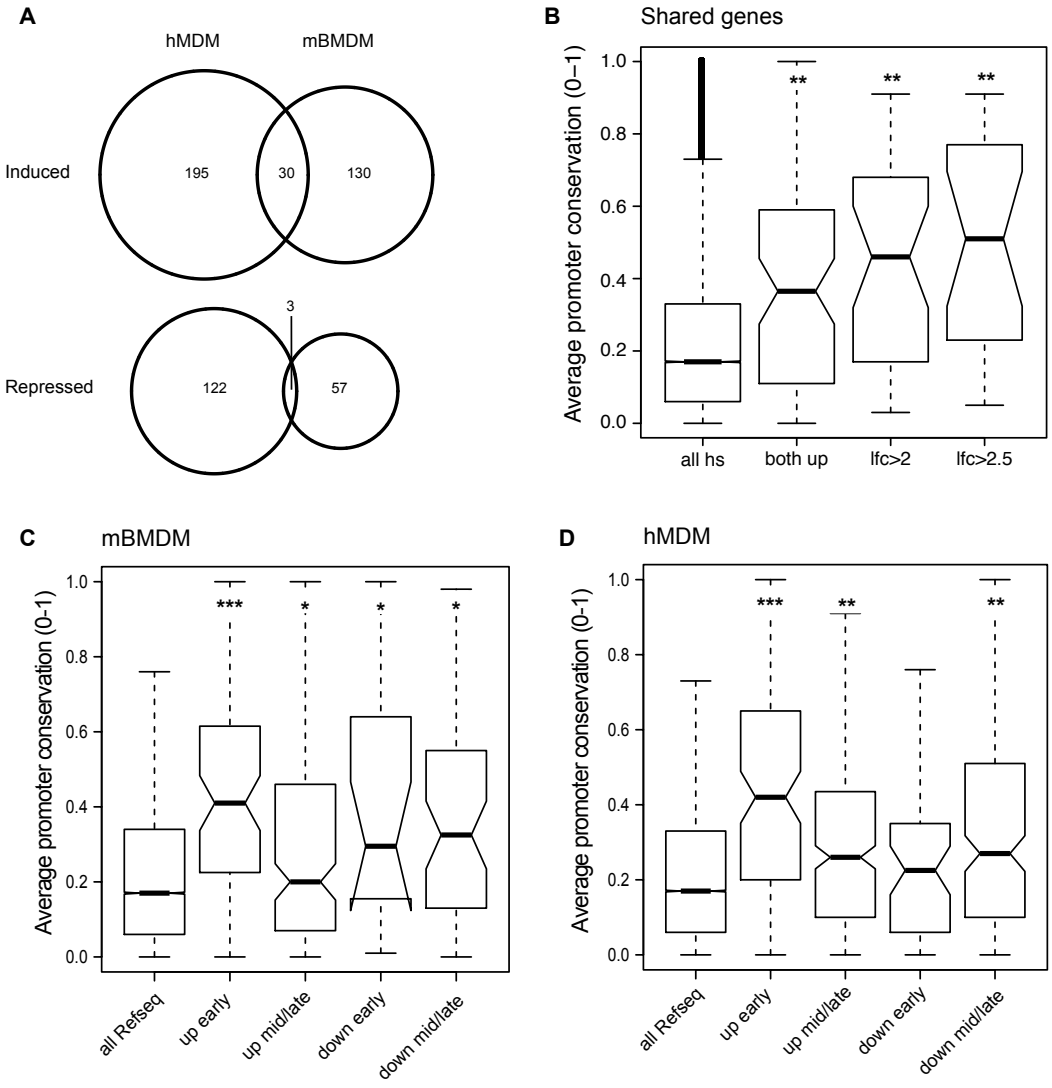

Figure 3.4 The expression response to dexamethasone is divergent despite promoter sequence conservation.

A Intersections between regulated orthologues in mBMDM and hMDM. **B** Average promoter (-300,+100bp of TSS) sequence conservation scores (phastCons) for all shared genes and subsets of increasing GC responsiveness. All human promoters are shown as background (all hs). **C&D** promoter sequence conservation for all genes regulated in mBMDM and hMDM respectively, categorised by response and kinetics. All Refseq promoters shown as background. Conservation scores from phastCons. *** = p-value <1x10-10, ** = p-value <1x10-4, * = p-value <0.05, Wilcoxon rank sum.

Induced

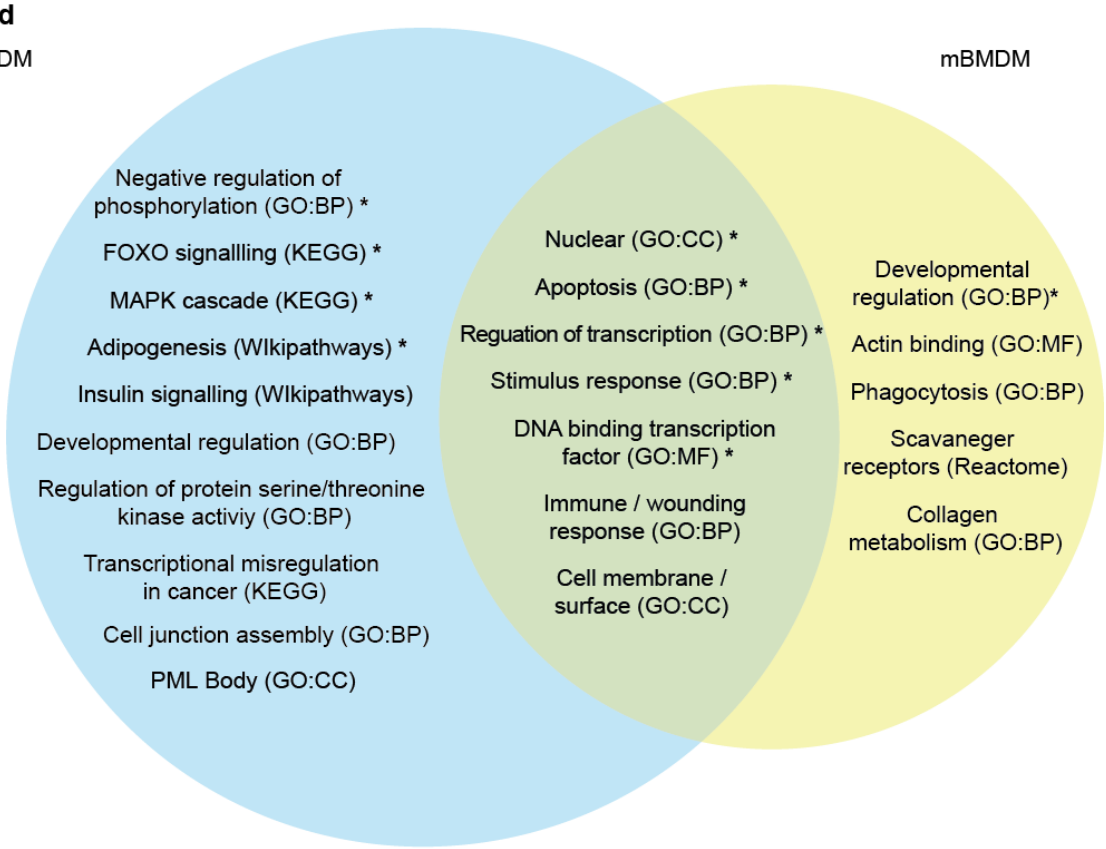

Repressed

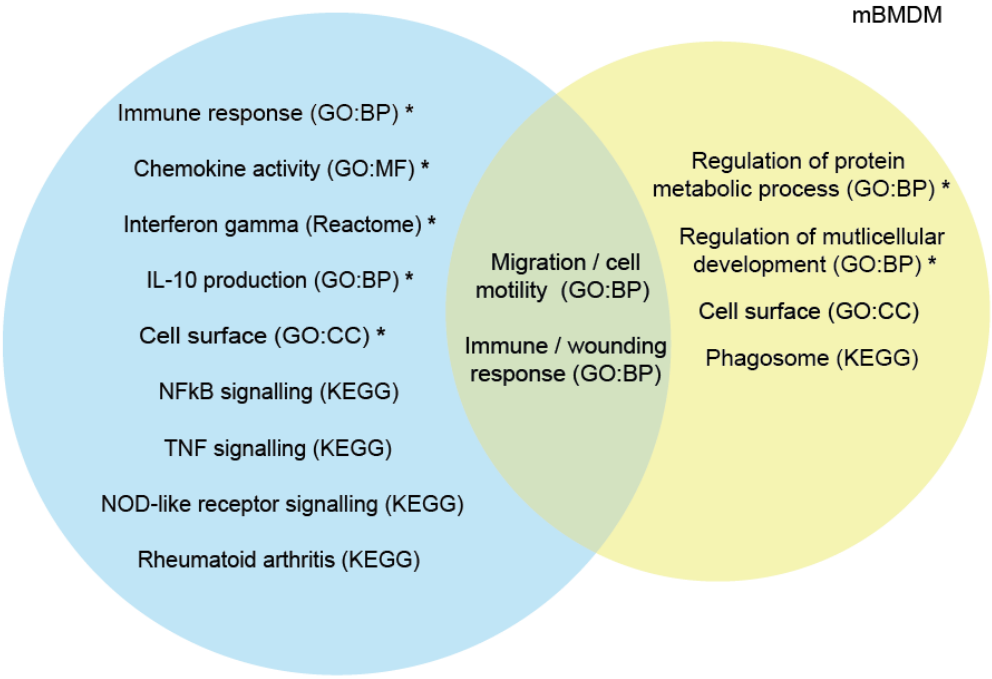

Figure 3.5 Enriched functional annotation terms for the response of macrophages to dexamethasone.

Multiple public databases of functional annotation were interrogated and significantly enriched terms are shown for induced (top), and repressed (bottom) gene sets. Data from mBMDM data are in yellow and hMDM in blue. Duplicate terms have been removed. All value terms shown are significant to at least -log p-value > 6.5. ***** = Enriched in genes regulated 0-2h. Abbreviations: KEGG = Kyoto Encyclopedia of Genes and Genomes, GO = Gene Ontology, BP = Biological Process, MF = Molecular Function

Table 3.3 Gene regulated in the same way in mBMDM and hMDM by dexamethasone

Up			Down
B3GNT5	*FILIP1L*	*MERTK*	*PLAU*
CYTIP	*FKBP5*	*MMP19*	*IFIT1*
DDIT4	*GLUL*	*MS4A6A*	*NR1D2*
DUSP1	*TSC22D3*	*P2RY12*	
FOS	*FPR1*	*PIK3IP1*	
KLF4	*GPR126*	*ZBTB16*	
PER1	*JDP2*	*MS4A4A*	
SLA	*KLF9*	*P2RY13*	
SSH2	*LDLRAD3*	*THBS1*	
CD163	*MAP3K6*	*PSTPIP2*	

Many species-specific differences in LPS responsiveness of individual genes could be attributed to highly divergent promoters between mice and man (Schroder et al., 2012). In GC regulated genes there was higher average promoter conservation when the GC target genes were regulated in both species (p-value = $1.32x10^{-5}$, Wilcoxon rank sum) (Figure 3.4B) and for the genes in each species that responded most rapidly to GC (3.4C&D). However overall, despite their discordant regulation between the species, the promoter regions of all GC-inducible genes had relatively high sequence conservation (Figure 3.4C&D).

Global conservation of sequence may not capture more subtle changes to information content within a given sequence. Specific motifs or regulatory elements may be gained or lost with only a marginal effect on the global conservation score but a substantial potential regulatory effect. To seek evidence of regulatory elements shared by GC-responsive genes in each species, the promoters (-300bp, +100bp of the TSS defined previously by CAGE analysis) (Forrest et al., 2014) were scanned for motifs associated with transcription factor (Heinz et al., 2010). Amongst the promoters of LPS-induced genes in both mouse and human there was clear enrichment for binding sites of many known inducible transcription factors, including NFkB and AP1 (Schroder et al., 2012). These sites were not enriched at the promoters of GC-induced genes. Comparing to all RefSeq promoters matched for GC content there was also no evidence of any motif, such as the GRE, that might be implicated in direct GR binding at the promoters of the GC responsive genes. Considering all induced genes in mBMDM only the *Cebpd* motif met stringent identification criteria for enrichment ($q<0.05$, Benjamini-Hochberg). No motifs reached significant enrichment in the promoters of early-repressed genes whilst late repression was marginally associated with TATA-box ($q = 0.052$) and p300 ($q=0.057$). In hMDM, promoters of rapidly induced genes showed no motif enrichments, but there was an overrepresentation of E-Box and TATA-Box motifs ($q=0.0469$) in the promoters of genes with delayed induction in response to GC. Early repression was associated with NFkB-p65 ($q=0.0006$), NF1 half-site ($q=0.0049$) and TATA box ($q=0.0337$) whilst late returned FOXO1 ($q=0.0065$), SREBP1 ($q=0.0123$), and multiple ETS motifs, including PU.1 ($q=0.0172$) (Figure

3.6A&B). Promoters may be divided by presence or absence of increased density of CG dinucloetides (CpG islands), with CpG island promoters tending to be broader with more than one possible initiation site whilst sharp, non CpG island promoters tend to be more lineage specific (Illingworth and Bird, 2009). Looking for motif enrichment in GC regulated CpG island and non CpG island promoters separately for mBMDM showed no motifs reaching significance in the CpG set but enrichment for ETS motifs including PU.1 in the non-CpG set (q=0.021 Benjamini-Hochberg, 2.1 fold enrichment). In hMDM GC regulated genes with CpG island promoters also showed no significant motif signature, whilst the non-CpG promoters had enrichment for ETS motifs (q=0.0219 Benjamini-Hochberg, 2.7 fold enrichment). In summary, there was no evidence of a consistent promoter-binding factor at GC-responsive genes in either species although non-CpG island promoters may have more reliance on the lineage defining ETS factor PU.1, consistent with their role in more tissue specific genes (Illingworth and Bird, 2009).

A Motifs enriched in promoters of genes regulated in hMDM by dexamethasone

Promoter subset	q-value	Motif
Up mid-late	0.0469	Atoh1
Up mid-late	0.0469	Ebox factor
Up mid-late	0.0469	TATA Box
Down early	0.0006	NFkB-p65
Down early	0.0049	NF1-halfsite
Down early	0.0337	TATA Box
Down mid-late	0.0065	Foxo1
Down mid-late	0.0123	Srebp1a
Down mid-late	0.0172	PU.1(ETS)
Down mid-late	0.0372	SPDEF(ETS)
Down mid-late	0.0372	Smad3
Down mid-late	0.0372	PU.1-IRF(ETS:IRF)
Down mid-late	0.0372	PAX5
Down mid-late	0.0372	STAT6
Down mid-late	0.0372	MafA

B Motifs enriched in promoters of genes regulated in mBMDM by dexamethasone

Promoter subset	q-value	Motif
Up (all)	0.046	Cepb
Down mid-late	0.051	TATA-box
Down mid-late	0.057	p300

Figure 3.6 Motifs over-represented in the promoters of dexamethasone regulated genes.

The promoters (-300bp to +100bp) of the high confidence sets of GC-regulated genes in **A** hMDM and **B** mBMDM were scanned for matches to known motifs. Motifs reaching a significance threshold of $q < 0.05$ were included (Benjamini-Hochberg).

3.5 Targets of glucocorticoids in human macrophages enrich for risk variants for inflammatory disease

Genes regulated by GC in human macrophages are candidates for involvement in inflammatory and metabolic disease and might therefore be implicated in genetic susceptibility. From the GWAS catalogue (www.ebi.ac.uk/gwas) I selected all loci with inflammatory or metabolic disease associations (1408 SNPs), including those defined as suggestive rather than fully genome wide significant in the original study. There was a significant enrichment: 48/350 GC regulated genes in hMDM have been reported to have an association with an inflammatory condition (3.7 fold over background, $p=1.1x10^{-5}$, Pearson's chi-squared, Table 3.4).

Table 3.4 Intersection between dexamethasone regulated genes in hMDM and reported GWAS hits for inflammatory disease

FOS	*SDC4*	*TFCP2L1*	*CXCL2*	*TNF*
ITPKC	*SLAMF1*	*SLC25A15*	*ICAM1*	*ZBTB46*
NFIL3	*SLC11A1*	*MYC*	*IL8*	*TAGAP*
PAPOLG	*SLC15A2*	*TNFAIP3*	*NFKBIE*	*SLAMF7*
GAB1	*TBC1D1*	*MET*	*NOD2*	*CD48*
GRB10	*TMEM39A*	*TMEM17*	*ASRGL1*	*ITGAL*
IL1R1	*C5*	*SOCS1*	*P2RX7*	*IRF1*
MERTK	*IL1R2*	*BCL11A*	*SLC29A3*	
PPM1L	*RGS1*	*CD83*	*TLR7*	
PRKCH	*CXCL1*	*CIITA*	*TNFSF15*	

Of the SNPs associated with GC-regulated genes 14 did not reach full genome wide significance in the original study and 9 were not reported in main article (Table 3.5). A similar analysis considering the specific genomic loci demonstrated enrichment for SNPs with reported associations to inflammatory conditions in the region of induced genes (Figure 3.7). Only 3% (43/1387) of this subset of GWAS catalogue SNPs map to promoters and only one SNP maps to the promoter of a GC regulated gene (rs1738074, Coeliac disease, *TAGAP*, repressed).

Table 3.5 Weak GWAS hits regulated by GC in hMDM

Abbreviations: N=Not in main text, Y=Yes, SUP = in supplementary materials

SNP	Symbol	Disease	Reported	PUBMEDID	First Author	Date
rs1008953	SDC4	Psoriasis	N	20953189	Stuart PE	2010
rs10243024	MET	Multiple sclerosis (severity)	N	19010793	Baranzini SE	2008
rs12540874	GRB10	Systemic sclerosis	Y	21779181	Gorlova O	2011
rs1738074	TAGAP	Celiac disease	Y	18311140	Hunt KA	2008
rs1738074	TAGAP	Multiple sclerosis	Y	22190364	Patsopoulos NA	2011
rs1957895	PRKCH	Rheumatoid arthritis	Y	22446963	Okada Y	2012
rs2230926	TNFAIP3	Rheumatoid arthritis	N	20453841	Kochi Y	2010
rs2252996	SLC29A3	Systemic lupus erythematosus	Y	23273568	Yang W	2012
rs3751143	P2RX7	COPD-related biomarkers	SUP	23144326	Kim DK	2012
rs3805236	GAB1	Asthma	N	21804548	Hirota T	2011
rs4781011	CIITA	Ulcerative colitis	N	20228799	McGovern DP	2010
rs6062314	ZBTB46	Multiple sclerosis	N	21833088	Sawcer S	2011
rs610604	TNFAIP3	Psoriasis	N	20953190	Strange A	2010
rs9290065	PPM1L	Kawasaki disease	SUP	22446961	Lee YC	2012

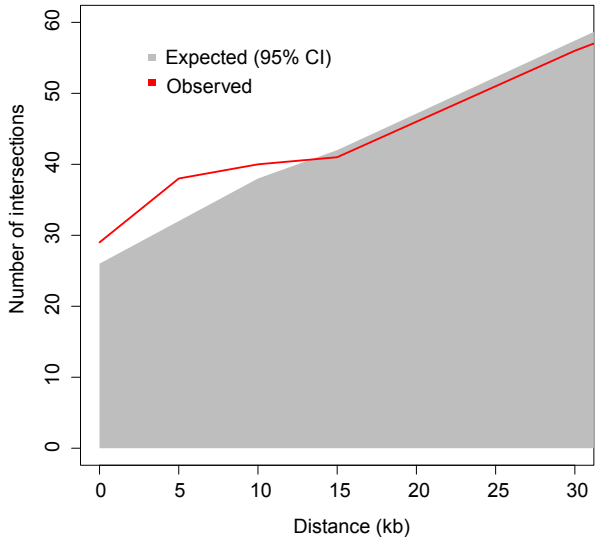

Figure 3.7. Enrichment for SNPs with GWAS link to inflammatory disease near dexamethasone regulated genes.

The incidence of SNPs that intersect with gene loci responsive to dexamethasone in hMDM for a range of windows surrounding the gene (red line). The 95% confidence limits for windows surrounding 10,000 permuted gene sets is plotted in grey.

3.6 Discussion

In both mouse and human macrophages there was a sequential cascade of gene regulation over 24h. Although much of the literature on GC has focussed on transcriptional repression of inflammatory genes, the results highlight the fact that GC acts as a classical transcriptional activator. The dominant response in both species was gene induction as measured at the level of steady state mRNA, and this response occurred more rapidly than repression. The faster kinetics for induction is

consistent with previous work in A549 cells (derived from human lung epithelial cells) (Reddy et al., 2009). In some cases, for example *PLAU*, the transcriptional repression may be a downstream consequence of gene induction (*DUSP1*). Whilst this was a non-stimulated setting rather than an inflammatory context, the reorganisation of the transcriptome measured here highlights the role of GC in macrophages beyond restraint of pro-inflammatory gene transcription. The approach taken here does not assess either loading of RNA polymerase or generation nascent transcripts so cannot capture a full picture regarding the initiation of transcription. It is inherent in this that for all but the least stable mRNAs repression will lag behind induction due to the lifespan of the mRNA already present. Given the translational output depends in some degree on the abundance of a mRNA this remains a reasonable comparison. A further limitation is I did not measure protein levels for these regulated genes so an additional layer of complexity lies above this response when considering cell function.

A core set of known glucocorticoid targets was shared between the two models, but the vast majority were not. The difference between the two species is even greater than that found in the inflammatory response to LPS, where the majority of target genes were regulated in a similar manner (Schroder et al., 2012). This is not necessarily surprising given the many differences between mice and man, but analysis of the local regulatory sequence does not provide an explanation as the promoters of these divergently responding genes are relatively conserved. Motif analysis did not find a common factor that binds to the promoters. There were some functional terms that are consistent with known human-mouse differences, for example roles in adipogenesis and insulin signalling enriched in the human data (Irvine et al., 2009; Stylianou et al., 2012). However given the limitations inherent in comparing these models discussed above there remains the possibility that some of this is cell type, not species difference.

Human genes identified in this response have an association with inflammatory risk variants. Genome wide association studies identify candidate loci with a role in disease(The Wellcome Trust Case Control Consortium, 2007). In order to avoid emphasising false positives from this genome wide data stringent thresholds are used

that therefore discard many sites that may have a true biological link. The role of reported genes is often not clear in the context of disease and they are often simply the nearest to the SNP with the strongest association. The over-representation of reported genes in the hMDM GC responders reflects the intersecting roles of this cell type and stimulus and gives confidence that I have identified relevant targets using this model system. Conversely the data provide biological support to the previously identified targets, including some not reported as true hits initially due to relatively low significance (Table 3.5).

3.7 Summary

Transcriptional activation is the hallmark of the macrophage response to GC in both hMDM and mBMDM, however beyond a small core set the genes induced are not shared. This divergence is greater than that seen for classical pro-inflammatory stimuli and cannot be linked to promoter sequence changes. It is possible therefore that the differences between the culture models could be a contributor to this effect, rather than it being primarily species driven.

Chapter 4: Glucocorticoid receptor binding in macrophages

4.1 Introduction

The primary mechanism by which glucocorticoids (GC) have their transcriptional effects is through binding to the glucocorticoid receptor (GR, gene symbol *NR3C1*). As discussed in section 1.1.2, GR is a nuclear hormone receptor that shares common domain structures with the androgen, estrogen, progesterone and mineralocorticoid (Figure 1.3) receptors. In the absence of GC, GR is held in the cytoplasm bound to chaperones including HSP70 and HSP90 and p23 (Oakley and Cidlowski, 2011). Ligand binding causes a dissociation of these and exposes a nuclear localisation signal thus allowing GR to enter the nucleus. Other factors such as the immunophilins *FKBP51* and *FKBP52* also bind GR at rest (Vandevyver et al., 2012), these have a role in modulating the interaction of GR with both ligand and the major chaperones. By this mechanism these partners can regulate GC sensitivity (Jääskeläinen et al., 2011).

GR binds to an inverted repeat motif (AGAACAnnnTGTTCT)(discussed in section 1.1.2). The absence of a consensus GRE motif at the promoters of GC-inducible genes, and previous data in other systems placing GR binding away from promoters (John et al., 2008, 2011; Reddy et al., 2009; Uhlenhaut et al., 2013),suggested that GR might induce transcription by binding to distal regulatory elements. To determine the location of these elements, chromatin immunoprecipitation and sequencing (ChIP-seq) was performed using antibodies against GR, in mouse and human macrophages stimulated with dexamethasone.

4.2 GR binding in Mouse Bone Marrow Derived Macrophages

One previous set of GR ChIP-seq data has been produced for glucocorticoid treated bone marrow macrophages (Uhlenhaut et al., 2013). However, the system used was not comparable. In the previous study the authors removed both serum and the macrophage growth factor CSF1 for 12 hours before the addition of dexamethasone. They also used a substantially higher (1uM) concentration of dexamethasone and only very limited expression data was generated to pair with the receptor binding. Receptor binding in this study was assessed by ChIP-seq using M20 a polyclonal anti-GR antibody from Santa Cruz (sc-1004). It is known that the enhancer landscape of macrophages is defined by the conditions it experiences both at steady state (Gosselin et al., 2014; Lavin et al., 2014) and in response to stimuli (Ostuni et al., 2013). Therefore data on GR binding in response to GC in the same culture system used to generate the expression data presented in chapter 3 was required.

Optimisation of this assay was challenging. Many ChIP-seq datasets for GR have used a cocktail of antibodies and a large amount of input material to gain good quality results (John et al., 2011). Figure 4.1 shows an example in which multiple antibodies and combinations of antibodies were screened for their ability to precipitate a known GRE -4.6kb from the TSS of *Dusp1* in standard ChIP-qPCR assays. GR ChIP-seq data was generated using a stringent protocol and the best performing antibody, which was a monoclonal (see methods). Here best performance was defined as the maximum signal at a positive locus (*Dusp1* -4.6kb) compared to untreated for the same locus as well as a control site (*ActB* promoter) (Figure 4.1).

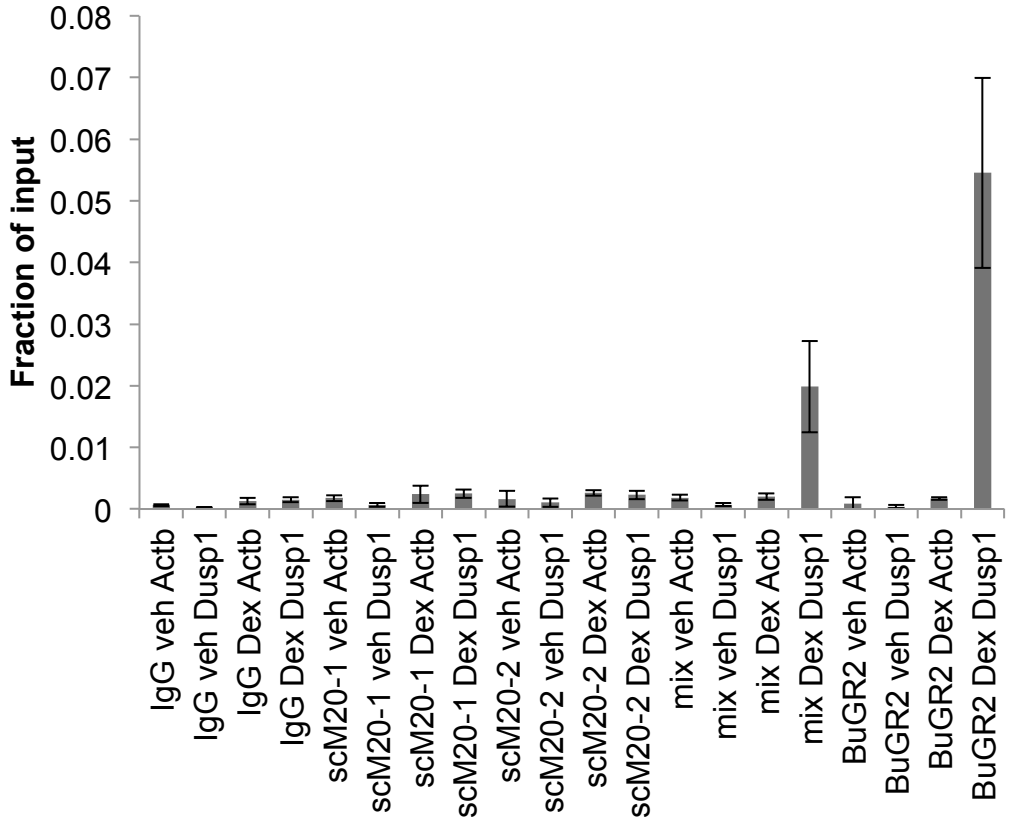

Figure 4.1 Optimisation of ChIP, example of antibody screening.

ChIP-qPCR at a known GR bound (Dusp1, -4.6kb from *Dusp1* TSS) and a control (Actb, *Actb* promoter) locus. From left to right results from normal IgG, 2 different batches of a highly cited commercial antibody (M20, Santa Cruz), a mix of M20 and BuGR2 monoclonal (John et al., 2011) and the monoclonal BuGR2 alone. Results shown are from a single representative biological replicate; error bars are 2x standard error of the mean for 3 technical replicates.

Figure 4.2 (A-D) shows representative UCSC browser tracks for measured GR binding in mBMDM. Binding was observed in the vicinity of many inducible genes, regardless of their time course of responsiveness. Examples are shown for genes induced by 1h (*Fos*), 2-4h (*Jdp2*), 2-10h (*Fkbp5, Klf9*), and at 24h (*F13a1*). This produced 488 high confidence GR peaks, 474 of which were induced by

dexamethasone. These peaks lie away from promoters in intergenic regions and introns (Figure 4.3A).

In the previous study noted above (Uhlenhaut et al., 2013), obtained by ChIP-seq after cross-linking with both disuccinimidyl glutarate and formaldehyde, only 5% of the ~10,000 called ChIP-peaks had a consensus GR response element (GRE). Previous ChIP-seq data from cell lines have reported 50-62% of GR bound sites having a motif matching the GRE (John et al., 2008; Reddy et al., 2009). To assess the association between GR binding and motifs, a region of +/-25bp surrounding the peak maxima was examined. Based upon *de novo* motif finding, the majority (78%) of our GR peaks contain a motif or motifs closely resembling the GRE at their centre (Figure 4.3B&C). The proportion of peaks with GRE rises further to 86% when considering a region +/-100bp from the peak centre (Figure 4.3D).

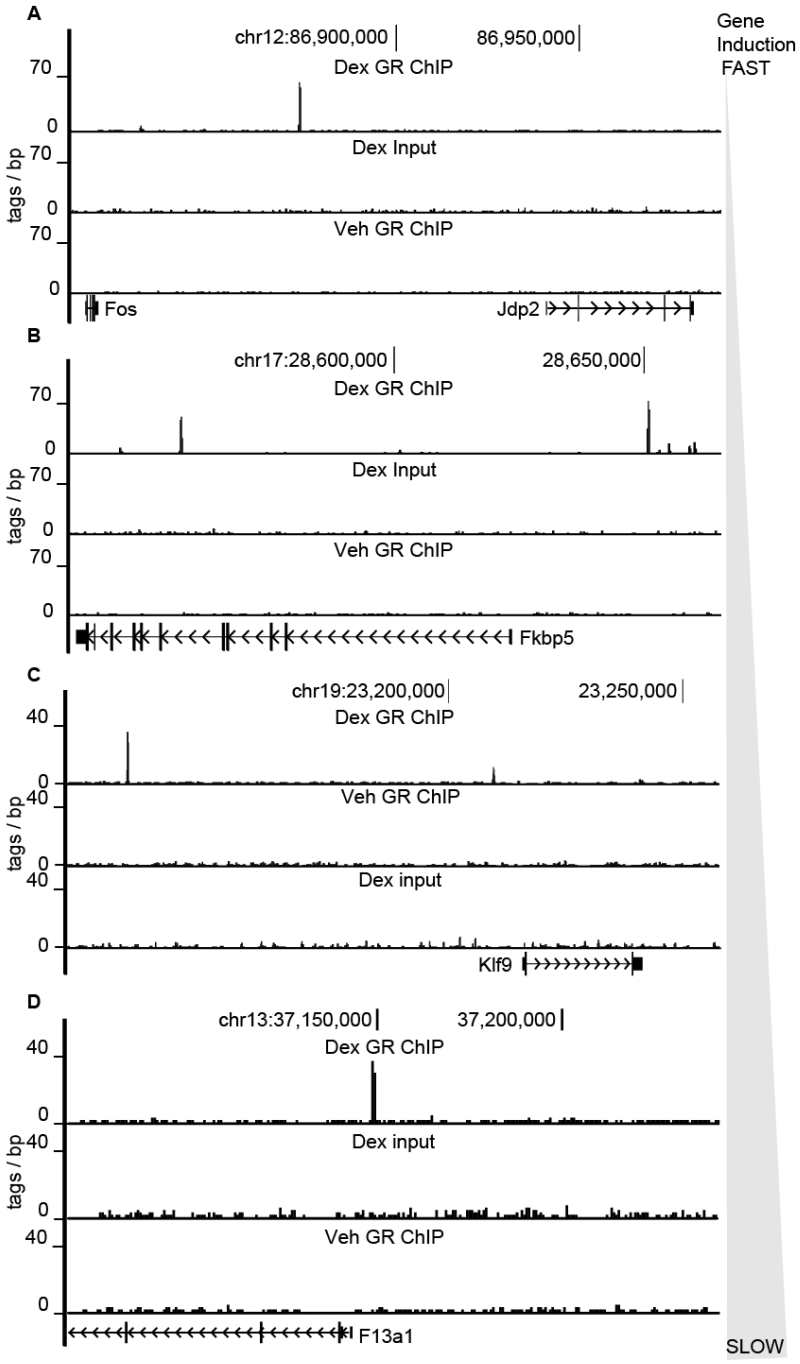

Figure 4.2 GR binding in dexamethasone treated mBMDM

(**A-D)** Representative genome browser tracks for 3 induced loci, showing two early responders (0-2h, *Fos,* 2-4h *Jdp2)*, two slower (2-10h, *Fkbp5, Klf9*) and one late responder (24h, *F13a1*). Data are for 100nM dexamethasone treated IP, vehicle IP and input. Genome co-ordinates are from mm9 assembly.

There is intersection with the previous data (Uhlenhaut et al., 2013) but 36% of the peaks in the current dataset, the vast majority of which contain a canonical GRE, are not present in their data. Peak score comparison between datasets is not straightforward. However, well-characterised GR peaks are present in both datasets with similar peak scores (e.g. *Per1* -600bp 73.5 vs 58.7 Uhlenhaut et al. , *Dusp1* -27kb 200.9 vs 146.9 Uhlenhaut et al), the slightly higher values in our data are most likely due to different relative sequence depth and library complexity. Considering the unique peaks for each dataset those from my data are again, likely for the same reasons, slightly higher (median 11.4 vs 8.1, p-value = 1.33×10^{-15} Wilcoxon rank sum). Taken together this suggests that the differences between the datasets are not simply due to sensitivity.

Gene repression driven from negative GRE (nGRE) has been reported to be a widespread phenomenon (Surjit et al., 2011). Although induction was the predominant response there were also many genes repressed therefore putative targets for nGRE mediated repression. However, *de-novo* motif analysis did not reveal any matches for the described nGRE (CTCC(n)0-2GGAGA, where (n)0-2 indicates flexibility in spacing) (Hudson et al., 2013; Surjit et al., 2011). Scanning permissively specifically for motifs similar to this selects 59/488 peaks. Of these only 4 have a repressed gene within 1Mb (*Plau, Egr2, Rgs2, Cy2s1),* one of which has a prominent canonical GRE-containing peak at 74kb(*Rgs2).*

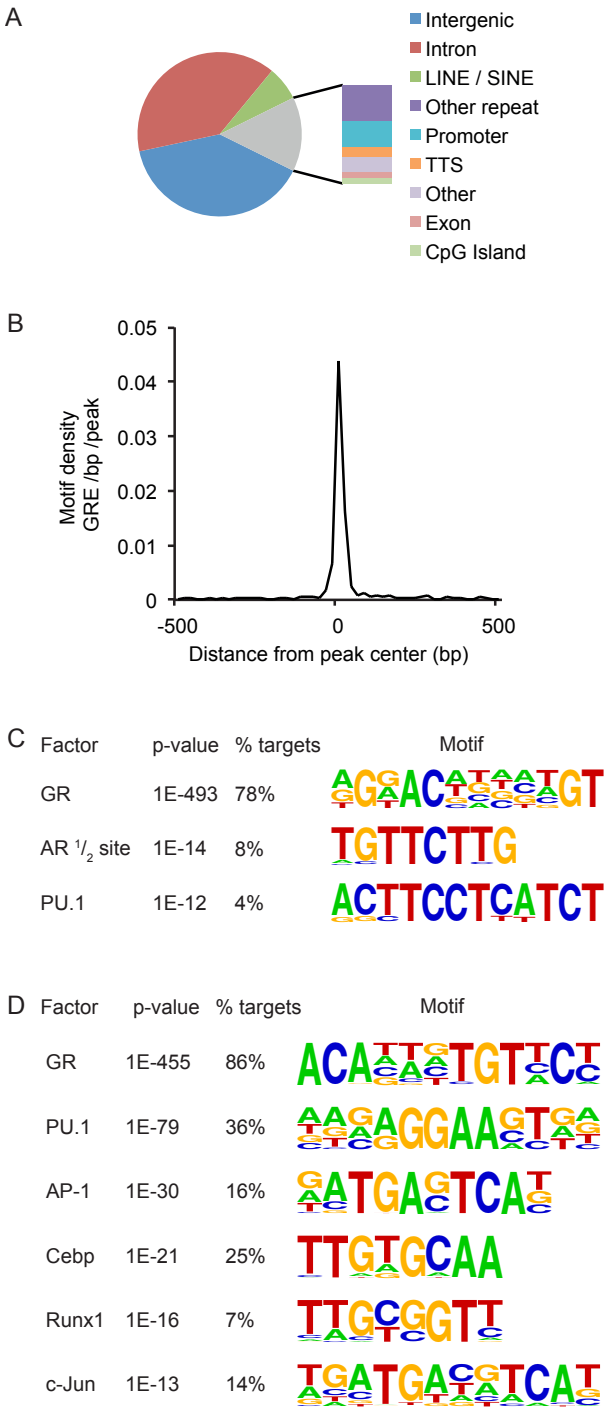

Figure 4.3 Characterisation of GR bound sites in mBMDM

A Classification of regions bound by GR. **B** Enrichment for GRE in peaks found by ChIP-seq. **C** Motifs found *de-novo* +/- 25bp of the peak centre, **D** Motifs found *de novo* in region +/-100bp of the peak centre.

GR is known to act in concert with other factors (Altonsy et al., 2014; Rao et al., 2011; Ratman et al., 2013) and combinatorial binding is a feature of nuclear receptor and other transcription factor function at distal regulatory sites in macrophages (Glass and Ogawa, 2006; Heinz et al., 2010). Enhancers average ~200-250bp in size (Andersson et al., 2014) and contain clusters of recognition sites for transcription factors. Other enriched motifs in the vicinity of mBMDM GR binding sites in this data include AP-1, Hif1b, Cepb and PU.1, (Figure 4.3D).

The ETS factor PU.1 is a master regulator of macrophage transcription (DeKoter and Singh, 2000; Natoli, 2010; Nerlov and Graf, 1998) and other stimulus induced transcription factors have been shown to bind at enhancers marked by PU.1 in activated macrophages (Ghisletti et al., 2010; Heinz et al., 2010). Profiles of PU.1-chromatin binding as well as active enhancer associated histone marks (H3K27ac, H3K4me1) and open chromatin have been published for non-stimulated mBMDM (Ostuni et al., 2013). In the data presented here 94% of GR bound sites overlapped with at least one of the other baseline datasets, particularly PU.1 (72%). The majority overlapped more than 2 of these features (Figure 4.4). The sequence required for binding by PU.1, originally defined as 5'-GAGGAA-3' (Klemsz et al., 1990), is variable around a core now reported as GGAAGT embedded in a 12bp motif (Heinz et al., 2013). The most specific consensus site may not be required for binding (Natoli et al., 2011), likely due to co-operation with other factors. PU.1 may require interaction with an alternate ETS factor (Ross et al., 1998) and in some cases can be substituted (Hoogenkamp et al., 2007). Based upon a more permissive ETS motif, 76% peaks of the GR bound sites were coincident with a potential PU.1 binding motif. Amongst the 65% of GR bound sites with a consensus GRE, there was an average separation of 40bp between the two motifs. Only 1.4% of peaks had neither GRE nor ETS motifs present.

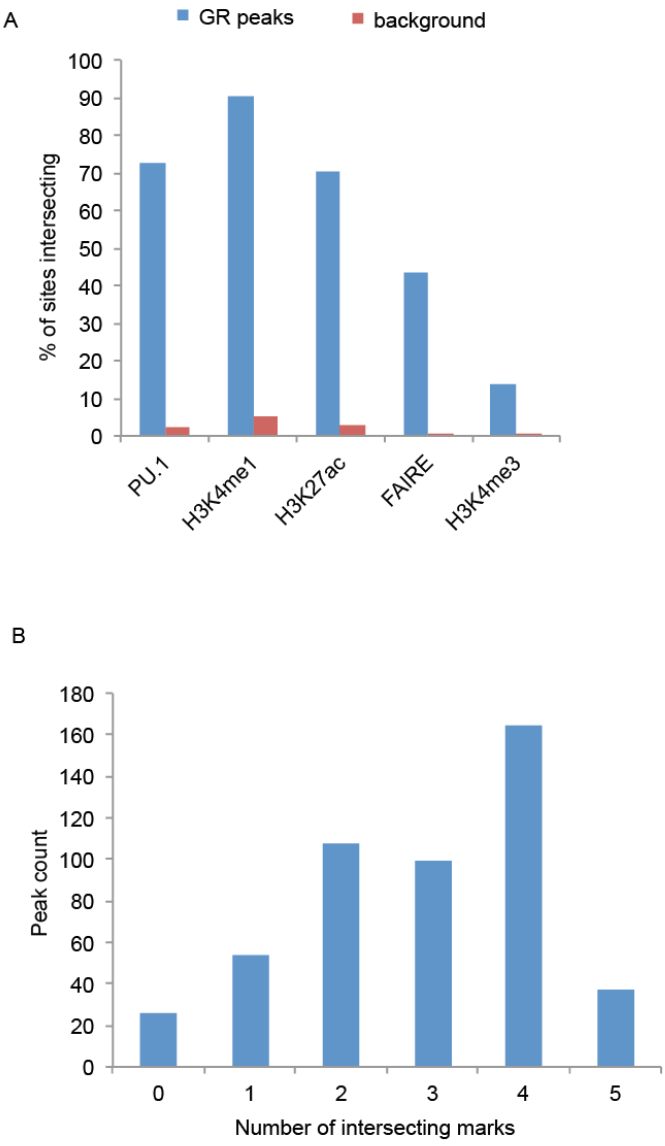

Figure 4.4 GR bound sites in mBMDM overlap sites previously reported to bear marks associated with enhancers

Comparison to published (Ostuni et al., 2013) data for marks found at enhancers (PU.1 binding, H3K4me1, H3K27ac, FAIRE-seq and H3K4me3). **A** Percentage of GR sites that overlap with the given features. Red bars indicate a GC matched genome permuted background set. **B** GR bound sites that overlap with the given number of listed features**.**

4.3 GR binding in Human Monocyte Derived Macrophages

Due to the constraints on cell number when using subpopulations of human primary cells, as well as the virtual absence of binding in untreated mouse macrophages, ChIP-seq for GR was focused solely on dexamethasone treated hMDM. It is known that GR primarily resides in the cytoplasm in the non-stimulated state (Miranda et al., 2013), as confirmed above by the mouse data. Therefore the majority of GR bound sites identified here are likely to be acutely induced.

Optimisation of the assay was again challenging. None of the antibodies that gave signal in mouse provided useful results in man for ChIP-qPCR, including the very efficient monoclonal used for ChIP-seq in mBMDM. However, after further antibody screening and alteration of assay conditions (see methods section 2.1.4) a ChIP-seq dataset comparable to that from mBMDM was obtained for hMDM.

As in the mouse, there was evidence of GR binding in the vicinity of inducible genes, regardless of the time course of induction. Representative browser images for the data are shown for peaks near genes regulated by 1h (*PER1, DUSP1*), 2-10h (*FKBP5, PDK4*), 10-24h (*ADORA3, IL1R1, IL1R2*) (Figure 4.5A-F). Using a stringent protocol in total there were 484 high confidence GR-binding peaks in dexamethasone stimulated hMDM. As in mBMDM, they lie away from promoters in non-coding regions of the genome (Figure 4.6A) and were highly enriched for a motif that closely matches the consensus GRE (52% within +/-25bp, 62% within +/-100bp, Figure 4.6B). Other motifs present in the 200bp region surrounding each GR peak include PU.1 (34%), IRF4 and RXR (both 5%) (Figure 4.6C&D). Using permissive criteria, as used for the mouse data above, the 34% with a strict PU.1 site increased to 62% of peaks containing any enriched ETS factor binding motif, including 70% of peaks with a GRE. The average separation was 43bp between ETS and GRE motifs where they were coincident (40bp in mouse), 18% of peaks did not contain either (1.4% in mouse).

GR binding sites are possible targets for disease-associated polymorphisms in inflammatory disease. None of the inflammatory SNPs identified in chapter 3 (section 3.5) directly overlapped with GR bound peaks, although 2 lie within 350bp (rs10499197, near *TNFAIP3* and linked to SLE and systemic sclerosis and rs12466022, linked to multiple sclerosis). The analysis was extended to include SNPs that are in significant linkage disequilibirum with reported risk SNPs, but this did not reveal any direct overlaps. Two additional disease associated variants were located in the region of GR bound sites: rs403439 and rs 2743403. The first lies 264bp from a GR peak and is in LD with rs12984174, which is linked to asthma. The second lies 468bp from a GR peak and is in LD with rs1008953 linked to psoriasis and lying adjacent to *SDC4*. Both of these alternative variants are common (allele frequencies ~25%) so the regulatory significance of this is uncertain.

Interestingly the GR bound peak adjacent to *SDC4* is conserved from hMDM to mBMDM (Table 4.1). *Sdc4* was weakly induced by dexamethasone in mBMDM although it did not meet the fold change threshold set to be included in the full analysis.

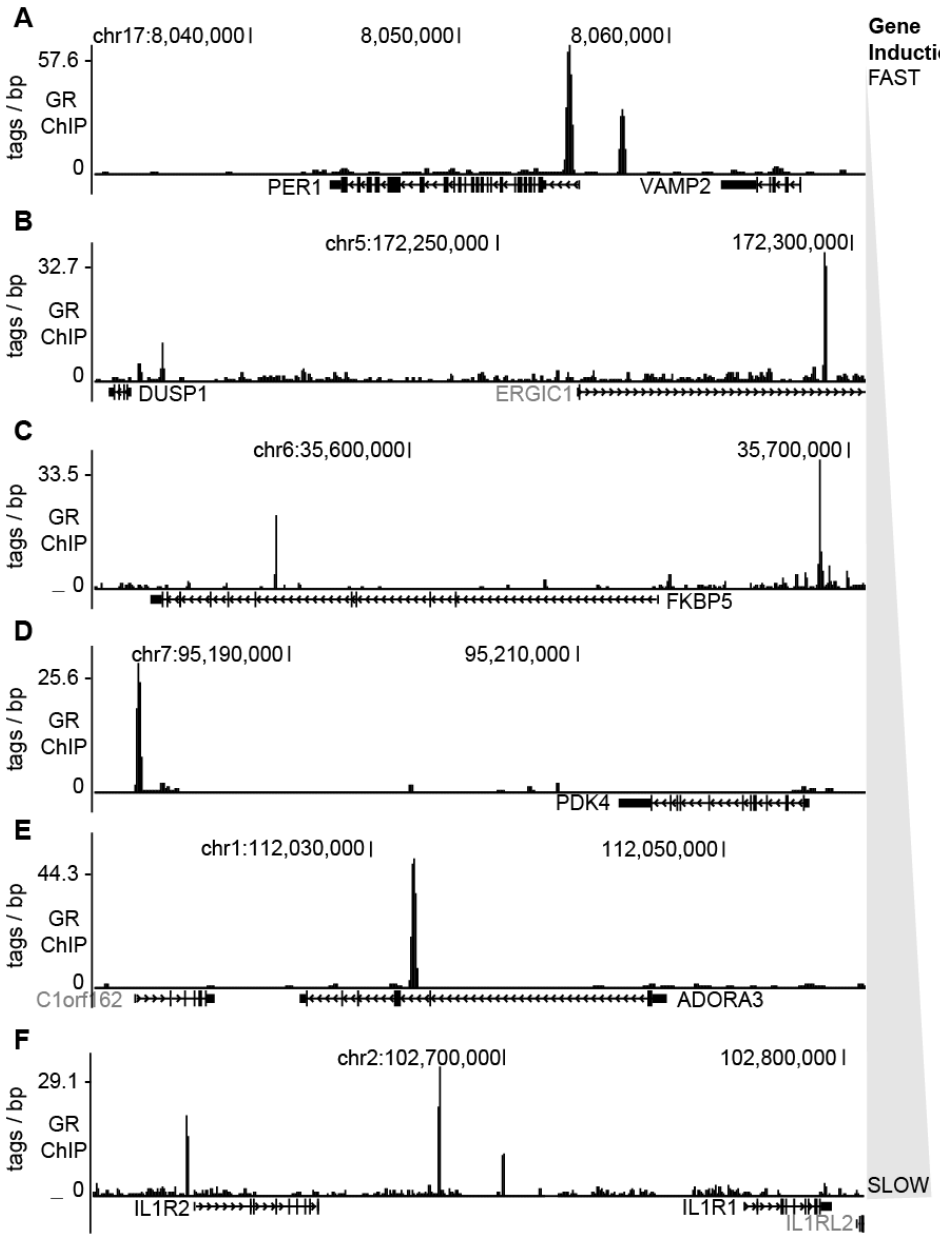

Figure 4.5 Genome wide binding of glucocorticoid receptor in hMDM

Representative browser tracks for loci regulated within 1h **A** PER1, **B** DUSP1, 2-10h **C** FKBP5, **D** PDK4, and 10-24h **E** ADORA3, **F** IL1R2 & IL1R1 (IL1R1 responds 4-10h). Gene names in light grey are non-regulated.

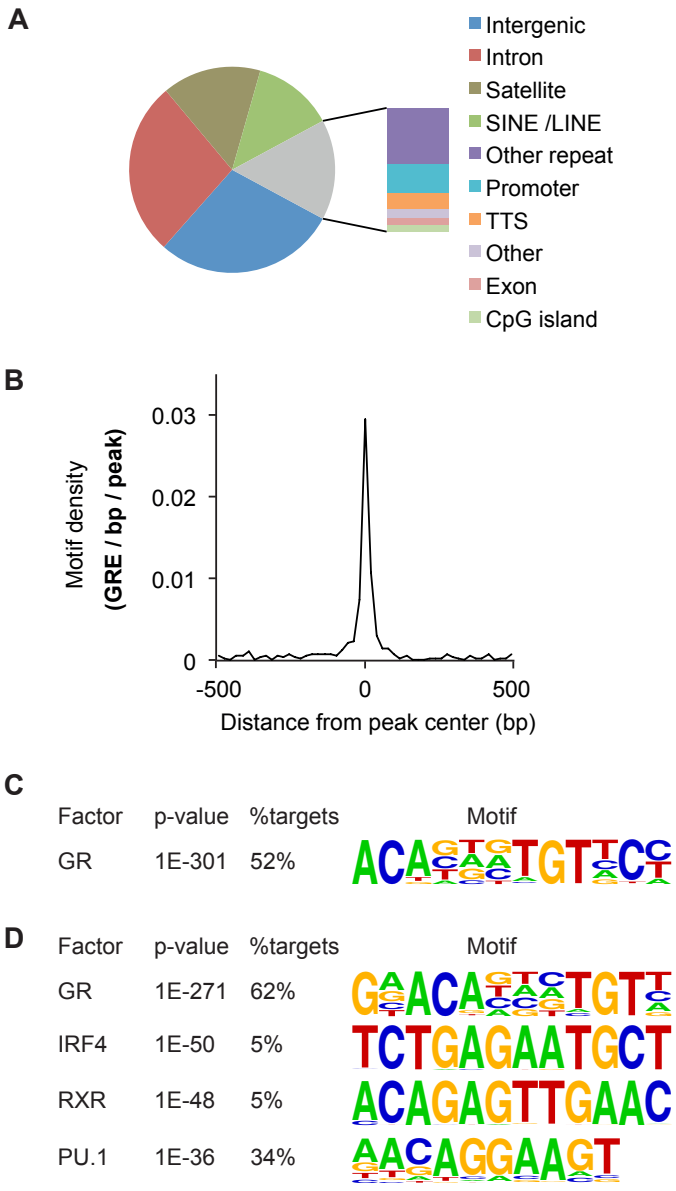

Figure 4.6 Characterisation of GR bound sites in hMDM

A Classification of regions bound by GR. **B** Enrichment for GRE in peaks found by ChIP-seq. **C** Motifs found *de-novo* +/- 25bp of the peak centre, **D** Motifs found *de novo* in region +/-100bp of the peak centre.

4.4 Glucocorticoid receptor binding is associated with induced, not repressed genes

There was a clear association between GR binding peaks and GC-induced genes in both species, greatest at 10kb from the TSS, but still marginally detectable at 1Mb. Conversely, there was no detectable relationship between GR-binding peaks and repressed genes (Figure 4.7A-D). Considered from a gene-centric view 77/160 induced transcripts in mBMDM showed evidence of GR binding within 200kb of the TSS (105/160 within 1Mb), compared to only 1/50 that were repressed. The hMDM equivalent figures were 78/225 induced, 8/125 repressed within 200kb (159/225 induced within 1Mb). There was no difference in the range of motifs found in peaks near early or late genes. From a peak-centric view 33% lay within 1Mb of an induced gene in mBMDM (32% in hMDM) and this subset of peaks had higher signal for GR binding than those more distant (mBMDM GR peaks <1Mb median peak score 18.8 vs. 12.6 for > 1Mb, $p=1.37x10^{-5}$; hMDM GR peaks <1Mb median peak score 28.5 vs. 22.1 for >1Mb, p=0.0078, Wilcoxon rank sum).

The expression response to GC was stronger where there were multiple GR peaks within 200kb of the TSS of an induced gene than if there was only a single GR bound site (mBMDM median $\log_2$ fold change 2.43 vs 1.43, p=0.0018, hMDM median $\log_2$ fold change 2.53 vs 1.76, p=0.031, Wilcoxon rank sum). Early (<2h) induction was not associated with greater peak proximity (mBMDM median distance 22kb vs 46kb, p=0.199, hMDM median distance 46kb vs 88kb, p=0.162, Wilcoxon rank sum) nor was there a difference in peak strength.

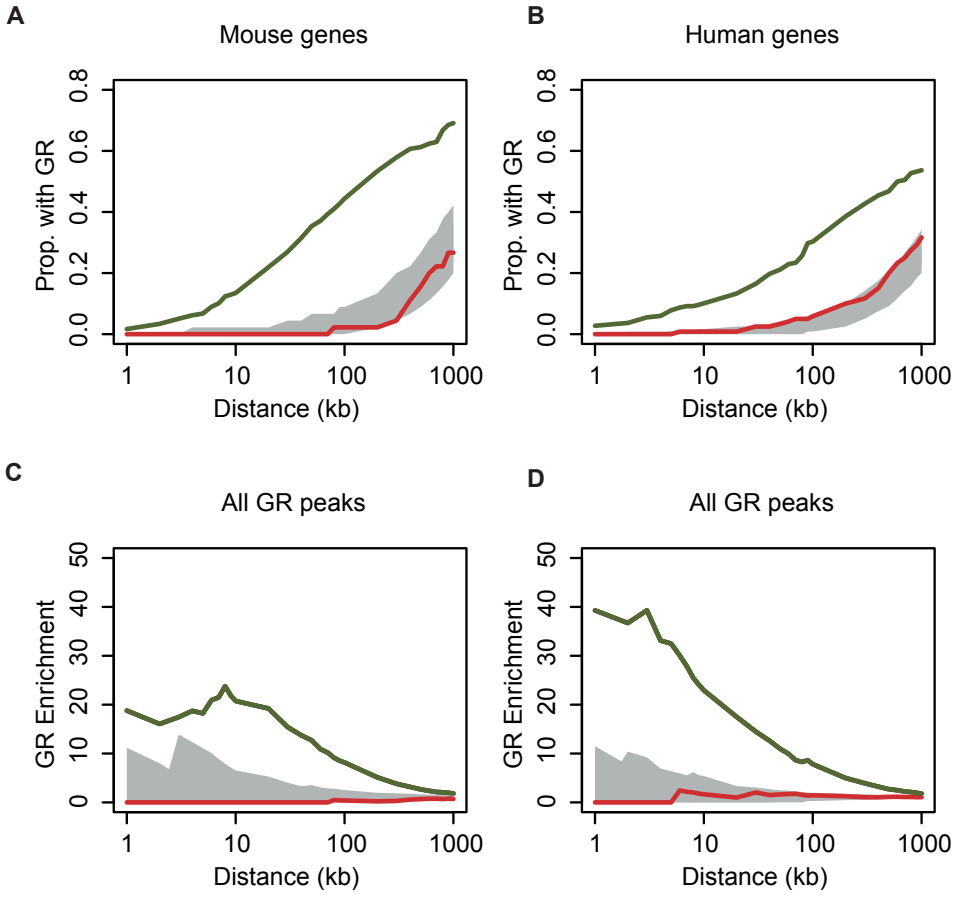

Figure 4.7 Induced genes are associated with GR binding

The proportion of peaks with induced (green) or repressed (red) genes within a given genomic interval for **A** mBMDM and **B** hMDM. The 95% confidence intervals from matched permuted distributions of GR peaks are shown in grey. The enrichment of the proportion of induced (green) genes with a GR peak within a given interval versus the proportion of induced genes without a GR peak within that interval for **C** mBMDM and **D** hMDM. No enrichment is seen for repressed genes (shown in red) The 95% CI from a permuted distribution of GR peaks is shown in grey. This analysis was performed with assistance from Rob Young, MRC HGU.

4.5 Inter-species differences of glucocorticoid receptor binding are associated with sequence changes that lead to motif loss

As noted in the introduction (section 1.4), turnover of enhancers has been linked to response divergence (Heinz et al., 2013; Stefflova et al., 2013). The landscape of enhancers is also different from mouse to man, particularly for immune genes (Stergachis et al., 2014; Yue et al., 2014).

The GR bound sites from hMDM were intersected with those bound in mBMDM, limiting to regions of conserved synteny (using *liftOver* from UCSC (Kent et al., 2002)). Amongst the human dataset there were only 22 bound sites that were both conserved and within 1Mb of a regulated gene (Table 4.1). Most of the GR bound sites could however be aligned between species (Figure 4.8). There was no difference between the rate of turnover between species (aligned sites vs. inserted/deleted sites) and as observed previously there was a minor deletion bias observed in mouse (Laurie et al., 2012).

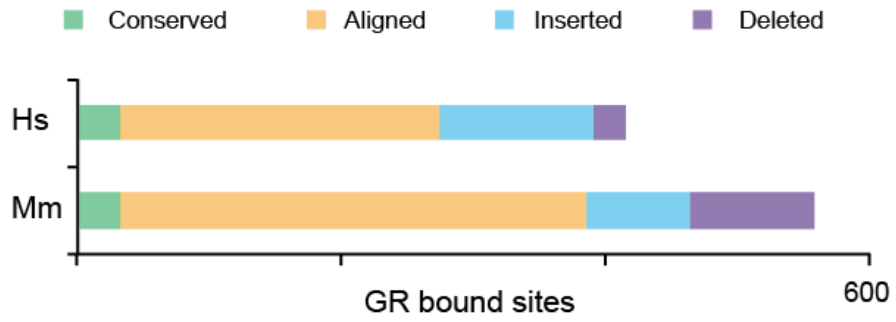

Figure 4.8 Evolutionary outcomes for GR peaks in human.

Aligned sites where the orthologous region is bound by GR in mouse are shown in green and in orange if the site is not bound by GR in mouse. Sites that could not be aligned are defined as either insertions (cya) or deletions (purple) by comparison with dog (CanFam2), horse (EquCab2), cow (BosTau6) and pig (SuScr3) genomes (see methods), Human GR sites were assigned as deletions in the mouse lineage.

Of the shared sites (16) were adjacent to genes induced in both species and are known regulators of the inflammatory response (e.g. *DUSP1, FKBP5* (Figure 4.9A&B)*, MAP3K6, TSC22D3, FOS, KLF4,*). Three of the others are adjacent to genes that are strongly regulated in hMDM but much less so in mBMDM, thus were filtered from the robust gene set used for comparisons (*C1qb*, *Sdc4* and *Mt2,*Table 4.1). Even at the conserved loci GR binding differed: the previously described proximal peaks at the DUSP1/Dusp1 locus were retained (Tchen et al., 2010) but the strongest binding site was not shared (Figure 4.9A). Overall, genes which were upregulated in both species were enriched for having GR bound within 1 Mb in both species (4.0-fold enrichment, chi-squared p = 2.9x10-7 ; Figure 4.9A).

The more common pattern was for GR binding to be divergent between the species; for example the GR peak upstream of *F13a1*, a component of the coagulation cascade, is mouse-specific (Figure 4.8C,). Mouse-specific GR binding

was more frequent in the region of genes that responded to GC only in mouse (2.0-fold enrichment over human, chi-squared $p = 0.0011$; Figure 4.8D). Similarly, human specific GR binding was enriched adjacent to human specific GC responders, for example *ADORA3,* which has a known role in driving the human macrophage phenotype (Barczyk et al., 2010) has an intronic GR peak that is not present in the mouse data. As for the mouse data, there was an overall 1.7-fold enrichment for a human-only GR peak within 1Mb of genes that were specifically upregulated in human macrophages (chi-squared, $p = 0.034$; Figure 4.9E&F).

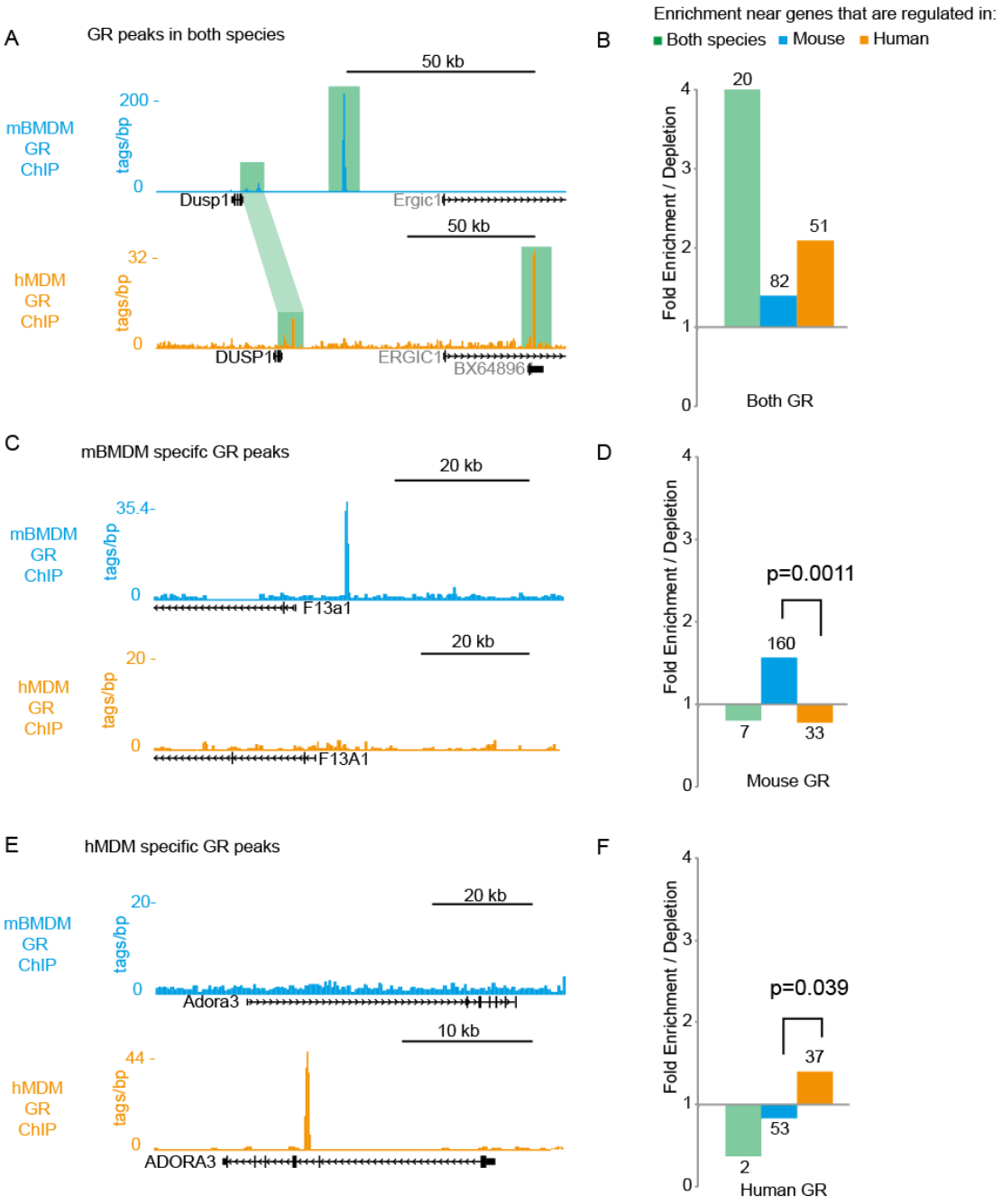

Figure 4.9 GR binding sites are minimally conserved between mouse and man and this is linked to the divergent transcriptional response to GC.

(A) GR ChIP-seq data from mBMDM (orange) and hMDM (cyan) showing conserved GR binding (green highlight) at a locus (DUSP1/Dusp1) whose expression is rapidly induced by GC in both mouse and human macrophages. GR bound sites aligned between species are linked by light green highlight: the

most prominent sites are bound in only one species. (B) Enrichment / depletion for mouse/human shared GR binding within 1Mb for GC-responsive genes that are; shared between mouse and human (green), mouse-specific (cyan), human-specific (orange). Numbers give raw counts for each category. (C) As in (A) but showing mouse-specific GR binding at F13a1/F13A1 which is induced in mBMDM but not hMDM. (D) As for B, but for mouse-specific GR binding sites. The chi squared p value for the difference between mouse and human specific sites is given. (E) As in (A) but showing human-specific GR binding at ADORA3/Adora3 which is induced in hMDM but not mBMDM. (F) As for (D) but for human-specific GR-binding sites.

Table 4.1 Conserved GR bound sites

Human Symbol	Distance(bp)	Peak Score	Mouse Symbol	Distance (bp)	Peak Score
MAP3K6	243	59.1	*Map3k6*	173	18.2
DDIT4	18650	81.1	*Ddit4*	18152	15.4
DDIT4	24921	166.4	*Ddit4*	22499	64.1
ZBTB16	100510	33.5	*Zbtb16*	95679	16.1
ZBTB16	119711	59.5	*Zbtb16*	112199	43.1
MMP19	5101	18.9	*Mmp19*	11362	22.7
FOS	62389	117.8	*Fos*	58829	65.7
PER1	506	114	*Per1*	460	73.5
PER1	2025	56.1	*Per1*	1885	47.4
PIK3IP1	6071	37.7	*Pik3ip1*	5257	13.9
DUSP1	4523	21.6	*Dusp1*	4261	18.8
FKBP5	86865	37.9	*Fkbp5*	65828	79.9
KLF9	66248	76.3	*Klf9*	84208	37.4
KLF9	5346	24.9	*Klf9*	6120	13.3
KLF4	271410	46.6	*Klf4*	209189	14.1
TSC22D3	42816	49.9	*Tsc22d3*	37204	33.2
Mouse orthologues are weakly regulated:					
C1QB	197	229.4	*Map3k6*	3645543	25.6
-	-	-	*C1qb*	174	25.6
MT2A	1223	16.3	*Ndrg4*	1531461	6.2
-	-	-	*Mt2*	942	6.2
SDC4	10723	75.8	*Ncoa5*	578851	33.8
-	-	-	*Sdc4*	13152	33.8
Gene - peak relationships uncertain					
TIFAB	985838	15	*Pdlim4*	2152809	61
TNFAIP3	159446	20	*Sgk1*	2695702	12.1
ARG2	648524	27	*Rab15*	2811132	6.4

As discussed in the introduction the enhancer landscape is highly dynamic and is a function of the conditions studied (Gosselin et al., 2014; Lavin et al., 2014; Ostuni et al., 2013). Thus, since mBMDM and hMDM are not perfectly equivalent the differences found may be due to differences between the models. However if the

differences are linked to sequence divergence then we can be more confident that this is a species difference

Shared GR bound sites that aligned across species showed significant enrichment for the GRE motif when compared to those sites that could be aligned but did not have measureable GR binding in the other species (Figure 4.10A&B). This was also true for PU.1, although less strongly, reflecting the lower prevalence in the baseline dataset (Figure 4.10A&B). In the same way the frequency of the GRE was higher in the aligned sites that retained GR binding in both species compared to the aligned but unbound sites (human origin fold enrichment 3.4, $p = 4.45x10^{-12}$, mouse origin fold enrichment 3.2, $p= 2.44x10^{-12}$, Pearson's chi-squared).

Species-specific GR bound sites were strongly enriched for GRE compared to the sites that could be aligned from the other species but were not bound (Figure 4.11A&B), with stronger enrichment for PU.1 in the mouse specific sites (Figure 4.11A&B). Consistent with some retention of PU.1 at the mouse specific sites, there was a weak but detectable relationship between the non-bound mouse sites that could be aligned in human and human specific induced genes (Figure 4.11C-F). Since most of the species-specific sites could be aligned (Figure 4.8) the changes that cause the motif loss are likely to be at the sequence level, such as nucleotide substitutions, rather than insertion or deletion of sequence. Overall this supports the hypothesis that these differences are due to species specific sequence changes, rather than being an artefact of the systems studied.

If the differences outlined above were driven by host pathogen interactions, as suggested for LPS (Schroder et al., 2012), there would be an active loss of conservation, indicative of positive selection, beyond that seen for background. Conversely increased conservation is seen at sites of purifying selection; the loss of such sites is deleterious. Using per base evolutionary constraint (Davydov et al., 2010) the shared sites in each species have increased constraint of the GRE (Figure 4.10C&D), consistent with a conserved biology. However there was not a signature consistent with substantial purifying or positive selection across the motif at the species-specific sites (Figure 4.10C&D).

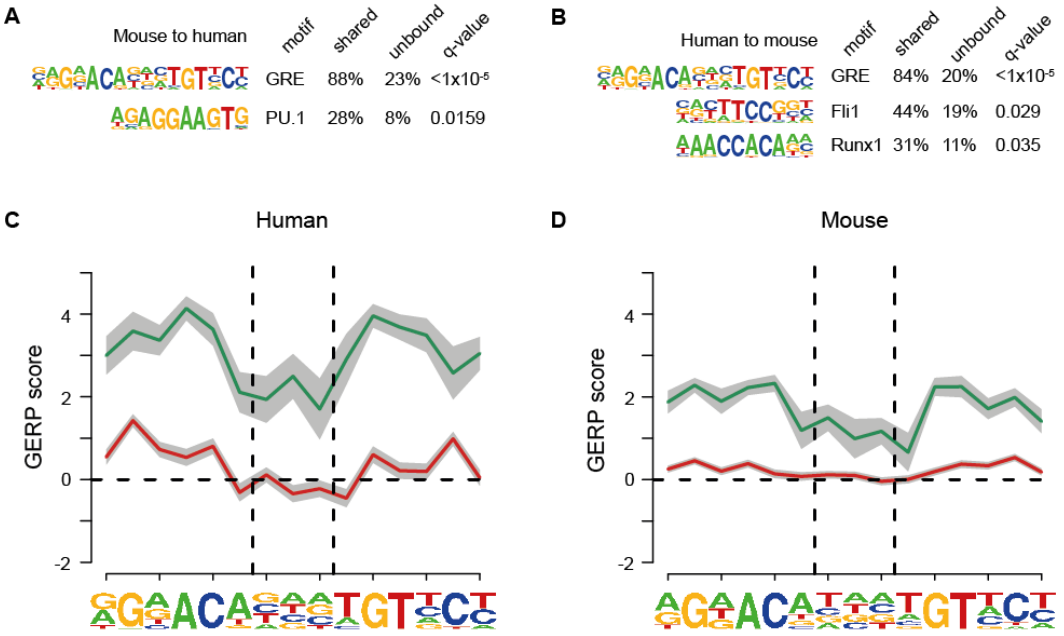

Figure 4.10 Conserved GR binding is linked to conservation of the GRE

(A) Motif enrichment for the sites bound by GR in mBMDM that aligned and were also bound in hMDM, using as background the sites that could be aligned but were not bound in hMDM (q values shown, Benjamini-Hochberg). (B) Analogous to (A) but for hMDM sites bound in mBMDM vs sites that could be aligned but were not bound in mBMDM. (C) Mean per base constraint scores calculated using GERP (Davydov et al., 2010) across the GRE in shared (green) and species-specific (red) peaks found in hMDM, where the grey bars represents the standard error of the mean. Vertical dashed lines delineate the centre NNN for the GRE, as derived de novo from our hMDM data. (D) Analogous to (C) for GR bound peaks and GRE motif found in mBMDM. Analysis performed with assistance from Rob Young, MRC HGU.

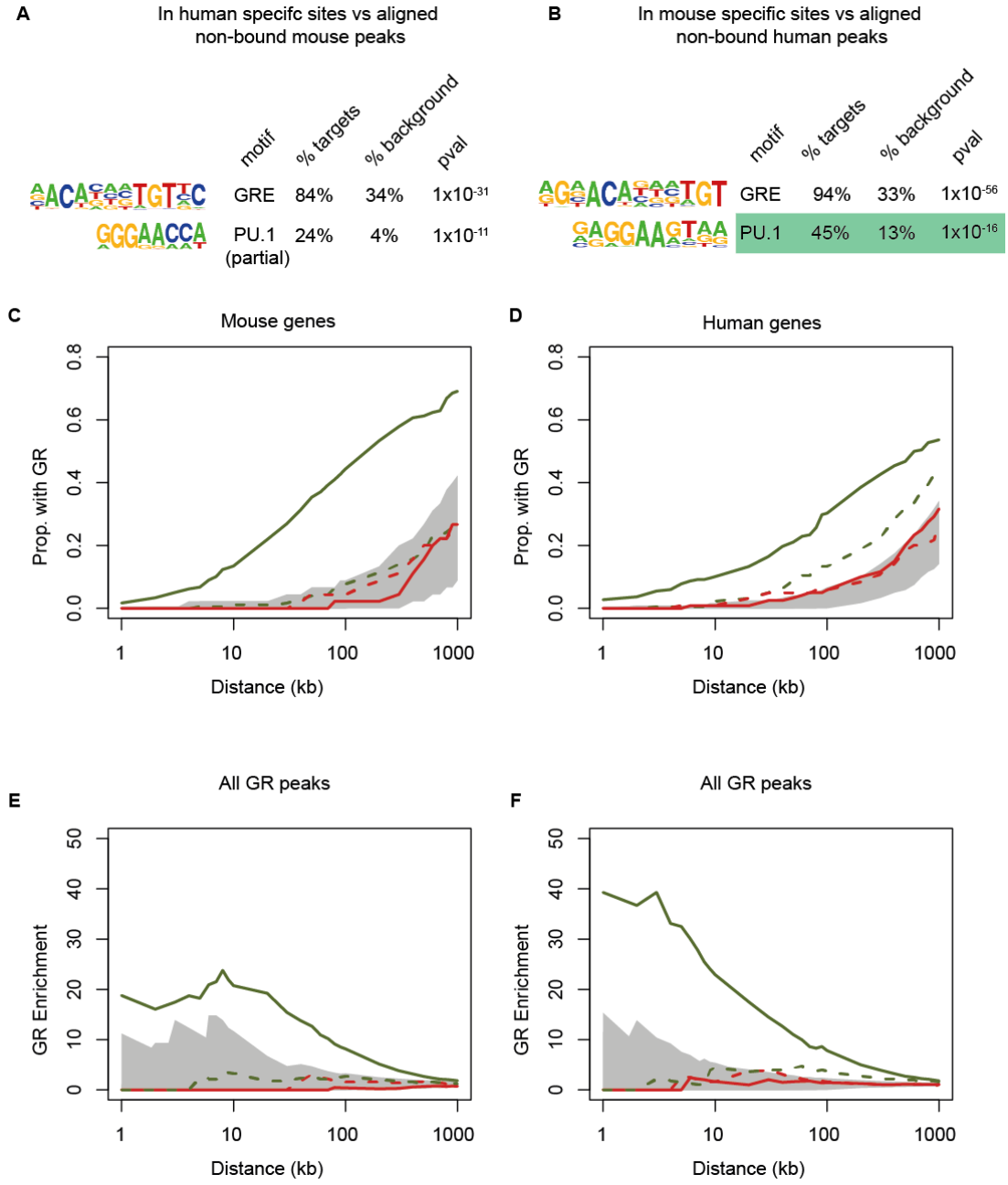

Figure 4.11 Loss of GRE motif is associated with species specific binding.

A motifs enriched in the human specific peaks compared to the aligned mouse sites that are not bound by GR in hMDM. **B** motifs enriched in the mouse specific peaks compared to the aligned human sites that are not bound by GR in mBMDM. The proportion of peaks with induced (green) or repressed (red) genes within a given genomic interval for **C** mBMDM and **D** hMDM. Dashed lines represent peaks from mouse, which align in human, but are not bound in

hMDM. The 95% confidence intervals from matched permuted distributions of GR peaks are shown in grey. The enrichment of the proportion of induced (green) genes with a GR peak within a given interval versus the proportion of induced genes without a GR peak within that interval for **E** mBMDM and **F** hMDM. No enrichment is seen for repressed genes (shown in red). Dashed lines represent the same test performed using the peaks from mouse that align in human but are not bound by GR in hMDM. The 95% CI from a permuted distribution of GR peaks is shown in grey. Analysis performed with assistance from Rob Young, MRC HGU.

Gene regulation occurs within a complex chromatin environment. A relatively stable higher order structure is proposed for the genome (Dixon et al., 2012) where interactions are relatively more likely within domains (topology associated domains, TAD). Regulatory interactions would then be enriched within these proposed topological domains. Comparison of the intervals between GR bound peaks and closest induced genes for each species shows no enrichment for the number of intervals contained within a single TAD vs randomly permuted intervals of the same size (hMDM 100/227 vs 109/227 p value = 0.45 Pearson's chi-squared). As expected from the location analysis above (Figure 4.7), the peaks are significantly more likely to be in the same TAD as the nearest induced gene when compared to a random set (hMDM 6.6 fold enrichment, p value $<2.2 \times 10^{-16}$, Pearson's chi squared).

4.6 Discussion

The data have revealed GR bound enhancers in the region of genes induced by GC, but promoters are not bound. Many modes of binding have been proposed for GR (Nixon et al., 2013). However, in both human and mouse macrophages GR bound sites, as assayed by ChIP, were strongly enriched for DNA sequence motifs matching the canonical inverted-repeat GR dimer binding site (GRE).

Conservation has been suggested to be a predictor of GR binding at sites adjacent to regulated genes (So et al., 2008) and there was a small subset of sites that fit this pattern. However, the large majority of the GR bound enhancers and GR motifs were not conserved between mouse and man. This confirms the prediction from the recently published mouse ENCODE data (Yue et al., 2014) that distal regulatory divergence is strongest for immunity. It is also consistent with previous work that shows variability of factor binding at distal sites can be a source of phenotype diversity between species (Villar et al., 2014) and this variation can accrue rapidly, even over the relatively short evolutionary distances between mouse strains (Stefflova et al., 2013).

The gain or loss of GR bound sites was linked to sequence changes that cause gain or loss of the canonical GRE and partner motifs such as PU.1. This correlates closely with the species differences in transcriptional regulation described in the previous chapter. As discussed above, the cell models are not directly comparable. However, the fact that GR binding can be linked to DNA sequence changes between species suggests that the divergent expression response is not just an artefact of different culture models. Given the immune roles of macrophages and glucocorticoids relating to the immune response it is perhaps surprising that there was not evidence of pathogen driven positive selection underlying the divergence. The lack of apparent adaptive selection amongst lineage specific enhancers that drive gene expression is consistent with recent work in Drosophila (Arnold et al., 2014), although in that setting enhancer function more generally appeared to be relatively well conserved.

Combinatorial binding of lineage determining and phenotype specific factors is known to play a critical role in macrophage biology (Glass and Ogawa, 2006; Heinz et al., 2010, 2013). For the GR response there was a role for PU.1 as there was a strong signal for both stringent and more lenient DNA motifs for this factor in the GR bound sites, along with majority overlap from previously reported PU.1 occupied sites (Ostuni et al., 2013). However the major motif that is gained or lost between species at species-specific GR bound sites is the GRE itself, with a weaker signal for PU.1. This indicates that whilst partner factors are important for GR binding, the

dominant effect remains within the GRE. This is in contrast to a study of human variants which lead to allelic imbalance where only a minority of differential transcription factor binding events found were associated with changes in the dominant motif. The majority were linked to subtler changes to motifs that were already more degenerate (Reddy et al., 2012).

The exact mechanism by which distal elements regulate transcription remains to be determined (Pennacchio et al., 2013). Interaction, redundancy and co-operativity for enhancers in a given locus have been proposed. For GR multiple bound sites have been associated with stronger gene regulation (Reddy et al., 2009). Macrophage GC targets also show this dose response relationship for GR binding, albeit weakly, which is supportive of an additive effect of multiple active distal regulatory elements (Section 4.4).

GC have commonly been studied as repressors of inflammatory gene expression. In the context studied here GC act on macrophages primarily as inducers of gene expression, when measured at the level of stable mRNA. As discussed above, the methodology does not address loading of RNA Polymerase, or initiation and elongation, which might be address by ChIP-seq and 'global run on' followed by sequencing respectively. The level of stable mRNA does however represent the complement of genes with detectable mRNA available for translation at any given time point, which remains a useful readout of gene regulation. The time series data revealed a cascade of gene regulation. Some of the later changes are likely to be secondary responses to the initial stimulus as explored recently for *Klf4* (Chinenov et al., 2014). However, the late-induced genes were equally likely to have a GR bound peak in the region. These peaks were of the same strength and had the same range of associated transcription factor binding motifs. One explanation for the lack of correlation between binding and temporal profile is that GR binding is permissive in some locations, producing activation only in combination with other transcription factors that are induced earlier in the temporal cascade.

Gene repression by GC was not associated with direct GR-DNA binding in either species. This is consistent with a report from candidate loci in cell lines (So et

al., 2008) and the finding of higher median distance between GR peaks and the nearest repressed vs. induced genes in the lung epithelial A549 cancer cell line (Reddy et al., 2009). Repression has been attributed by others to interaction with other chromatin-binding transcription factors rather than direct DNA binding DNA (Ratman et al., 2013). The difference in expression response between species was just as large for repressed as for induced genes. This is consistent with GR exerting its repressive effects by interacting with other factors bound at regulatory sites that are distant from promoters and evolving between the species. There was no signal from secondary crosslinking between GR and other factors bound to such sites in the vicinity of repressed genes. The previous study by Uhlenhaut et al (Uhlenhaut et al., 2013) used dual cross-linking with formaldehyde and disuccinimidyl glutaraldehdye in an explicit attempt to capture indirect interactions. This approach enabled them to report enrichment for motifs of known GR partners, but the large number and wide distribution of reported peaks prevented the assignment of any quantitative relationship with specific genes either induced or repressed by GC.

Previous studies in other systems reported negative GR binding elements (Hudson et al., 2013; Surjit et al., 2011), but they were not present in either our mouse or human data. Lower binding affinity and faster turnover time could compromise their detection under the conditions employed here. Alternatively, there may be context dependent use of different types of regulatory element. For example, the nGRE may only be relevant in macrophages when GR acts to suppress inflammatory gene induction, rather than in the basal CSF1-dependent state we examined (Uhlenhaut et al., 2013). An alternative mechanism that may underlie some of the repressive effects is secondary repression driven by the early-induced genes such as DUSP1 and NFKBIE.

4.7 Summary

In keeping with more generalised mouse-human comparisons by the mouse ENCODE consortium (Cheng et al., 2014; Stergachis et al., 2014) the principles of the macrophage response to GC are strongly conserved between mouse and man. There are also a small number of loci where conservation can be found in both the regulatory architecture and expression response. At these sites it may be more likely that specific findings will translate well from mouse to man (and vice-versa). However, the extensive expression divergence that is attributable to sequence changes at distal regulatory sites, in combination with the profound differences in macrophage responses to LPS between mouse and human (Schroder et al., 2012), underline the caution that must be employed when attempting to directly translate many locus or pathway specific findings from mouse models to human medicine.

Chapter 5: Dynamic regulation of chromatin structure in macrophages by glucocorticoids

5.1 Introduction

The data presented in chapters 3&4 confirm that in macrophages the majority of genomic sites bound by glucocorticoid receptor (GR) after treatment with dexamethasone lie away from promoters of regulated genes. It is also clear that GR binding is enriched in the vicinity of induced genes.

The mechanisms of gene regulation from a distance remain uncertain (section 1.2.2) (Pennacchio et al., 2013). The data presented here and that by others (Reddy et al., 2009) indicates that GR acts in this way, at least for gene activation, leaving open the question of how the effect is mediated.

Chromatin remodelling complexes are implicated in the regulation of a subset of genes by GR. Further, the pattern in which GR binds to DNA is defined by and then influences chromatin organisation (section 1.2.3) (Burd and Archer, 2013; John et al., 2011). However, Hakim et al. did not observe large scale re-organisation of chromatin in response to GC (Hakim et al., 2011). Instead an increased frequency of pre-existing regulatory contacts is suggested (Hakim et al., 2011). A model consistent with this was presented for the GC responsive *FKBP5* locus using 3C based techniques in A549 cells (Klengel et al., 2013; Paakinaho et al., 2010). In that study an increase in contacts between distal enhancers and the promoter was found on stimulation with GC. If GR works by increasing the frequency of dynamic loop formation between enhancer and promoter then it may be possible to identify this using 3D DNA FISH across responsive loci.

Work on the kinetics of GR binding and loading of remodelling complexes suggests that conformational changes may be rapid, within minutes (Johnson et al., 2008; Nagaich et al., 2004; Voss et al., 2011). More generally, local chromatin

dynamics have not been visualised after GC stimulation at native loci. It is not known to what extent measurable remodelling occurs at this scale and what role GR might play. The studies presented here begin to address this in the context of primary mouse macrophages.

5.2 GR binding is associated with rapid and prolonged chromatin decompaction

The genome wide expression and binding data outlined in chapters 3&4 identified regions of the genome that were both responsive to GC and bound by GR. From these loci, sites with strong binding and regulation were chosen for further investigation using 3D DNA FISH. The initial focus was a locus in which GR binding and inducible expression was highly conserved between mouse and man: *Fkbp5*. This gene produces a co-chaperone of GR in the cytoplasm and has known roles in feedback control and sensitivity to GC (section 1.1.2) (Jääskeläinen et al., 2011), thus is also potentially of clinical interest.The gene locus and fosmid probes used to span the mouse Fkbp5 are shown in Figure 5.1. For comparison *Tmod1,* which was in the same expression profile cluster (Chapter 3, Figure 1.), but lacks the strong local GR binding peaks (Figure 5.2)..

A detailed time series demonstrated by 3D DNA FISH that decompaction occurred across the *Fkbp5* locus within 5 minutes of exposure of mBMDM to dexamethasone and was sustained to 24h (Figure 5.3A&B) By contrast, the distance across *Tmod1*increased with the same kinetics as transcription, reaching significance only at 4h and then reducing towards baseline by 24h (Figure 5.3C&D). Since there was no apparent decline in the apparent decompaction after 24 hrs, the experiment was repeated with even longer treatment (Figure 5.4A). In this experiment, across the *Fkbp5,* locus decompaction remained statistically significant after 5 days following a single dexamethasone treatment (Figure 5.4A). The prolonged change in 3D chromatin conformation was not dependent upon ongoing transcription. Expression

of *Fkbp5* after 2h treatment followed by 22h in fresh culture media returns to close to baseline (Figure 5.4B)

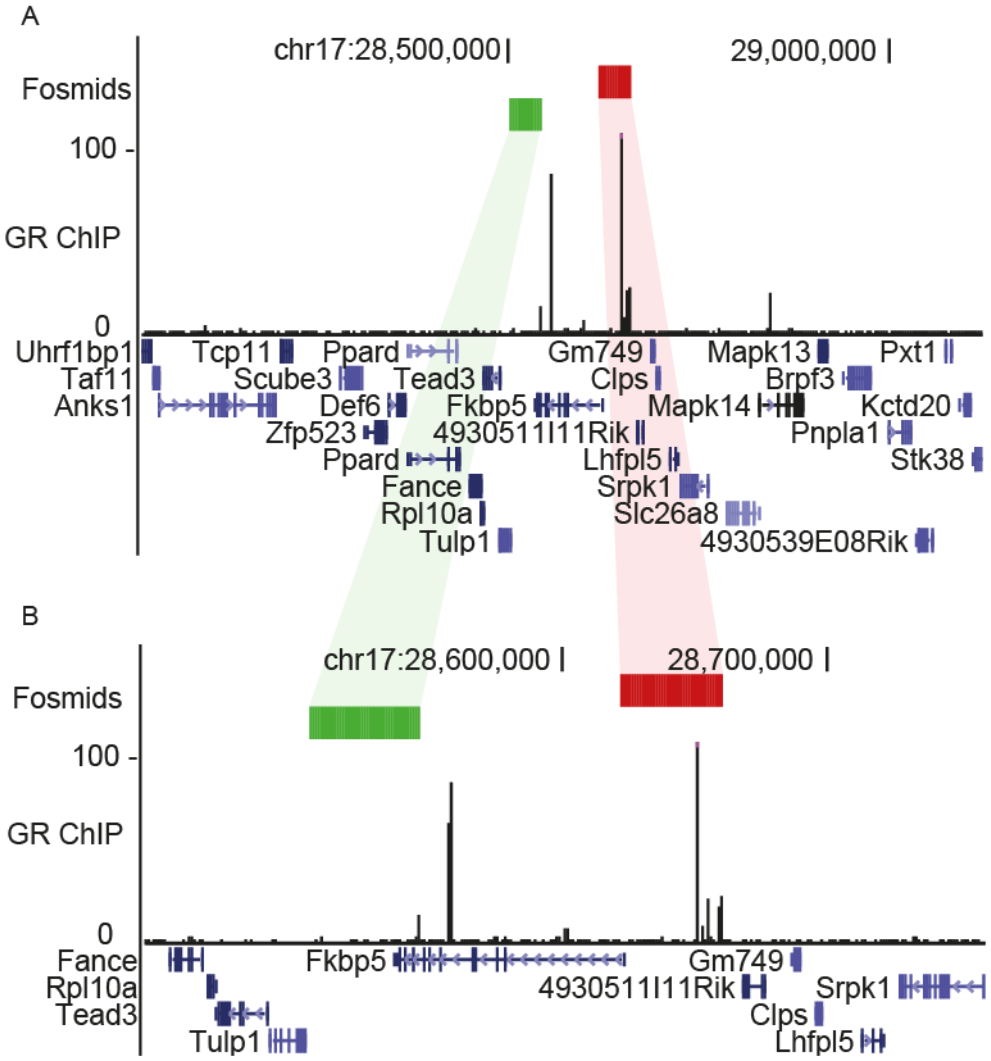

Figure 5.1 Location of fosmids used for 3D DNA FISH at *Fkbp5* locus

A Wide view of murine *Fkbp5* locus. The position of the fosmid probes is shown as red and green boxes. ChIP-seq for GR is shown as tags/base pair. **B** Analogous to A but zoomed in on the gene to show finer detail.

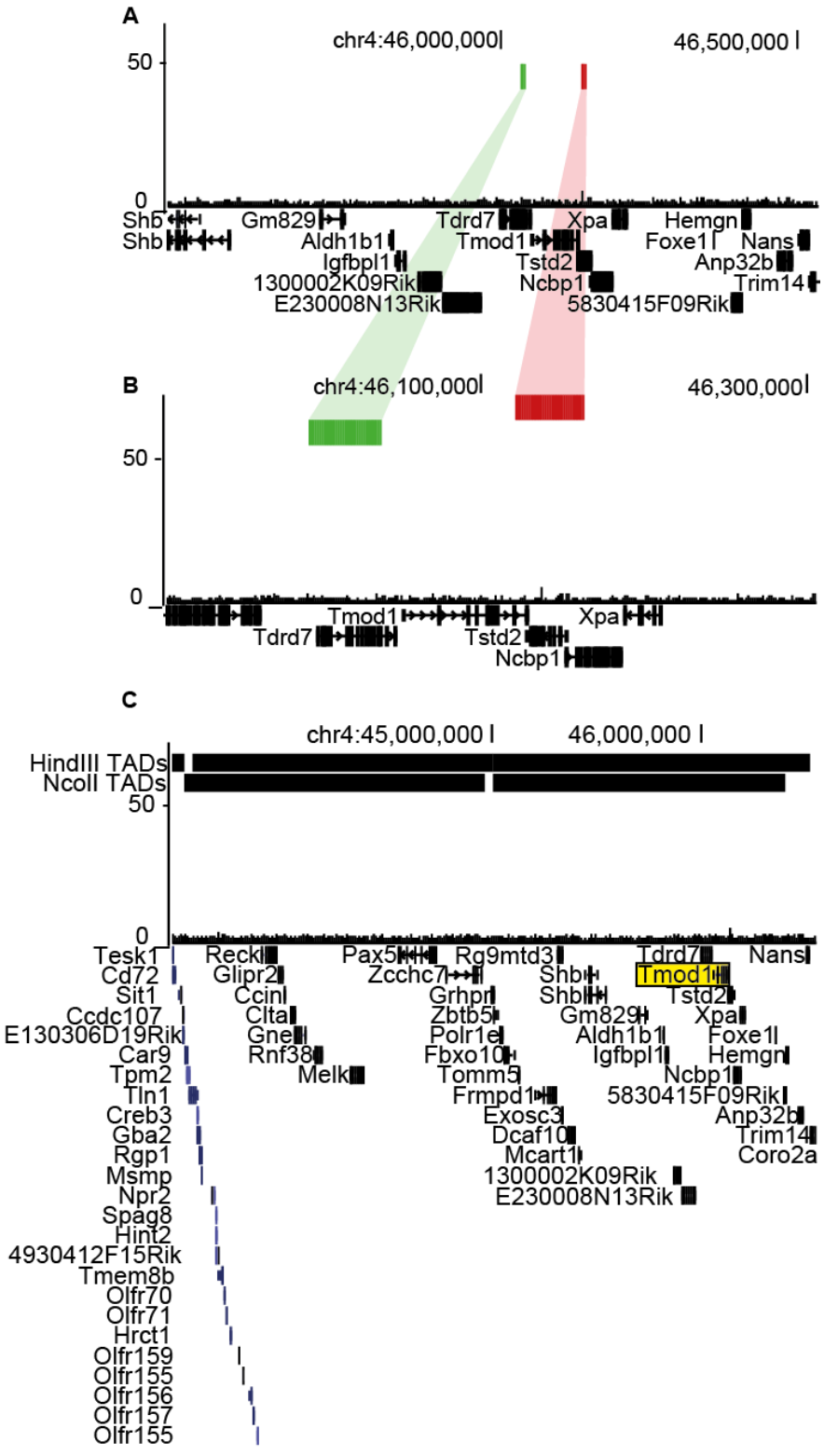

Figure 5.2 Location of fosmid probes used for 3D DNA FISH at *Tmod1* locus

Figure 5.2 Location of fosmid probes used for 3D DNA FISH at *Tmod1* locus

A Wide view of murine *Tmod1* locus. The position of the fosmid probes is shown as red and green boxes. ChIP-seq for GR is shown as tags/base pair. **B** Analogous to A but zoomed in on the gene to show finer detail. **C** Very wide view to show no GR bound within either of the two sets of TADs reported in (Dixon et al., 2012) using HindIII and NcolI restriction enzymes, TADs shown in black above locus.

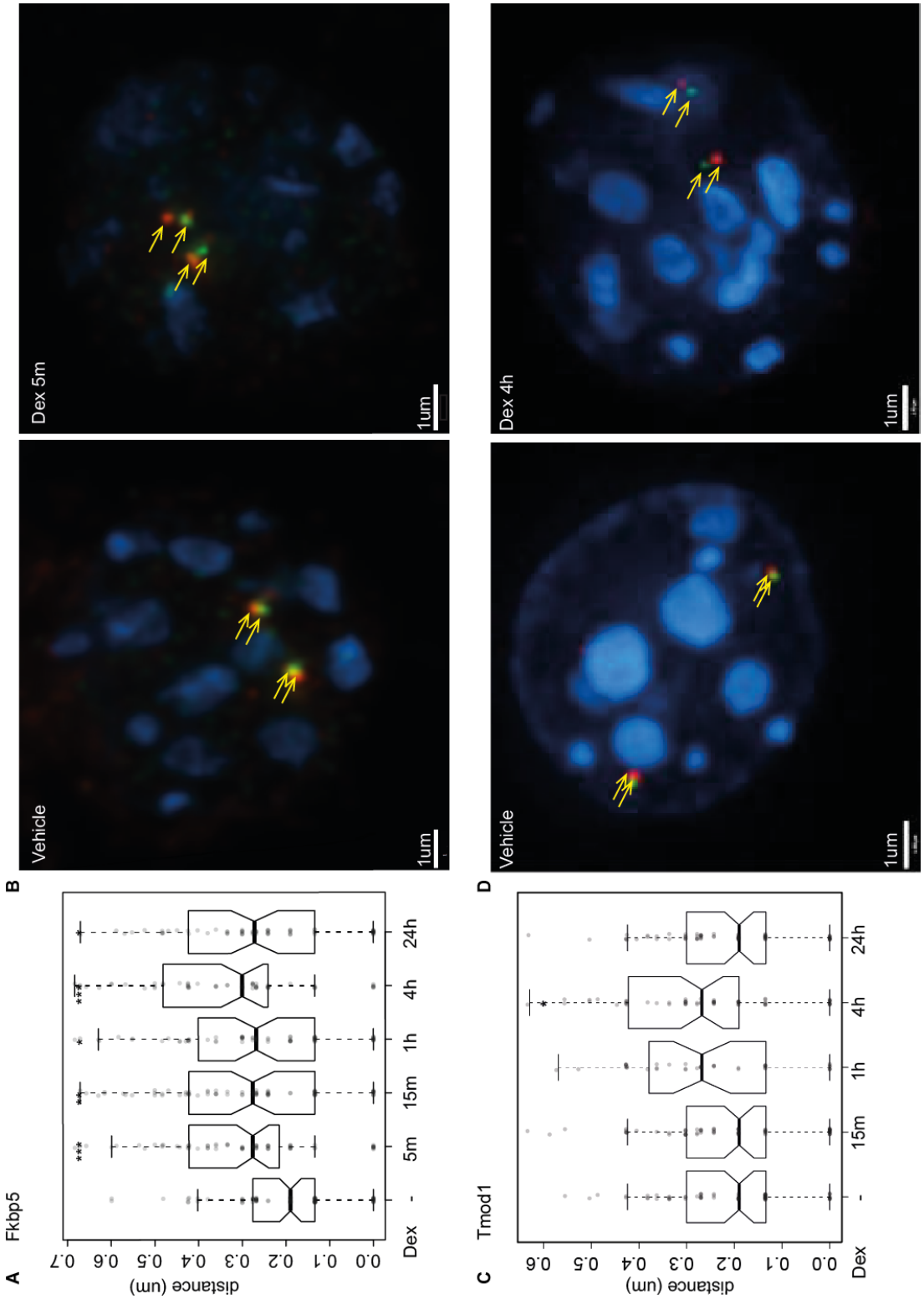

Figure 5.3 Chromatin decompaction in response to glucocorticoids

Figure 5.3 Chromatin decompaction in response to glucocorticoids

A Inter-probe distance measured across *Fkbp5* locus after treatment of mouse BMDM with 100nM dexamethasone for the indicated times as described in Methods (section). **B** Representative images of nuclei measured in A. Note the clear separation of the two probes on both loci in the treated cells , probes indicated by arrows. **C&D** Analogous to A&B but measured across *Tmod1* locus for comparison. n = 80 for each dataset. Horizontal line = median; grey circles = data points; whiskers = 1.5x interquartile range; n= ~80 for each dataset;* = $p<0.05$, ** =$p<0.005$, ***=$p<0.0005$ Wilcoxon rank sum;Dex = dexamethasone 100nM. Data was taken blinded to the treatment condition.

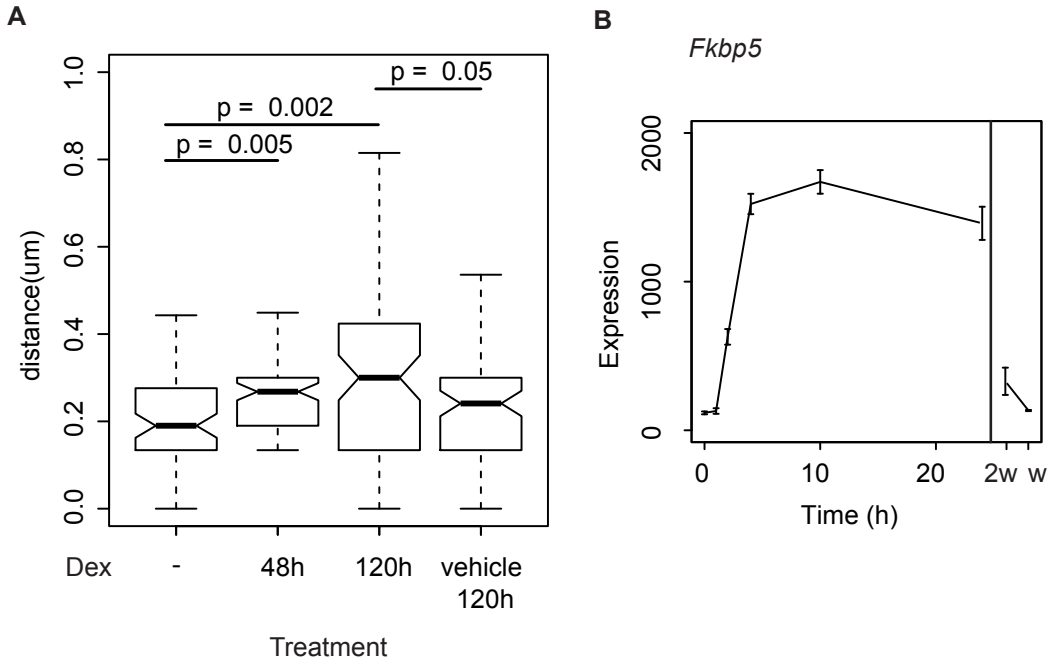

Figure 5.4 Prolonged chromatin decompaction at *Fkbp5* locus

AInter-probe distance across the *Fkbp5* locus in mBMDM stimulated with dexamethasone 100nM for the given times. Comparison is also shown with a vehicle treated sample that had been in culture for the same length of time. n=80 for each dataset. Dex = dexamethasone 100nM; - = vehicle treated 48h; Median = horizontal black line; p values = Wilcoxon rank sum; whiskers are 1.5x interquartile range.**B** raw expression values for *Fkbp5* over a 24h timeseries measured by microarray. **2w** = treated for 2h with dexamethasone 100nM followed by replacing the media and leaving in culture for a further 22h;**w** = media change only, no dexamethasone.

5.3 Rapid chromatin decompaction of *Fkbp5* locus does not depend on transcription

The rapid change in the structure of the *Fkbp5*locus precedes transcriptional output by an hour and it was therefore unlikely that active transcription was pre-requisite for the effect. The toxin α-amanitin causes a transcriptional block by irreversibly binding to the Rpb1 (*Polr2a* gene) subunit of RNA Polymerase II. Consistent with a transcription independent mechanism, pre-treatment of mBMDM with α-amanitin 2.5ug/ml for 4 hours did not block the decompaction at *Fkbp5,* although it was marginally slowed, reaching statistical significance between 5 and 15 minutes treatment rather than by 5 minutes (Figure 5.5A&B). By contrast and as predicted, α-amanitin ablated the chromatin changes across the *Tmod1* locus (Figure 5.5C&D), consistent with a transcription dependent mechanism at this locus. This suggests that there may be a different, transcription independent, mechanism underlying the changes at *Fkbp5*.

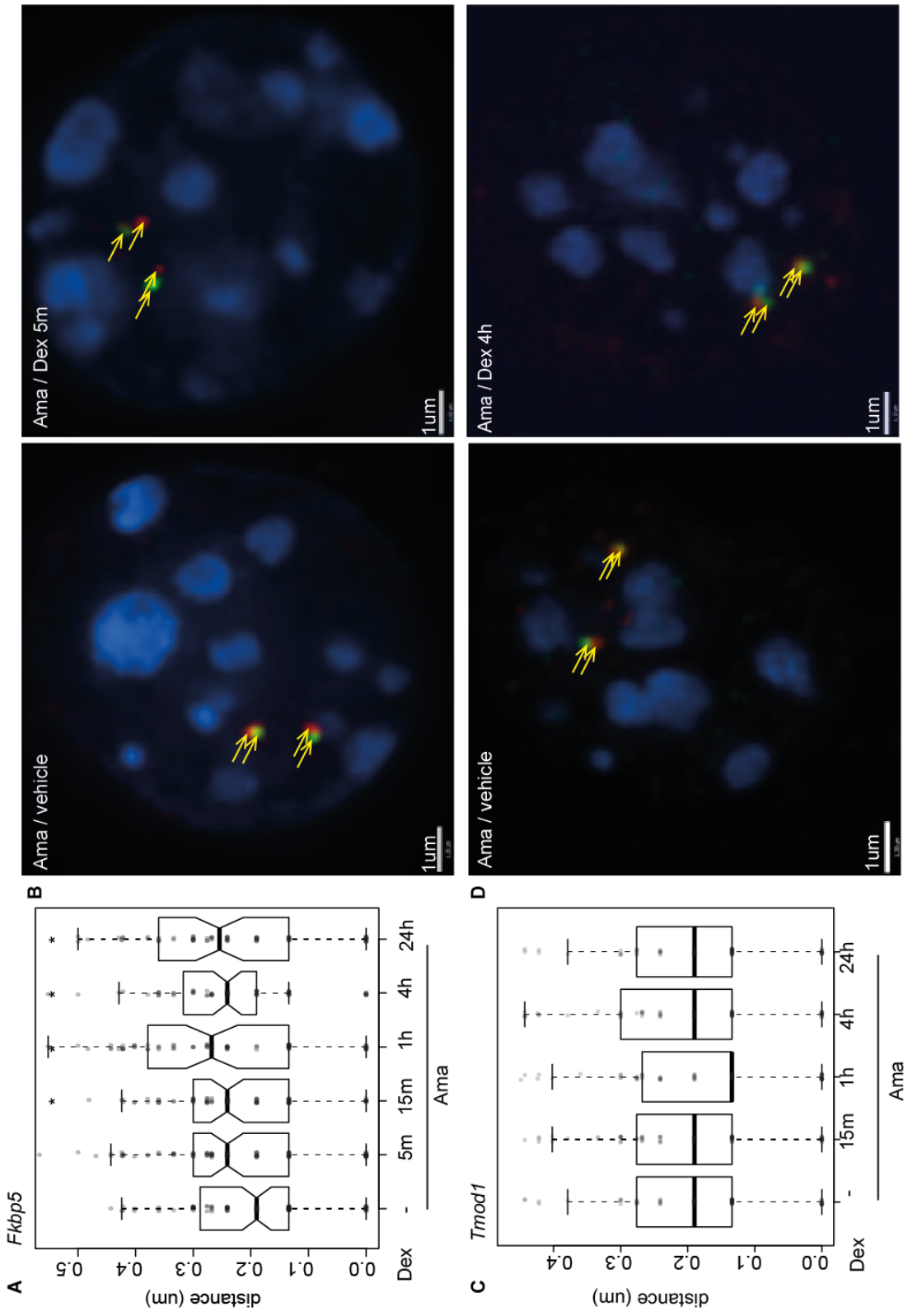

Figure 5.5 Alpha-amanitin does not block rapid decompaction at *Fkbp5*

Figure 5.5Alpha-amanitin does not block rapid decompaction at *Fkbp5*

A Inter-probe distance measured across *Fkbp5* locus after treatment with dexamethasone 100nM for the indicated times. **B** Representative images of nuclei measured in A. **C&D** Analogous to A&B but measured across *Tmod1* locus for comparison. Horizontal line = median; grey circles = data points; whiskers = 1.5x interquartile range, n= 80 for each dataset; * = $p<0.05$, Wilcoxon rank sum; Dex = dexamethasone 100nM; Ama = pre-treated with 2.5ug/ml alpha amanitin for 4h.

5.4 GR binds rapidly at enhancers in the *Fkbp5* locus

The marked difference between the changes to chromatin architecture between the two loci discussed above suggested that the strong local GR peaks at *Fkbp5*, absent at *Tmod1*, may be involved. The ChIP-seq data was measured at 2h treatment. To confirm that GR bound on a timescale that would be consistent with a genomic role in the rapid effect, binding was measured at the upstream (-28kb), downstream (+65) and promoter by ChIP-qPCR for shorter time points. Consistent with a direct role of binding, GR binding to the -28kb element was detectable within 5 minutes, and binding to the +65 element by 15 minutes (Figure 5.6).

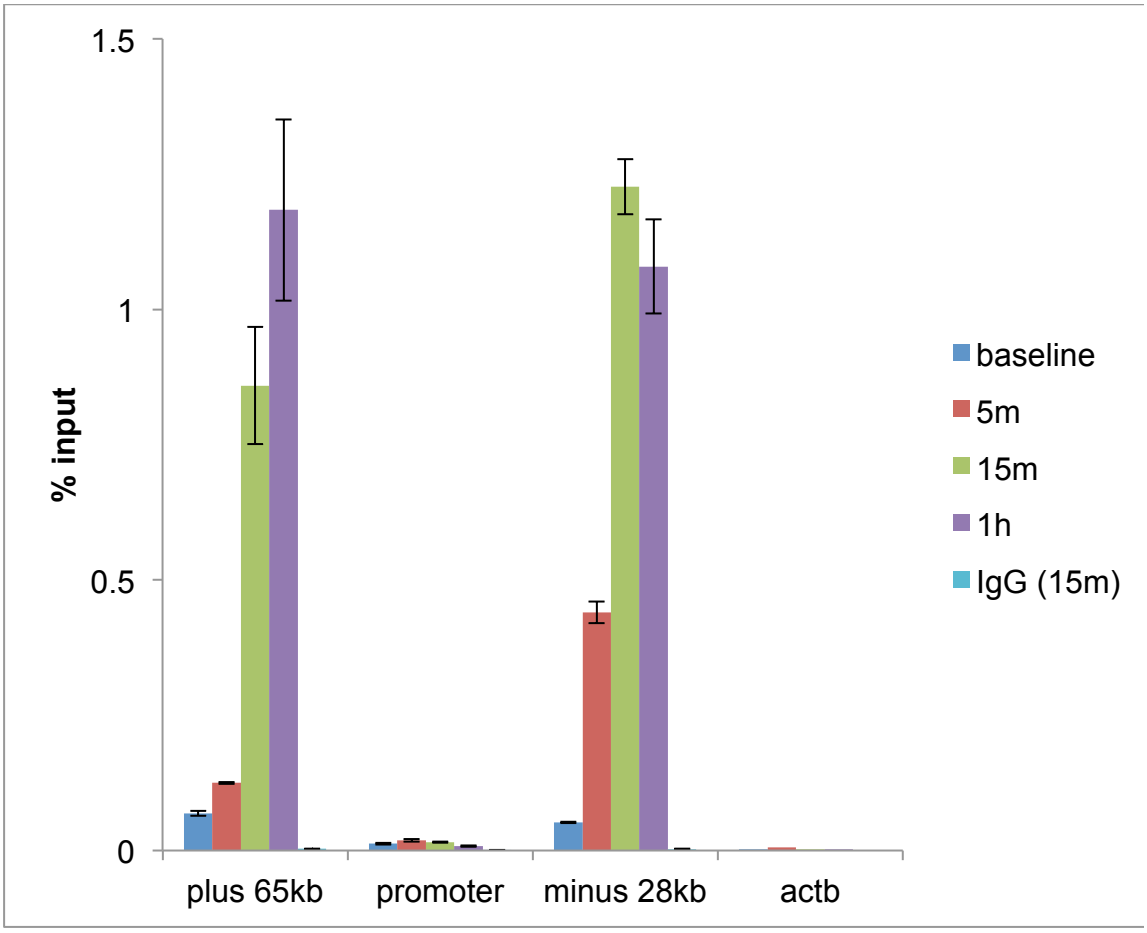

Figure 5.6 Glucocorticoid receptor binding at *Fkbp5* locus

Glucocorticoid receptor binding measured by ChIP-qPCR for the downstream enhancer (+65kb), promoter and upstream enhancer (-28kb) of Fkbp5. Data is shown for a 4 point time series (baseline, 5min, 15min,1h) of treatment with 100nM dexamethasone. Normal IgG and a control site in the promoter of *Actb* (actb) is also shown. Error bars are 2xSEM for technical replicates, data is shown is one of two biological replicates and is representative of both.

The data presented above show the distal regulatory elements and promoters moving apart on activation, albeit that the resolution of DNA FISH is not sufficient to resolve the 28kb distance to the upstream element. This does not immediately fit with prevailing models that requires increased interaction of enhancers with promoters to induce transcription (Krivega and Dean, 2012). The models might be reconciled if a decompact state reflects greater freedom of movement, so that on average the decompact state is permissive to transient, activating, enhancer-promoter contacts. If this were the case, and the enhancer promoter interactions were of sufficient duration, one might see two populations of apparent inter-marker distance within the data, a smaller one with shorter distances, the other larger with longer. The smaller set may be insufficient to show in a single data set the relatively low throughput techniques employed here (n=80 for each time point).

Pooling the total DNA FISH data for *Fkbp5* in mBMDM yielded 245 measurements for vehicle treated and 929 for dexamethasone treated cells. There was no detectable shift in the distribution to a bimodal pattern on treatment (Figure 5.7A), indeed the pattern of the distribution remained very similar (Pearson's product moment correlation =0.93). Furthermore, analysis by single cell RT-qPCR did not show a subpopulation of responding cells (Figure 5.7B).

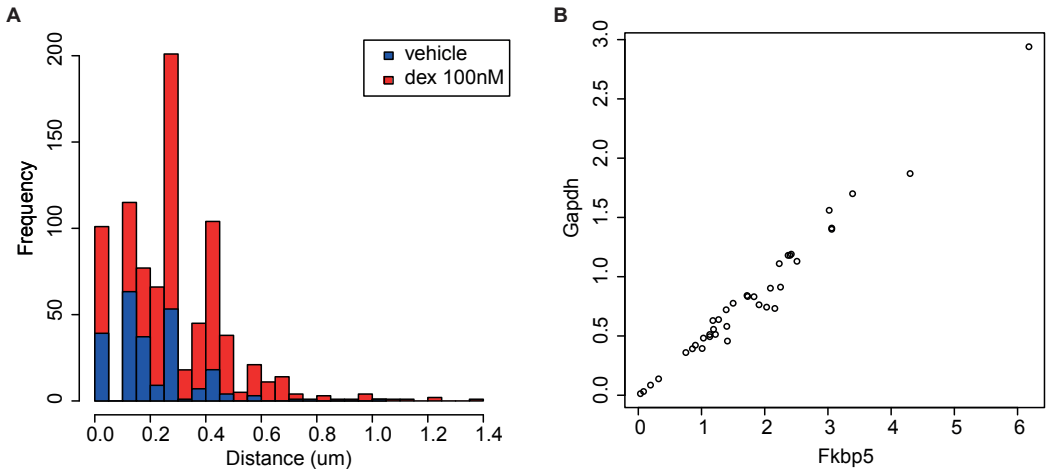

Figure 5.7 Characteristics of the response to dexamethasone at *Fkbp5*

A Pooled measurements across the *Fkbp5* locus for vehicle (blue, n=245) and dexamethasone treated (red, all time points included, n=929) mBMDM. **B** Relative expression level of *Fkbp5* and *Gapdh* in single mBMDM cells. Values are normalized to measurements taken from 10 cells for each gene. If a specific sub-population of cells respond to dexamethasone by disproportionately increasing *Fkbp5* then the distribution would divert (down) from the diagonal, (n=69).

5.5 Rapid decompaction may be a feature of GR bound loci

The locus studied above, *Fkbp5*, has a role in GC biology (section 1.1.2). To determine whether the decompaction was a generalizable feature of GC-responsive loci, the same time series analysis was repeated at an alternate GR bound GC responsive locus. A site on chromosome 19 (chr19:11,551,990-11,673,273)had five regulated genes from a family of transmembrane proteins, with one major and one minor GR bound peak in the vicinity(Figure 5.8A). The expression response was slower than *Fkbp5*, sustained at 24h and two of the genes have significant activity at baseline (Figure 5.8B).

Rapid decompaction was detectable across the locus after dexamethasone treatment (Figure 5.9A&B). As in the case of Fkbp5, decompaction clearly preceded gene induction (Figure 5.8B) despite the baseline activity and more decompact initial structure. As in the case of Fkbp5, and despite the baseline transcription, the effect of dexamethasone treatment was marginally slowed but not ablated by pre-treatment with α-amanitin (Figure 5.9C&D).

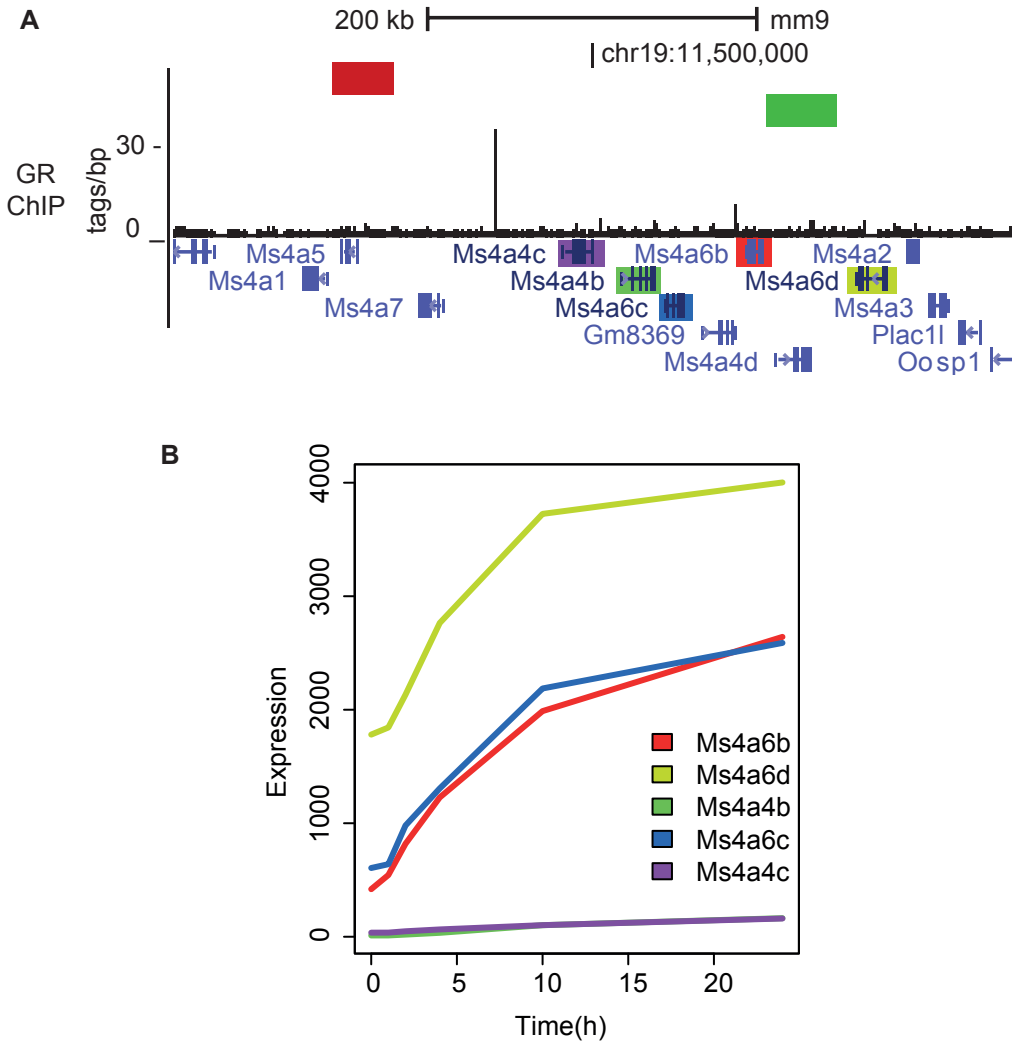

Figure 5.8 The site and response of a dexamethasone sensitive locus on chromosome 19

A UCSC browser image showing the locus. Shown are the genomic site, GR binding, regulated genes (highlighted, colours match to panel B) and the position of fosmid probes used for 3D DNA FISH (red and green boxes above track). **B** Raw expression values for each of the regulated genes within the locus from the microarray time series reported in chapter 3. Colours match highlights in panel A.

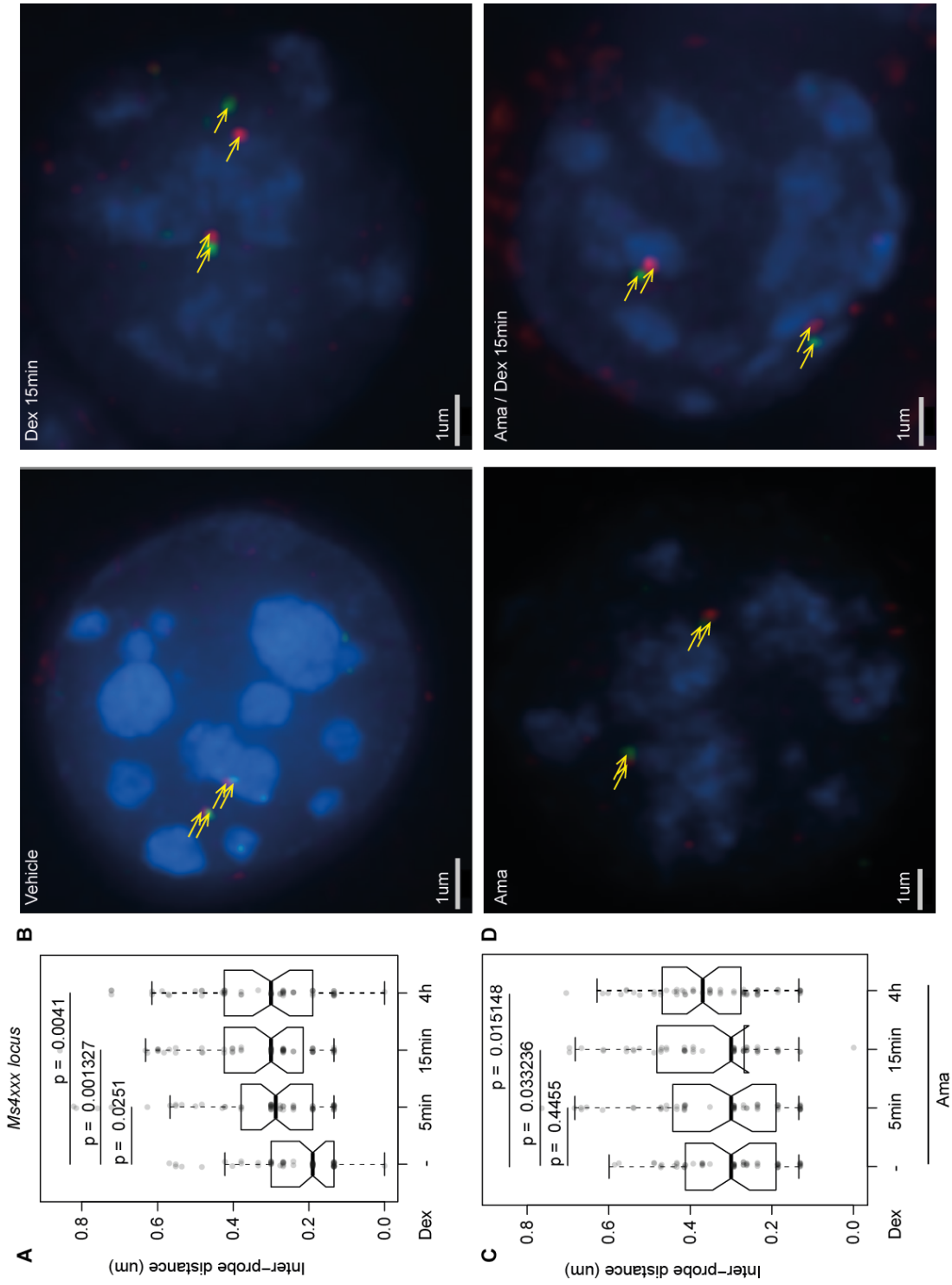

Figure 5.9 Chromatin decompaction at a GR bound locus on mouse chromosome 19

Figure 5.9 Chromatin decompaction at a GR bound locus on mouse chromosome 19

A Inter-probe distance measured across chr19 locus illustrated in (Figure 5.8) after treatment of mBMDM with dexamethasone for the indicated times. **B** Representative images of nuclei measured in A showing the position of labelled fosmid probes flanking the locus detected using red and green fluorophores. **C** Inter-probe distance measured across chr19 locus after treatment with dexamethasone following pre-treatment with alpha amanitin. **D** representative images of nuclei measured in C. Horizontal line = median; grey circles = data points; whiskers = 1.5x interquartile range, n=60 for each dataset; p-values as given, Wilcoxon rank sum; Dex = dexamethasone 100nM; Ama = pre-treated with 2.5ug/ml alpha amanitin for 4h.

5.6 Discussion

The data show that there are rapid changes to local chromatin structure around induced genes in response to GC in primary macrophages. This correlates with binding of GR and precedes the induction of transcription. The effect was not blocked by inhibiting transcription, therefore it is unlikely this effect is dependent on a transcribed eRNA (section 1.2.2.2).

Dynamic exchange of transcription factors at regulatory sites has been proposed to be directly linked to chromatin remodelling (John et al., 2008). Nuclear hormone receptors bind rapidly and in a combinatorial fashion (Glass and Ogawa, 2006; Métivier et al., 2003). Binding and turnover has been shown to be ATP dependent for GR (Stavreva et al., 2009). There is rapid recruitment of ATP utilising chromatin remodellers Brm and Brg1 to GREs (subunits of the SWI/SNF complex) within the GR responsive MMTV array (Johnson et al., 2008; Nagaich et al., 2004). The murine *Fkbp5* locus specifically was one of many reported to be less responsive (reduced to 0.64x wild type) in a cell line engineered to have a dominant negative version of the ATP requiring remodeller Brg1 (John et al., 2011).

Directly linking the binding of GR to rapid decompaction is difficult. Absence of Brg1 did not ablate the transcriptional response, only restrained it to two thirds of wild type levels (John et al., 2011), so it is not specifically required. Unfortunately an attempt to assess Brg1 loading at the sites shown in (Figure 5.6) by ChIP-qPCR was uninformative, with very low and invariant signal at all sites and treatments (data not shown). The other loci studied here were not GC responsive in that system.

The *FKBP5* locus in humans has been examined specifically in two studies and is well conserved in mouse. The first used ChIP-qPCR in A549 cells and identified GR binding similar to that presented here and in chapter 4 (Paakinaho et al., 2010). They suggest that the Brm subunit of the SWI/SNF complex is required to achieve a full response (24 fold reduced to 12 fold induction by Brm knockdown). However they were not able to demonstrate recruitment of this complex to the enhancers on GC treatment. They suggest a role for CTCF and cohesin in formation of a putative loop containing the gene, consistent with growing literature implicating these factors in the regulatory organisation of the genome (Ong and Corces, 2014). In their model the loop then compacts further on activation; the opposite of what has been demonstrated directly here by 3D DNA FISH.

Other studies in human cell lines have linked GR and BRM (Engel and Yamamoto, 2011). They showed that a subset of genes require BRM for full response and that GR binding may be reduced by BRM knockdown at the downstream *FKBP5* enhancer. For other loci they find that there was reduced nuclease accessibility on GC treatment in BRM knockdown, but they do not study *FKBP5*.

The *FKBP5* locus is of specific interest in human disease susceptibility. Links between SNPs within the *FKBP5* locus and multiple psychiatric diagnoses have been described(Binder, 2009). Further, specific risk SNPs and altered DNA methylation and chromatin conformation across the locus have been linked to higher risk of post traumatic stress disorder (Klengel et al., 2013). The association again is with increased enhancer-promoter contacts by 3C for the risk phenotype, suggested to increase the level of FKBP5 and hence alter the feedback control of the stress

response. The mechanism described is not certain since the methylation change reported is at a different enhancer to the risk allele, but the association of the SNP identified and primarily anxiety and depressive disorders appears robust. In this context the prolonged effect found in the present study (Figure 5.4) is of interest, as it hints at a structural change that can persist beyond the initial stimulus. This plasticity in chromatin may therefore be a contributor to prolonged effects following GC exposure and could have relevance to many areas of physiology and pathology involving severe stress or high doses of exogenous GC.

5.7 Summary

For the loci studied there is an association between rapid decompaction of chromatin and GR binding. The mechanism of this is not clear but does not require transcription. Other studies have implicated ATP dependent chromatin remodellers in the response to GC, but without reference to the kinetics. The phenomenon occurs at but is not limited to a locus of clinical relevance in GC biology. Overall the findings are not easy to align with a model of increased enhancer-promoter interaction driving transcription, at least where these interactions are occurring in anything more than a tiny fraction of the cell population at a given moment. In fact the opposite, where GR binding appears to rapidly release constraint on a locus is more consistent with the data.

Chapter 6: Conclusions and future work

6.1 Conclusions

6.1.1 The genome wide response to GC in macrophages

The work described in this thesis has demonstrated that GC act primarily as inducers of gene expression in primary macrophages from both mouse and man, but the set of induced genes is very different between the two species. GR bound to candidate enhancers in the vicinity of inducible genes that were generally not shared between mouse and man. The differences in binding were correlated with DNA sequence changes at the enhancer sites between the two species, which caused gain or loss of predicted GR receptor-binding motifs within the enhancer.

The inter-species divergence identified is striking, for both the GR binding and downstream expression response. However equally striking is the similarity in the pattern observed: both show binding at sites distant from promoters and enriched near induced genes. The data therefore argue strongly for the mouse as a model for understanding the principles of human, and specifically macrophage, biology. Concurrently it provides evidence for where (conserved loci) and where not (divergent loci) locus specific conclusions might be extrapolated more successfully between species.

6.1.2 GC effects on chromatin organisation in macrophages

The mechanism of action of GC was investigated by imaging several different target loci using labelled probes in macrophage nuclei. The DNA at specific GC responsive loci increased the average spatial separation of probes flanking responsive

loci within minutes of exposure of macrophages to the ligand. The apparent decondensation effect was maintained for at least 24 hours and was not prevented by inhibitors of transcription.

6.2 Future work

6.2.1 Enhancer turnover and variability

The data indicate that the major change driving loss of GC response at induced genes between species is turnover of the GRE motif. Confirmation that the turnover of GR binding sites is the cause of the expression divergence could be achieved by re-engineering a degenerate GRE, from a GR bound enhancer that aligns between species but is not bound. Improving the match to the GRE consensus motif in a stepwise base-by-base process should induce binding and cause induction of the target gene. If this re-engineering is not effective it may indicate that other elements such as PU.1 may also be required, albeit that GR appears dominant in the systems studied here. Editing the genome in this manner could be achieved using, for example, the now widespread Clustered Regularly Interspaced Palindromic Repeats / Cas (CRISPR/Cas) system (Cong et al., 2013; Jinek et al., 2013). Transfection of primary mBMDM leads to activation (Stacey et al., 1996) and cell death (Roberts et al., 2009). The murine macrophage like cell line RAW264.7 is GC responsive and can be transfected with less adverse effects (Stacey et al., 1996) thus could provide a model in which to attempt the recreation of a functional GRE.

Studying an intermediate species would provide an alternate approach. Pig macrophages, both BMDM and MDM, can be grown using equivalent in vitro protocols to those used in this study and have been shown to be closer to human than mouse in response to LPS (Schroder et al., 2012). Expression and ChIP data from pig would be required to provide confirmation. Studying a conserved enhancer in human and pig that drives gene induction, that aligns but has lost the GRE and gene induction response in mouse, would support the hypothesis that it is the presence of a

consensus GRE that is causing the observed differences. The antibodies used for GR ChIP in mouse and man in this study did not work in the other species. It is possible therefore that GR ChIP in pigs may be challenging, although partly mitigated by the large numbers of cells readily available.

This thesis has not attempted to address inter-individual variability between the human volunteers, as insufficient samples were included to draw valid conclusions. People differ in their response to GC and variability is present in the expression data, for example at *CCL7* (Figure 6.1). The data presented here predict that the difference will stem, at least in part, from genetic variation at regulatory sites (Heinz et al., 2013). The ideal study to address this would include a large number of individuals, as a meaningful effect size is difficult to estimate, and match expression and ChIP-seq data. There are practical limitations to this, in addition to the cost implications. The major issue is the challenge of generating ChIP-seq data for pure macrophages from a single individual within a reasonable donation of blood. To gain good data in this study, material from 4 volunteers was pooled. Therefore an average of the GR binding patterns for these individuals had been obtained. An alternative approach is that the identified sites could be used as candidate loci within which to search for variants using sequence capture technology and re-sequencing. Far less material is required for expression analysis therefore paired RNA samples from macrophages treated with GC could be obtained for comparison at loci where variants are identified.

From a clinician's perspective a key objective is to limit the side effects of glucocorticoid therapy (section 1.1.1,Table 1.1). Different GR ligands may cause altered GR binding by favouring a particular GR conformation. Exploring the GR binding pattern induced by novel ligands is an exciting avenue to increase understanding of how they may have differential effects on gene transcription. This is the focus of on-going work with collaborators (Dr. Ruth Andrew's lab, BHF Centre for Cardiovascular Sciences, QMRI, University of Edinburgh).

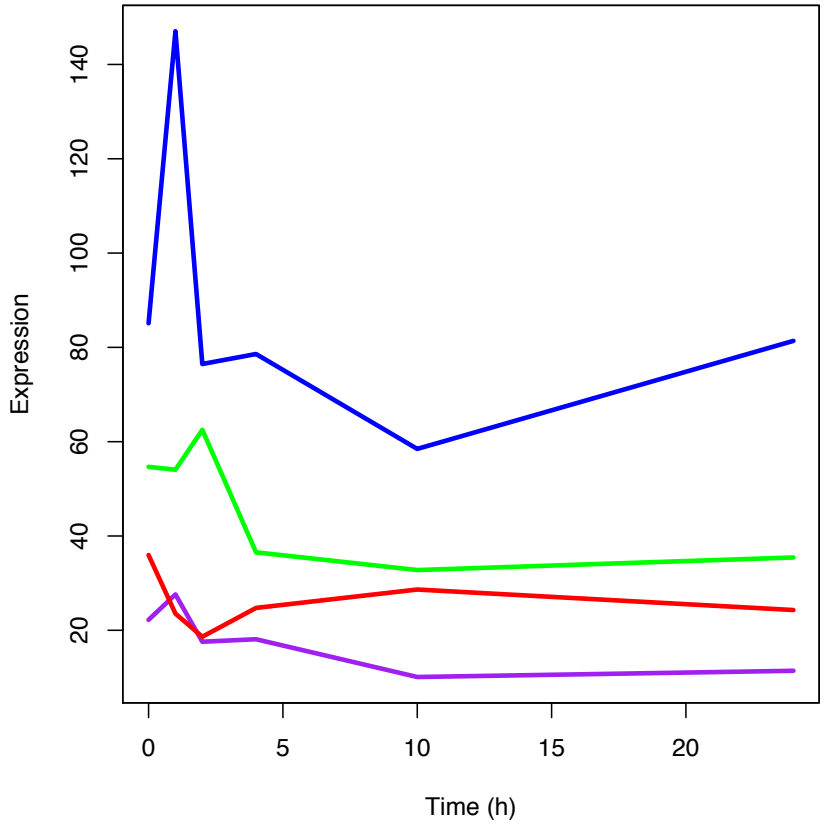

Figure 6.1 Variability in expression of CCL7 in response to GC

Expression values of *CCL7* for, each individual volunteer's monocyte derived macrophages, extracted from the microarray dataset presented in section 3.3. Each colour represents a volunteer.

6.2.2 Kinetics of the macrophage response to GC and mechanisms of repression

The data in chapter 4 show that late responding genes are equally likely to have a GR peak as early responding genes. Previous work has also shown that GR binding and transcription may not be simply correlated in time (John et al., 2009). GR dynamics are also critically affected by ligand choice. Dexamethasone has high affinity for GR, which has consequently prolonged association times compared to cortisol (in man) or corticosterone (in mice), which is likely to alter the dynamics of the global binding pattern. An ideal experiment to describe the response of macrophages to GC further would therefore have several time points with matched data from stimulation with multiple GR ligands; a non-trivial undertaking especially in the context of human primary cells.

This study does not provide a mechanism for repression by GR, although some will be due to changes in the expressed transcription factor profile (Table 3.1, Table 3.2). Time series data for the histone modifications that are associated with poised and active enhancers (section 1.2.2.1) would provide additional insight into the nature of the regulatory landscape, as would a measure of chromatin accessibility such as DNaseI hypersensitivity. Transrepression by GR predicts that a set of regulatory sites associated with the repressed genes will exist that are not marked by direct GR binding, but have active histone marks such as H3K27ac and H3K4me1 and are bound by other factors such as AP-1 (Ratman et al., 2013; Uhlenhaut et al., 2013). Study of the position and sequence of these sites, if they exist, would shed light on the mechanisms by which GC repress.

6.2.3 GC driven chromatin dynamics

Rapid, transcription independent, decompaction is found at loci responding to GC that are bound by GR (section 5.2). Acetylation of histones can produce

decompaction (section 1.2.2). The histone acetyl-transferase p300 has been implicated in pulsatile association with GR at GRE (Conway-Campbell et al., 2011) and has been shown to co-immunoprecipitate with GR (Wang et al., 2012). High quality ChIP data for p300 across a candidate region such as *Fkbp5*, either by ChIP-seq or ChIP followed by microarray (ChIP-chip), after dexamethasone treatment would determine whether p300 is dynamically recruited to the GR binding site, and whether the recruitment correlates with regulated histone aceylation in the vicinity of the bound GR. Quality time series ChIP-seq or ChIP-chip data for Brg1 following dexamethasone treatment, would also be informative.

Knockout mice for both p300 / CBP and Brg1 exist but are embryonic lethal. The homozygotes also have substantial phenotypic abnormalities, particularly in the haematopoietic system, therefore are not ideal models for study (Blake et al., 2014). Small molecule inhibitors are available for both p300 and Brg1 but the effects would not be targeted to specific loci. The overall cell phenotype and chromatin environment would therefore be changed.

To probe the mechanism further in a more specific manner it would be interesting to delete, individually and together, the enhancer elements and thereby establish whether they are required for both decompaction and the transcriptional response to GC. The decompaction detected in mBMDM at the *Fkbp5* locus was recapitulated in the murine macrophage like cell line RAW264.7 treated with GC (Figure 6.2). Deletion of the enhancers in RAW264.7 cells, for example using the CRISPR/Cas system, could therefore serve as a model for this locus. Another option would involve the use of CRISPRs to generate deletion of the control element in murine ES cells, followed by the production of macrophages in culture via the generation of embryoid bodies (Subramanian et al., 2009). This approach is currently being tested in the Hume laboratory.

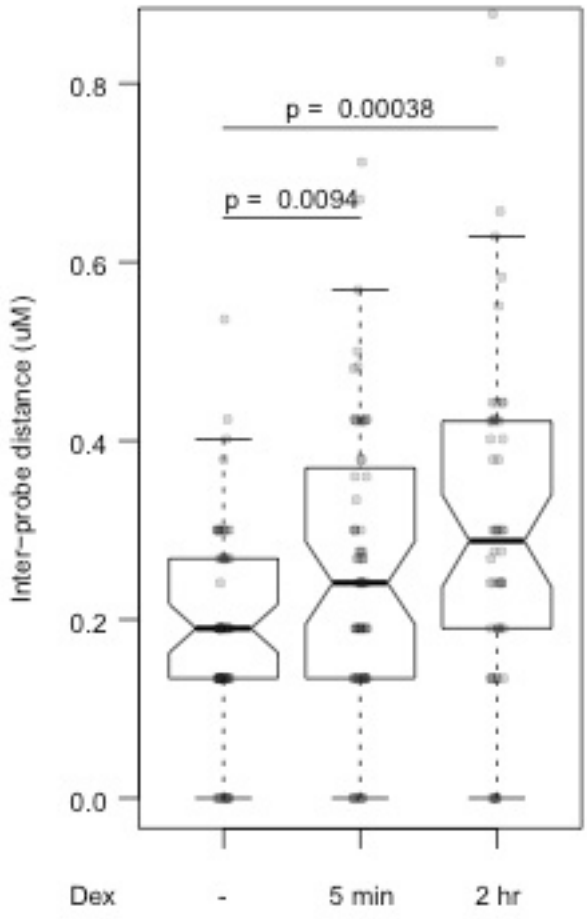

Figure 6.2 Rapid chromatin decompaction occurs in RAW264.7 cells

Inter probe distance measured across *Fkbp5* locus in RAW264.7 cells treated with dexamethasone 100nM for the indicated times.

The role of GR at the enhancers could also be probed in the RAW264.7 cell model. Transcription Activator Like (TAL) effectors (Ding et al., 2013; Zhang et al., 2011) fused to the activator VP64 can target and activate specific genes (Therizols et al., 2014). Recruiting domains of GR to the enhancers by fusing them to custom transcription factors which specifically target a single enhancer (Therizols et al., 2014) would confirm that GR is required and might also identify the domains

involved at each site. Again, ChIP for potential partners such as p300 / CBP or Mediator subunits (section 1.2.2.1), under each different condition would begin to dissect the mechanism.

Rapid decompaction can be produced by supercoiling, where twist is induced in the DNA helix by the passage of RNA polymerase II (Naughton et al., 2013; Villeponteau et al., 1984). Given the transcription independence of the GC response found in the present study supercoiling is an unlikely cause, but it could be tested. Bleomycin treatment induces DNA nicks thus relaxing the twisted formation (Naughton et al., 2013; Villeponteau and Martinson, 1987), which should then collapse any decompaction due to supercoiling.

The results for *Fkbp5* contradict previous findings by 3C in the human A549 cell line, where the downstream element increased its interaction frequency with the gene promoter in response to GC (Paakinaho et al., 2010). A central question in long-range control of gene expression is the nature of the interaction between regulatory sites and the genes they influence. Time series interaction data from mBMDM responding to GC using 3C may be highly informative and is a focus of current ongoing work.

Prolonged changes in chromatin structure following a bolus of GC may be important (section 5.2). Dysregulation of the HPA axis in severe illness is linked to worse outcomes (Annane et al., 2009; Boonen et al., 2013). Severe illness is also linked to prolonged reductions in functional capacity (Lone and Walsh, 2012). A stable change to the local organisation of GC responsive loci is therefore a candidate mechanism for involvement in the prolonged functional deficit. In the context of a prolonged response choice of ligand is important. This study used dexamethasone, which has a high affinity and long association time with GR (section 1.1.2). Comparison of the duration of effect after treatment with different GR ligands such as cortisol, which has a much shorter association time with GR, will be of interest. Further experiments might examine the compaction at *Fkbp5* (a highly conserved locus) in various cell types for treated and untreated mice. Progress to human healthy

volunteer and patient studies would be feasible if mouse results were positive, given the number of cells required for these assays is relatively small.

6.3 Summary

The data presented in this thesis describes the transcriptional response of macrophages to GC in mice and humans and demonstrates significant differences between the two species. The differences in the majority of induced genes were linked to changes in the DNA sequence at regulatory enhancers located at a distance from the genes that change. Rapid and prolonged local decondensation of chromatin was found at GC sensitive loci in macrophages.

Bridging the gap between fundamental mechanisms and physiological effects is the ultimate goal of my research. The data provide multiple exciting avenues for further investigation, some of which in due course may have important clinical implications.

References

Altonsy, M.O., Sasse, S.K., Phang, T.L., and Gerber, A.N. (2014). Context-dependent cooperation between nuclear factor κB (NF-κB) and the glucocorticoid receptor at a TNFAIP3 intronic enhancer: a mechanism to maintain negative feedback control of inflammation. J. Biol. Chem. *289*, 8231–8239.

Andersson, R., Gebhard, C., Miguel-Escalada, I., Hoof, I., Bornholdt, J., Boyd, M., Chen, Y., Zhao, X., Schmidl, C., Suzuki, T., et al. (2014). An atlas of active enhancers across human cell types and tissues. Nature *507*, 455–461.

Andrews, S. (2010). FastQC: a quality control tool for high throughput sequence data. http://www.bioinformatics.babraham.ac.uk/projects/fastqc

Annane, D., Sébille, V., Troché, G., Raphaël, J.C., Gajdos, P., and Bellissant, E. (2000). A 3-level prognostic classification in septic shock based on cortisol levels and cortisol response to corticotropin. JAMA *283*, 1038–1045.

Annane, D., Bellissant, E., Bollaert, P.-E., Briegel, J., Confalonieri, M., De Gaudio, R., Keh, D., Kupfer, Y., Oppert, M., and Meduri, G.U. (2009). Corticosteroids in the treatment of severe sepsis and septic shock in adults: a systematic review. JAMA *301*, 2362–2375.

Annane, D., Timsit, J.-F., Megarbane, B., Martin, C., Misset, B., Mourvillier, B., Siami, S., Chagnon, J.-L., Constantin, J.-M., Petitpas, F., et al. (2013). Recombinant human activated protein C for adults with septic shock: a randomized controlled trial. Am. J. Respir. Crit. Care Med. *187*, 1091–1097.

Arnold, C.D., Gerlach, D., Spies, D., Matts, J. a, Sytnikova, Y. a, Pagani, M., Lau, N.C., and Stark, A. (2014). Quantitative genome-wide enhancer activity maps for five Drosophila species show functional enhancer conservation and turnover during cis-regulatory evolution. Nat. Genet. *46*, 685–692.

Banerji, J., Rusconi, S., and Schaffner, W. (1981). Expression of a Beta-Globin Gene Is Enhanced by Remote SV40 DNA Sequences. Cell *27*, 299–308.

Barczyk, K., Ehrchen, J., Tenbrock, K., Ahlmann, M., Kneidl, J., Viemann, D., and Roth, J. (2010). Glucocorticoids promote survival of anti-inflammatory macrophages via stimulation of adenosine receptor A3. Blood *116*, 446–455.

Barozzi, I., Simonatto, M., Bonifacio, S., Yang, L., Rohs, R., Ghisletti, S., and Natoli, G. (2014). Coregulation of transcription factor binding and nucleosome occupancy through DNA features of mammalian enhancers. Mol. Cell *54*, 844–857.

Bernstein, B.E., Birney, E., Dunham, I., Green, E.D., Gunter, C., and Snyder, M. (2012). An integrated encyclopedia of DNA elements in the human genome. Nature *489*, 57–74.

Biddie, S.C., John, S., Sabo, P.J., Thurman, R.E., Johnson, T. a, Schiltz, R.L., Miranda, T.B., Sung, M.-H., Trump, S., Lightman, S.L., et al. (2011). Transcription factor AP1 potentiates chromatin accessibility and glucocorticoid receptor binding. Mol. Cell *43*, 145–155.

Binder, E.B. (2009). The role of FKBP5, a co-chaperone of the glucocorticoid receptor in the pathogenesis and therapy of affective and anxiety disorders. Psychoneuroendocrinology *34S*, S186–S195.

Blake, J.A., Bult, C.J., Eppig, J.T., Kadin, J.A., and Richardson, J.E. (2014). The Mouse Genome Database: Integration of and access to knowledge about the laboratory mouse. Nucleic Acids Res. *42*, D810–D817.

Bolger, A.M., Lohse, M., and Usadel, B. (2014). Trimmomatic: a flexible trimmer for Illumina sequence data. Bioinformatics *30*, 2114–2120.

Boonen, E., Vervenne, H., Meersseman, P., Andrew, R., Mortier, L., Declercq, P.E., Vanwijngaerden, Y.-M., Spriet, I., Wouters, P.J., Vander Perre, S., et al. (2013). Reduced cortisol metabolism during critical illness. N. Engl. J. Med. *368*, 1477–1488.

Bulger, M., and Groudine, M. (1999). Looping versus linking: Toward a model for long-distance gene activation. Genes Dev. *13*, 2465–2477.

Bulger, M., and Groudine, M. (2011). Functional and mechanistic diversity of distal transcription enhancers. Cell *144*, 327–339.

Burd, C.J., and Archer, T.K. (2013). Chromatin architecture defines the glucocorticoid response. Mol. Cell. Endocrinol. *380*, 25–31.

Chambeyron, S., and Bickmore, W. a (2004). Chromatin decondensation and nuclear reorganization of the HoxB locus upon induction of transcription. Genes Dev. *18*, 1119–1130.

Chambeyron, S., Da Silva, N.R., Lawson, K. a, and Bickmore, W. a (2005). Nuclear re-organisation of the Hoxb complex during mouse embryonic development. Development *132*, 2215–2223.

Chapman, K.E., Coutinho, A., Gray, M., Gilmour, J.S., Savill, J.S., and Seckl, J.R. (2006). Local amplification of glucocorticoids by 11beta-hydroxysteroid dehydrogenase type 1 and its role in the inflammatory response. Ann. N. Y. Acad. Sci. *1088*, 265–273.

Cheng, Y., Ma, Z., Kim, B.-H., Wu, W., Cayting, P., Boyle, A.P., Sundaram, V., Xing, X., Dogan, N., Li, J., et al. (2014). Principles of regulatory information conservation between mouse and human. Nature *515*, 371–375.

Chinenov, Y., Coppo, M., Gupte, R., Sacta, M. a, and Rogatsky, I. (2014). Glucocorticoid receptor coordinates transcription factor-dominated regulatory network in macrophages. BMC Genomics *15*, 656.

Chrivia, J.C., Kwok, R.P., Lamb, N., Hagiwara, M., Montminy, M.R., and Goodman, R.H. (1993). Phosphorylated CREB binds specifically to the nuclear protein CBP. Nature *365*, 855–859.

Clapier, C.R., and Cairns, B.R. (2009). The biology of chromatin remodeling complexes. Annu. Rev. Biochem. *78*, 273–304.

Cong, L., Ran, F.A., Cox, D., Lin, S., Barretto, R., Habib, N., Hsu, P.D., Wu, X., Jiang, W., Marraffini, L. a, et al. (2013). Multiplex genome engineering using CRISPR/Cas systems. Science *339*, 819–823.

Conway-Campbell, B.L., George, C.L., Pooley, J.R., Knight, D.M., Norman, M.R., Hager, G.L., and Lightman, S.L. (2011). The HSP90 molecular chaperone cycle regulates cyclical transcriptional dynamics of the glucocorticoid receptor and its coregulatory molecules CBP/p300 during ultradian ligand treatment. Mol. Endocrinol. *25*, 944–954.

D'Alessio, S., and Blasi, F. (2009). The urokinase receptor as an entertainer of signal transduction. Front. Biosci. *14*, 4575–4587.

Davydov, E. V, Goode, D.L., Sirota, M., Cooper, G.M., Sidow, A., and Batzoglou, S. (2010). Identifying a high fraction of the human genome to be under selective constraint using GERP++. PLoS Comput. Biol. *6*, e1001025.

Dekker, J., Rippe, K., Dekker, M., and Kleckner, N. (2002). Capturing chromosome conformation. Science *295*, 1306–1311.

DeKoter, R.P., and Singh, H. (2000). Regulation of B lymphocyte and macrophage development by graded expression of PU.1. Science *288*, 1439–1441.

Deng, W., Lee, J., Wang, H., Miller, J., Reik, A., Gregory, P.D., Dean, A., and Blobel, G. a (2012). Controlling long-range genomic interactions at a native locus by targeted tethering of a looping factor. Cell *149*, 1233–1244.

Denny, W.B., Valentine, D.L., Reynolds, P.D., Smith, D.F., and Scammell, J.G. (2000). Squirrel monkey immunophilin FKBP51 is a potent inhibitor of glucocorticoid receptor binding. Endocrinology *141*, 4107–4113.

Ding, Q., Lee, Y.-K., Schaefer, E. a K., Peters, D.T., Veres, A., Kim, K., Kuperwasser, N., Motola, D.L., Meissner, T.B., Hendriks, W.T., et al. (2013). A TALEN genome-editing system for generating human stem cell-based disease models. Cell Stem Cell *12*, 238–251.

Dixon, J., Selvaraj, S., Yue, F., Kim, A., Li, Y., and Shen, Y. (2012). Topological Domains in Mammalian genomes identified by Analysis of Chromatin Interactions. Nature *485*, 376–380.

Dostie, J., and Bickmore, W. a (2012). Chromosome organization in the nucleus - charting new territory across the Hi-Cs. Curr. Opin. Genet. Dev. *22*, 125–131.

Dostie, J., Richmond, T.A., Arnaout, R.A., Selzer, R.R., Lee, W.L., Honan, T.A., Rubio, E.D., Krumm, A., Lamb, J., Nusbaum, C., et al. (2006). Chromosome Conformation Capture Carbon Copy (5C): A massively parallel solution for mapping interactions between genomic elements. Genome Res. *16*, 1299–1309.

Duttke, S.H.C., Lacadie, S. a, Kadonaga, J.T., Ohler, U., Duttke, S.H.C., Lacadie, S. a, Ibrahim, M.M., Glass, C.K., and Corcoran, D.L. (2015). Human Promoters Are Intrinsically Directional. Mol. Cell *57*, 1–11.

Ehrchen, J., Steinmüller, L., Barczyk, K., Tenbrock, K., Nacken, W., Eisenacher, M., Nordhues, U., Sorg, C., Sunderkötter, C., and Roth, J. (2007). Glucocorticoids induce differentiation of a specifically activated, anti-inflammatory subtype of human monocytes. Blood *109*, 1265–1274.

Engel, K.B., and Yamamoto, K.R. (2011). The Glucocorticoid Receptor and the Coregulator Brm Selectively Modulate Each Other's Occupancy and Activity in a Gene-Specific Manner. Mol. Cell. Biol. *31*, 3267–3276.

Eskeland, R., Leeb, M., Grimes, G.R., Kress, C., Boyle, S., Sproul, D., Gilbert, N., Fan, Y., Skoultchi, A.I., Wutz, A., et al. (2010). Ring1B compacts chromatin structure and represses gene expression independent of histone ubiquitination. Mol. Cell *38*, 452–464.

Fairbairn, L., Kapetanovic, R., Sester, D.P., and Hume, D. a (2011). The mononuclear phagocyte system of the pig as a model for understanding human innate immunity and disease. J. Leukoc. Biol. *89*, 1–17.

Fardet, L., Petersen, I., and Nazareth, I. (2011). Prevalence of long-term oral glucocorticoid prescriptions in the UK over the past 20 years. Rheumatology (Oxford). *50*, 1982–1990.

Felsenfeld, G., Boyes, J., Chung, J., Clark, D., and Studitsky, V. (1996). Chromatin structure and gene expression. Proc. Natl. Acad. Sci. U. S. A. *93*, 9384–9388.

Forrest, A.R.R., Kawaji, H., Rehli, M., Baillie, J.K., de Hoon, M.J.L., Lassmann, T., Itoh, M., Summers, K.M., Suzuki, H., Daub, C.O., et al. (2014). A promoter-level mammalian expression atlas. Nature *507*, 462–470.

Frazer, K.A., Elnitski, L., Church, D.M., Dubchak, I., and Hardison, R.C. (2003). Cross-species sequence comparisons: a review of methods and available resources. Genome Res. *13*, 1–12.

Frijters, R., Fleuren, W., Toonen, E.J.M., Tuckermann, J.P., Reichardt, H.M., van der Maaden, H., van Elsas, A., van Lierop, M.-J., Dokter, W., de Vlieg, J., et al. (2010). Prednisolone-induced differential gene expression in mouse liver carrying wild type or a dimerization-defective glucocorticoid receptor. BMC Genomics *11*, 359.

Fromm, G., Cadiz-rivera, B., Vries, C. De, Getman, M., Mcgrath, K.E., Kingsley, P.D., Fields, J., Fiering, S., and Bulger, M. (2011). An embryonic stage – specific enhancer within the murine ɴʟ -globin locus mediates domain-wide histone hyperacetylation. Blood *117*, 5207–5215.

Galon, J., Franchimont, D., Hiroi, N., Frey, G., Boettner, A., Ehrhart-Bornstein, M., O'Shea, J.J., Chrousos, G.P., and Bornstein, S.R. (2002). Gene profiling reveals unknown enhancing and suppressive actions of glucocorticoids on immune cells. FASEB J. *16*, 61–71.

Van de Garde, M.D.B., Martinez, F.O., Melgert, B.N., Hylkema, M.N., Jonkers, R.E., and Hamann, J. (2014). Chronic exposure to glucocorticoids shapes gene expression and modulates innate and adaptive activation pathways in macrophages with distinct changes in leukocyte attraction. J. Immunol. *192*, 1196–1208.

Gautier, L., Cope, L., Bolstad, B.M., and Irizarry, R.A. (2004). affy---analysis of Affymetrix GeneChip data at the probe level. Bioinformatics *20*, 307–315.

Gavrilov, A. a., Gushchanskaya, E.S., Strelkova, O., Zhironkina, O., Kireev, I.I., Iarovaia, O. V., and Razin, S. V. (2013). Disclosure of a structural milieu for the proximity ligation reveals the elusive nature of an active chromatin hub. Nucleic Acids Res. *41*, 3563–3575.

Ghisletti, S., and Natoli, G. (2013). Deciphering cis-regulatory control in inflammatory cells. Philos. Trans. R. Soc. Lond. B. Biol. Sci. *368*, 20120370.

Ghisletti, S., Barozzi, I., Mietton, F., Polletti, S., De Santa, F., Venturini, E., Gregory, L., Lonie, L., Chew, A., Wei, C.-L., et al. (2010). Identification and characterization of enhancers controlling the inflammatory gene expression program in macrophages. Immunity *32*, 317–328.

Gilbert, N., Boyle, S., Fiegler, H., Woodfine, K., Carter, N.P., and Bickmore, W. a. (2004). Chromatin Architecture of the Human Genome. Cell *118*, 555–566.

Giorgetti, L., Galupa, R., Nora, E.P., Piolot, T., Lam, F., Dekker, J., Tiana, G., and Heard, E. (2014). Predictive polymer modeling reveals coupled fluctuations in chromosome conformation and transcription. Cell *157*, 950–963.

Glass, C.K., and Ogawa, S. (2006). Combinatorial roles of nuclear receptors in inflammation and immunity. Nat. Rev. Immunol. *6*, 44–55.

Gosselin, D., and Glass, C.K. (2014). Epigenomics of macrophages. Immunol. Rev. *262*, 96–112.

Gosselin, D., Link, V.M., Romanoski, C.E., Fonseca, G.J., Eichenfield, D.Z., Spann, N.J., Stender, J.D., Chun, H.B., Garner, H., Geissmann, F., et al. (2014). Environment Drives Selection and Function of Enhancers Controlling Tissue-Specific Macrophage Identities. Cell *159*, 1327–1340.

Gray, K. a, Daugherty, L.C., Gordon, S.M., Seal, R.L., Wright, M.W., and Bruford, E. a (2013). Genenames.org: the HGNC resources in 2013. Nucleic Acids Res. *41*, D545–D552.

Gross, K.L., and Cidlowski, J. a (2008). Tissue-specific glucocorticoid action: a family affair. Trends Endocrinol. Metab. *19*, 331–339.

Hadoke, P.W.F., Kipari, T., Seckl, J.R., and Chapman, K.E. (2013). Modulation of 11β-hydroxysteroid dehydrogenase as a strategy to reduce vascular inflammation. Curr. Atheroscler. Rep. *15*, 320.

Häggström, M. (2014). Diagram of the pathways of human steroidogenesis. Wikiversity J. Med.

Hakim, O., Sung, M.H., Voss, T.C., Splinter, E., John, S., Sabo, P.J., Thurman, R.E., Stamatoyannopoulos, J. a, De Laat, W., and Hager, G.L. (2011). Diverse gene reprogramming events occur in the same spatial clusters of distal regulatory elements. Genome Res. *21*, 697–706.

Hargreaves, D.C., Horng, T., and Medzhitov, R. (2009). Control of inducible gene expression by signal-dependent transcriptional elongation. Cell *138*, 129–145.

Heintzman, N.D., Stuart, R.K., Hon, G., Fu, Y., Ching, C.W., Hawkins, R.D., Barrera, L.O., Van Calcar, S., Qu, C., Ching, K. a, et al. (2007). Distinct and predictive chromatin signatures of transcriptional promoters and enhancers in the human genome. Nat. Genet. *39*, 311–318.

Heintzman, N.D., Hon, G.C., Hawkins, R.D., Kheradpour, P., Stark, A., Harp, L.F., Ye, Z., Lee, L.K., Stuart, R.K., Ching, C.W., et al. (2009). Histone modifications at human enhancers reflect global cell-type-specific gene expression. Nature *459*, 108–112.

Heinz, S., Benner, C., Spann, N., Bertolino, E., Lin, Y.C., Laslo, P., Cheng, J.X., Murre, C., Singh, H., and Glass, C.K. (2010). Simple combinations of lineage-determining transcription factors prime cis-regulatory elements required for macrophage and B cell identities. Mol. Cell *38*, 576–589.

Heinz, S., Romanoski, C.E., Benner, C., Allison, K.A., Kaikkonen, M.U., Orozco, L.D., and Glass, C.K. (2013). Impact of natural genetic variation on enhancer selection and function. Nature *503*, 487–492.

Hench PS, Slocumb CH, Polley HF, K.E. (1950). Effect of Cortisone and Pituitary Adrenocorticotrophic Hormone (ACTH) on Rhuematic Diseases. JAMA *144*, 1327–1335.

Hindorff, L. a, Sethupathy, P., Junkins, H. a, Ramos, E.M., Mehta, J.P., Collins, F.S., and Manolio, T. a (2009). Potential etiologic and functional implications of genome-wide association loci for human diseases and traits. Proc. Natl. Acad. Sci. U. S. A. *106*, 9362–9367.

Hollenberg, S., Weinberger, C., Ong, E., Cerelli, G., Oro, A., Lebo, R., Thompson, E., Rosenfeld, M.G., and Evans, R.M. (1985). Primary structure and expression of a functional human glucocorticoid receptor cDNA. Nature *318*, 635–641.

Holmqvist, P.-H., and Mannervik, M. (2013). Genomic occupancy of the transcriptional co-activators p300 and CBP. Transcription *4*, 18–23.

Hoogenkamp, M., Krysinska, H., Ingram, R., Huang, G., Barlow, R., Clarke, D., Ebralidze, A., Zhang, P., Tagoh, H., Cockerill, P.N., et al. (2007). The Pu.1 locus is differentially regulated at the level of chromatin structure and noncoding transcription by alternate mechanisms at distinct developmental stages of hematopoiesis. Mol. Cell. Biol. *27*, 7425–7438.

Hsieh, C.-L., Fei, T., Chen, Y., Li, T., Gao, Y., Wang, X., Sun, T., Sweeney, C.J., Lee, G.-S.M., Chen, S., et al. (2014). Enhancer RNAs participate in androgen receptor-driven looping that selectively enhances gene activation. Proc. Natl. Acad. Sci. U. S. A. *111*, 7319–7324.

Hu, D., Gao, X., Morgan, M. a, Herz, H.-M., Smith, E.R., and Shilatifard, A. (2013). The MLL3/MLL4 branches of the COMPASS family function as major histone H3K4 monomethylases at enhancers. Mol. Cell. Biol. *33*, 4745–4754.

Hudson, W.H., Youn, C., and Ortlund, E.A. (2013). The structural basis of direct glucocorticoid-mediated transrepression. Nat. Struct. Mol. Biol. *20*, 53–58.

Hume, D. (2008). Differentiation and heterogeneity in the mononuclear phagocyte system. Mucosal Immunol. *1*, 432–441.

Hume, D. (2012). Plenary perspective: the complexity of constitutive and inducible gene expression in mononuclear phagocytes. J. Leukoc. Biol. *92*, 433–444.

Hume, D., and Gordon, S. (1984). The correlation between plasminogen activator activity and thymidine incorporation in mouse bone marrow-derived macrophages.

Opposing actions of colony-stimulating factor, phorbol myristate acetate, dexamethasone and prostaglandin E. Exp. Cell Res. *150*, 347–355.

Hume, D.A., and Freeman, T.C. (2014). Transcriptomic analysis of mononuclear phagocyte differentiation and activation. Immunol. Rev. *262*, 74–84.

Hume, A., Stephens, W., Warren, H.S., and Curtin, J. (1985). Preparation and Characterization of Human Bone Marrow-Derived Macrophages. J. Leukoc. Biol. *38*, 541–552.

Illingworth, R.S., and Bird, A.P. (2009). CpG islands--'a rough guide'. FEBS Lett. *583*, 1713–1720.

Ingersoll, M. a, Spanbroek, R., Lottaz, C., Gautier, E.L., Frankenberger, M., Hoffmann, R., Lang, R., Haniffa, M., Collin, M., Tacke, F., et al. (2010). Comparison of gene expression profiles between human and mouse monocyte subsets. Blood *115*, e10–e19.

Irvine, K.M., Andrews, M.R., Fernandez-Rojo, M. a, Schroder, K., Burns, C.J., Su, S., Wilks, A.F., Parton, R.G., Hume, D. a, and Sweet, M.J. (2009). Colony-stimulating factor-1 (CSF-1) delivers a proatherogenic signal to human macrophages. J. Leukoc. Biol. *85*, 278–288.

Jääskeläinen, T., Makkonen, H., and Palvimo, J.J. (2011). Steroid up-regulation of FKBP51 and its role in hormone signaling. Curr. Opin. Pharmacol. *11*, 326–331.

Jenkins, S.J., and Hume, D. a (2014). Homeostasis in the mononuclear phagocyte system. Trends Immunol. *35*, 358–367.

Jinek, M., East, A., Cheng, A., Lin, S., Ma, E., and Doudna, J. (2013). RNA-programmed genome editing in human cells. Elife *2013*, 1–9.

John, S., Sabo, P.J., Johnson, T. a, Sung, M.-H., Biddie, S.C., Lightman, S.L., Voss, T.C., Davis, S.R., Meltzer, P.S., Stamatoyannopoulos, J. a, et al. (2008). Interaction of the glucocorticoid receptor with the chromatin landscape. Mol. Cell *29*, 611–624.

John, S., Johnson, T. a, Sung, M.-H., Biddie, S.C., Trump, S., Koch-Paiz, C. a, Davis, S.R., Walker, R., Meltzer, P.S., and Hager, G.L. (2009). Kinetic complexity of the global response to glucocorticoid receptor action. Endocrinology *150*, 1766–1774.

John, S., Sabo, P.J., Thurman, R.E., Sung, M.-H., Biddie, S.C., Johnson, T. a, Hager, G.L., and Stamatoyannopoulos, J. a (2011). Chromatin accessibility pre-determines glucocorticoid receptor binding patterns. Nat. Genet. *43*, 264–268.

Johnson, T.A., Elbi, C., Parekh, B.S., Hager, G.L., and John, S. (2008). Chromatin Remodeling Complexes Interact Dynamically with a Glucocorticoid Receptor – regulated Promoter. Mol. Biol. Cell *19*, 3308–3322.

Kagey, M.H., Newman, J.J., Bilodeau, S., Zhan, Y., Orlando, D. a, van Berkum, N.L., Ebmeier, C.C., Goossens, J., Rahl, P.B., Levine, S.S., et al. (2010). Mediator and cohesin connect gene expression and chromatin architecture. Nature *467*, 430–435.

Kaikkonen, M.U., Spann, N.J., Heinz, S., Romanoski, C.E., Allison, K.A., Stender, J.D., Chun, H.B., Tough, D.F., Prinjha, R.K., Benner, C., et al. (2013). Remodeling of the Enhancer Landscape during Macrophage Activation Is Coupled to Enhancer Transcription. Mol. Cell *51*, 310–325.

Kapetanovic, R., Fairbairn, L., Beraldi, D., Sester, D.P., Archibald, A.L., Tuggle, C.K., and Hume, D. a (2012). Pig bone marrow-derived macrophages resemble human macrophages in their response to bacterial lipopolysaccharide. J. Immunol. *188*, 3382–3394.

Kauffmann, A., Gentleman, R., and Huber, W. (2009). arrayQualityMetrics--a bioconductor package for quality assessment of microarray data. Bioinformatics *25*, 415–416.

Kent, W.J., Sugnet, C.W., Furey, T.S., Roskin, K.M., Pringle, T.H., Zahler, A.M., and Haussler, D. (2002). The Human Genome Browser at UCSC. 996–1006.

Kerschen, E.J., Fernandez, J. a, Cooley, B.C., Yang, X. V, Sood, R., Mosnier, L.O., Castellino, F.J., Mackman, N., Griffin, J.H., and Weiler, H. (2007). Endotoxemia and sepsis mortality reduction by non-anticoagulant activated protein C. J. Exp. Med. *204*, 2439–2448.

Klemsz, M., McKercher, S., and Celada, A. (1990). The macrophage and B cell-specific transcription factor PU. 1 is related to the ets oncogene. Cell *61*, 113–124.

Klengel, T., Mehta, D., Anacker, C., Rex-Haffner, M., Pruessner, J.C., Pariante, C.M., Pace, T.W.W., Mercer, K.B., Mayberg, H.S., Bradley, B., et al. (2013). Allele-specific FKBP5 DNA demethylation mediates gene-childhood trauma interactions. Nat. Neurosci. *16*, 33–41.

Krivega, I., and Dean, A. (2012). Enhancer and promoter interactions-long distance calls. Curr. Opin. Genet. Dev. *22*, 79–85.

Krivega, I., Dale, R.K., and Dean, A. (2014). Role of LDB1 in the transition from chromatin looping to transcription activation. Genes Dev. *28*, 1278–1290.

Lam, M.T.Y., Cho, H., Lesch, H.P., Gosselin, D., Heinz, S., Tanaka-Oishi, Y., Benner, C., Kaikkonen, M.U., Kim, A.S., Kosaka, M., et al. (2013). Rev-Erbs repress

macrophage gene expression by inhibiting enhancer-directed transcription. Nature *498*, 511–515.

Lan, N.C., Graham, B., Bartter, F.C., and Baxter, J.D. (1982). Binding of Steroids to Mineralocorticoid Receptors: Implications for in Vivo Occupancy by Glucocorticoids. J. Clin. Endocrinol. Metab. *54*, 332–342.

Langmead, B., and Salzberg, S. (2012). Fast gapped-read alignment with Bowtie 2. Nat. Methods *9*, 357–359.

Lattin, J.E., Schroder, K., Su, A.I., Walker, J.R., Zhang, J., Wiltshire, T., Saijo, K., Glass, C.K., Hume, D. a, Kellie, S., et al. (2008). Expression analysis of G Protein-Coupled Receptors in mouse macrophages. Immunome Res. *4*, 5.

Laurie, S., Toll-Riera, M., Radó-Trilla, N., and Albà, M.M. (2012). Sequence shortening in the rodent ancestor. Genome Res. *22*, 478–485.

Lavin, Y., Winter, D., Blecher-Gonen, R., David, E., Keren-Shaul, H., Merad, M., Jung, S., and Amit, I. (2014). Tissue-Resident Macrophage Enhancer Landscapes Are Shaped by the Local Microenvironment. Cell *159*, 1312–1326.

Lee, J., Smith, E., and Shilatifard, A. (2010). The language of histone crosstalk. Cell *142*, 682–685.

Lee, W., Haslinger, A., Karin, M., and Tjian, R. (1987). Activation of transcription by two factors that bind promoter and enhancer sequences of the human metallothionein gene and SV40. Nature *325*, 368–372.

Lenhard, B., Sandelin, A., and Carninci, P. (2012). Metazoan promoters: emerging characteristics and insights into transcriptional regulation. Nat. Rev. Genet. *13*, 233–245.

Lettice, L. a., Heaney, S.J.H., Purdie, L. a., Li, L., de Beer, P., Oostra, B. a., Goode, D., Elgar, G., Hill, R.E., and de Graaff, E. (2003). A long-range Shh enhancer regulates expression in the developing limb and fin and is associated with preaxial polydactyly. Hum. Mol. Genet. *12*, 1725–1735.

Levine, M. (2010). Transcriptional enhancers in animal development and evolution. Curr. Biol. *20*, R754–R763.

Li, G., and Reinberg, D. (2011). Chromatin higher-order structures and gene regulation. Curr. Opin. Genet. Dev. *21*, 175–186.

Li, W., Notani, D., Ma, Q., Tanasa, B., Nunez, E., Chen, A.Y., Merkurjev, D., Zhang, J., Ohgi, K., Song, X., et al. (2013). Functional roles of enhancer RNAs for oestrogen-dependent transcriptional activation. Nature *498*, 516–520.

Lieberman-Aiden, E., van Berkum, N.L., Williams, L., Imakaev, M., Ragoczy, T., Telling, A., Amit, I., Lajoie, B.R., Sabo, P.J., Dorschner, M.O., et al. (2009). Comprehensive mapping of long-range interactions reveals folding principles of the human genome. Science *326*, 289–293.

Lonard, D.M., and O'Malley, B.W. (2012). Nuclear receptor coregulators: modulators of pathology and therapeutic targets. Nat. Rev. Endocrinol. *8*, 598–604.

Lone, N.I., and Walsh, T.S. (2012). Impact of intensive care unit organ failures on mortality during the five years after a critical illness. Am. J. Respir. Crit. Care Med. *186*, 640–647.

Lu, N.Z., and Cidlowski, J. a (2004). The origin and functions of multiple human glucocorticoid receptor isoforms. Ann. N. Y. Acad. Sci. *1024*, 102–123.

Luger, K., Mader, A.W., Richmond, R.K., Sargent, D.F., and Richmond, T.J. (1997). Crystal structure of the nucleosome core particle at 2.8A˚ resolution. Nature *389*, 251–260.

Malik, S., and Roeder, R.G. (2010). The metazoan Mediator co-activator complex as an integrative hub for transcriptional regulation. Nat. Rev. Genet. *11*, 761–772.

Markaki, Y., Smeets, D., Fiedler, S., Schmid, V.J., Schermelleh, L., Cremer, T., and Cremer, M. (2012). The potential of 3D-FISH and super-resolution structured illumination microscopy for studies of 3D nuclear architecture: 3D structured illumination microscopy of defined chromosomal structures visualized by 3D (immuno)-FISH opens new perspectives for stud. Bioessays *34*, 412–426.

McNally, J.G., Müller, W.G., Walker, D., Wolford, R., and Hager, G.L. (2000). The glucocorticoid receptor: rapid exchange with regulatory sites in living cells. Science *287*, 1262–1265.

Meijsing, S.H., Pufall, M.A., So, A.Y., Bates, D.L., Chen, L., and Yamamoto, K.R. (2009). DNA Binding Site Sequence Directs Glucocrticoid Receptor Structure and Activity. Science (80-.). *324*, 407–410.

Métivier, R., Penot, G., Hübner, M.R., Reid, G., Brand, H., Koš, M., and Gannon, F. (2003). Estrogen receptor-α directs ordered, cyclical, and combinatorial recruitment of cofactors on a natural target promoter. Cell *115*, 751–763.

Miranda, T.B., Morris, S. a, and Hager, G.L. (2013). Complex genomic interactions in the dynamic regulation of transcription by the glucocorticoid receptor. Mol. Cell. Endocrinol. *380*, 16–24.

Montavon, T., Soshnikova, N., Mascrez, B., Joye, E., Thevenet, L., Splinter, E., de Laat, W., Spitz, F., and Duboule, D. (2011). A regulatory archipelago controls Hox genes transcription in digits. Cell *147*, 1132–1145.

Morey, C., Da Silva, N.R., Perry, P., and Bickmore, W. a (2007). Nuclear reorganisation and chromatin decondensation are conserved, but distinct, mechanisms linked to Hox gene activation. Development *134*, 909–919.

Nagaich, A.K., Walker, D. a, Wolford, R., and Hager, G.L. (2004). Rapid periodic binding and displacement of the glucocorticoid receptor during chromatin remodeling. Mol. Cell *14*, 163–174.

Natoli, G. (2010). Maintaining Cell Identity through Global Control of Genomic Organization. Immunity *33*, 12–24.

Natoli, G., Ghisletti, S., and Barozzi, I. (2011). The genomic landscapes of inflammation. Genes Dev. *25*, 101–106.

Naughton, C., Avlonitis, N., Corless, S., Prendergast, J.G., Mati, I.K., Eijk, P.P., Cockroft, S.L., Bradley, M., Ylstra, B., and Gilbert, N. (2013). Transcription forms and remodels supercoiling domains unfolding large-scale chromatin structures. Nat. Struct. Mol. Biol. *20*, 387–395.

Nerlov, C., and Graf, T. (1998). PU.1 induces myeloid lineage commitment in multipotent hematopoietic progenitors. Genes Dev. *12*, 2403–2412.

Nicolaides, N.C., Kyratzi, E., Lamprokostopoulou, A., Chrousos, G.P., and Charmandari, E. (2015). Stress, the stress system and the role of glucocorticoids. Neuroimmunomodulation *22*, 6–19.

Nixon, M., Andrew, R., and Chapman, K.E. (2013). It takes two to tango: dimerisation of glucocorticoid receptor and its anti-inflammatory functions. Steroids *78*, 59–68.

Noordermeer, D., Leleu, M., Splinter, E., Rougemont, J., De Laat, W., and Duboule, D. (2011). The dynamic architecture of Hox gene clusters. Science *334*, 222–225.

Noordermeer, D., Leleu, M., Schorderet, P., Joye, E., Chabaud, F., and Duboule, D. (2014). Temporal dynamics and developmental memory of 3D chromatin architecture at Hox gene loci. Elife *3*, e02557.

Ntini, E., Järvelin, A.I., Bornholdt, J., Chen, Y., Boyd, M., Jørgensen, M., Andersson, R., Hoof, I., Schein, A., Andersen, P.R., et al. (2013). Polyadenylation site-induced decay of upstream transcripts enforces promoter directionality. Nat. Struct. Mol. Biol. *20*, 923–928.

Oakley, R.H., and Cidlowski, J. a (2011). Cellular processing of the glucocorticoid receptor gene and protein: new mechanisms for generating tissue-specific actions of glucocorticoids. J. Biol. Chem. *286*, 3177–3184.

Ogawa, S., Lozach, J., Benner, C., Pascual, G., Tangirala, R.K., Westin, S., Hoffmann, A., Subramaniam, S., David, M., Rosenfeld, M.G., et al. (2005). Molecular determinants of crosstalk between nuclear receptors and toll-like receptors. Cell *122*, 707–721.

Ong, C.-T., and Corces, V.G. (2014). CTCF: an architectural protein bridging genome topology and function. Nat. Rev. Genet. *15*, 234–246.

Ostuni, R., Piccolo, V., Barozzi, I., Polletti, S., Termanini, A., Bonifacio, S., Curina, A., Prosperini, E., Ghisletti, S., and Natoli, G. (2013). Latent Enhancers Activated by Stimulation in Differentiated Cells. Cell *152*, 157–171.

Paakinaho, V., Makkonen, H., Jääskeläinen, T., and Palvimo, J.J. (2010). Glucocorticoid receptor activates poised FKBP51 locus through long-distance interactions. Mol. Endocrinol. *24*, 511–525.

Pennacchio, L. a, Bickmore, W., Dean, A., Nobrega, M. a, and Bejerano, G. (2013). Enhancers: five essential questions. Nat. Rev. Genet. *14*, 288–295.

Phillips-Cremins, J.E., Sauria, M.E.G., Sanyal, A., Gerasimova, T.I., Lajoie, B.R., Bell, J.S.K., Ong, C.-T., Hookway, T. a, Guo, C., Sun, Y., et al. (2013). Architectural protein subclasses shape 3D organization of genomes during lineage commitment. Cell *153*, 1281–1295.

Pott, S., and Lieb, J.D. (2014). What are super-enhancers? Nat. Genet. *47*, 8–12.

Presman, D.M., Ogara, M.F., Stortz, M., Alvarez, L.D., Pooley, J.R., Schiltz, R.L., Grøntved, L., Johnson, T. a, Mittelstadt, P.R., Ashwell, J.D., et al. (2014). Live cell imaging unveils multiple domain requirements for in vivo dimerization of the glucocorticoid receptor. PLoS Biol. *12*, e1001813.

Quinlan, A.R., and Hall, I.M. (2010). BEDTools: a flexible suite of utilities for comparing genomic features. Bioinformatics *26*, 841–842.

Rao, N.S., McCalman, M.T., Moulos, P., Francoijs, K.-J.J., Chatziioannou, A., Kolisis, F.N., Alexis, M.N., Mitsiou, D.J., and Stunnenberg, H.G. (2011). Coactivation of GR and NFKB alters the repertoire of their binding sites and target genes. Genome Res. *21*, 1404–1416.

Rao, S.S.P., Huntley, M.H., Durand, N.C., Stamenova, E.K., Bochkov, I.D., Robinson, J.T., Sanborn, A.L., Machol, I., Omer, A.D., Lander, E.S., et al. (2014). A 3D Map of the Human Genome at Kilobase Resolution Reveals Principles of Chromatin Looping. Cell *159*, 1665–1680.

Ratman, D., Vanden Berghe, W., Dejager, L., Libert, C., Tavernier, J., Beck, I.M., and De Bosscher, K. (2013). How glucocorticoid receptors modulate the activity of

other transcription factors: a scope beyond tethering. Mol. Cell. Endocrinol. *380*, 41–54.

Raza, S., Barnett, M.W., Barnett-Itzhaki, Z., Amit, I., Hume, D. a, and Freeman, T.C. (2014). Analysis of the transcriptional networks underpinning the activation of murine macrophages by inflammatory mediators. J. Leukoc. Biol. *96*, 167–183.

Reddy, T.E., Pauli, F., Sprouse, R.O., Neff, N.F., Newberry, K.M., Garabedian, M.J., and Myers, R.M. (2009). Genomic determination of the glucocorticoid response reveals unexpected mechanisms of gene regulation. Genome Res. *19*, 2163–2171.

Reddy, T.E., Gertz, J., Pauli, F., Kucera, K.S., Varley, K.E., Newberry, K.M., Marinov, G.K., Mortazavi, A., Williams, B. a, Song, L., et al. (2012). Effects of sequence variation on differential allelic transcription factor occupancy and gene expression. Genome Res. *22*, 860–869.

Reichardt, H.M., Tuckermann, J.P., Göttlicher, M., Vujic, M., Weih, F., Angel, P., Herrlich, P., and Schütz, G. (2001). Repression of inflammatory responses in the absence of DNA binding by the glucocorticoid receptor. EMBO J. *20*, 7168–7173.

Richard-Foy, H., and Hager, G.L. (1987). Sequence-specific positioning of nucleosomes over the steroid inducible MMTV promoter. EMBO J. *6*, 2321–2328.

Roberts, T.L., Idris, A., Dunn, J. a, Kelly, G.M., Burnton, C.M., Hodgson, S., Hardy, L.L., Garceau, V., Sweet, M.J., Ross, I.L., et al. (2009). HIN-200 Proteins Regulate Caspase. Science. *323*, 1057–1060.

Rogatsky, I., Luecke, H.F., Leitman, D.C., and Yamamoto, K.R. (2002). Alternate surfaces of transcriptional coregulator GRIP1 function in different glucocorticoid receptor activation and repression contexts. Proc. Natl. Acad. Sci. U. S. A. *99*, 16701–16706.

Ross, I.L., Yue, X., Ostrowski, M.C., and Hume, D.A. (1998). Interaction between PU.1 and Another Ets Family Transcription Factor Promotes Macrophage-specific Basal Transcription Initiation. J. Biol. Chem. *273*, 6662–6669.

De Santa, F., Barozzi, I., Mietton, F., Ghisletti, S., Polletti, S., Tusi, B.K., Muller, H., Ragoussis, J., Wei, C.-L., and Natoli, G. (2010). A Large Fraction of Extragenic RNA Pol II Transcription Sites Overlap Enhancers. PLoS Biol. *8*, e1000384.

Schiller, B.J., Chodankar, R., Watson, L.C., Stallcup, M.R., and Yamamoto, K.R. (2014). Glucocorticoid receptor binds half sites as a monomer and regulates specific target genes. Genome Biol. *15*, 418.

Schroder, K., Irvine, K.M., Taylor, M.S., Bokil, N.J., Le Cao, K.-A., Masterman, K.-A., Labzin, L.I., Semple, C. a, Kapetanovic, R., Fairbairn, L., et al. (2012). Conservation and divergence in Toll-like receptor 4-regulated gene expression in

primary human versus mouse macrophages. Proc. Natl. Acad. Sci. U. S. A. *109*, E944–E953.

Seila, A.C., Calabrese, J.M., Levine, S.S., Yeo, G.W., Rahl, P.B., Flynn, R. a, Young, R. a, and Sharp, P. a (2008). Divergent transcription from active promoters. Science *322*, 1849–1851.

Seok, J., Warren, H.S., Cuenca, A.G., Mindrinos, M.N., Baker, H. V, Xu, W., Richards, D.R., McDonald-Smith, G.P., Gao, H., Hennessy, L., et al. (2013). Genomic responses in mouse models poorly mimic human inflammatory diseases. Proc. Natl. Acad. Sci. U. S. A. *110*, 3507–3512.

Shilatifard, A. (2006). Chromatin modifications by methylation and ubiquitination: implications in the regulation of gene expression. Annu. Rev. Biochem. *75*, 243–269.

Silverman, M.N., and Sternberg, E.M. (2012). Glucocorticoid regulation of inflammation and its functional correlates: from HPA axis to glucocorticoid receptor dysfunction. Ann. N. Y. Acad. Sci. *1261*, 55–63.

Smith, E., and Shilatifard, A. (2010). The Chromatin Signaling Pathway: Diverse Mechanisms of Recruitment of Histone-Modifying Enzymes and Varied Biological Outcomes. Mol. Cell *40*, 689–701.

Smyth, G.K. (2005). Limma: linear models for microarray data. In Bioinformatics and Computational Biology Solutions Using {R} and Bioconductor, R. Gentleman, V. Carey, S. Dudoit, R. Irizarry, and W. Huber, eds. (New York: Springer), pp. 397–420.

So, a. Y.-L., Cooper, S.B., Feldman, B.J., Manuchehri, M., and Yamamoto, K.R. (2008). Conservation analysis predicts in vivo occupancy of glucocorticoid receptor-binding sequences at glucocorticoid-induced genes. Proc. Natl. Acad. Sci. *105*, 5745–5749.

Van Staa, T.P., Leufkens, H.G., Abenhaim, L., Begaud, B., Zhang, B., and Cooper, C. (2000). Use of oral corticosteroids in the United Kingdom. QJM *93*, 105–111.

Stacey, K.J., Fowles, L.F., Colman, M.S., Ostrowski, M.C., and Hume, D. a (1995). Regulation of urokinase-type plasminogen activator gene transcription by macrophage colony-stimulating factor. Mol. Cell. Biol. *15*, 3430–3441.

Stacey, K.J., Sweet, M.J., and Hume, D.A. (1996). Macrophages ingest and are activated by bacterial DNA. J. Immunol. *157*, 2116–2122.

Stahn, C., and Buttgereit, F. (2008). Genomic and nongenomic effects of glucocorticoids. Nat. Clin. Pract. Rheumatol. *4*, 525–533.

Stavreva, D. a, Wiench, M., John, S., Conway-Campbell, B.L., McKenna, M. a, Pooley, J.R., Johnson, T. a, Voss, T.C., Lightman, S.L., and Hager, G.L. (2009). Ultradian hormone stimulation induces glucocorticoid receptor-mediated pulses of gene transcription. Nat. Cell Biol. *11*, 1093–1102.

Steer, J.H., Vuong, Q., and Joyce, D. a (1997). Suppression of human monocyte tumour necrosis factor-alpha release by glucocorticoid therapy: relationship to systemic monocytopaenia and cortisol suppression. Br. J. Clin. Pharmacol. *43*, 383–389.

Stefflova, K., Thybert, D., Wilson, M.D., Streeter, I., Aleksic, J., Karagianni, P., Brazma, A., Adams, D.J., Talianidis, I., Marioni, J.C., et al. (2013). Cooperativity and rapid evolution of cobound transcription factors in closely related mammals. Cell *154*, 530–540.

Stergachis, A.B., Neph, S., Sandstrom, R., Haugen, E., Reynolds, A.P., Zhang, M., Byron, R., Canfield, T., Stelhing-Sun, S., Lee, K., et al. (2014). Conservation of trans-acting circuitry during mammalian regulatory evolution. Nature *515*, 365–370.

Strahle, U., Klock, G., and Schutz, G. (1987). A DNA sequence of 15 base pairs is sufficient to mediate both glucocorticoid and progesterone induction of gene expression. Proc. Natl. Acad. Sci. U. S. A. *84*, 7871–7875.

Stylianou, I.M., Bauer, R.C., Reilly, M.P., and Rader, D.J. (2012). Genetic basis of atherosclerosis: insights from mice and humans. Circ. Res. *110*, 337–355.

Subramanian, A., Guo, B., Marsden, M.D., Galic, Z., Kitchen, S., Kacena, A., Brown, H.J., Cheng, G., and Zack, J.A. (2009). Macrophage differentiation from embryoid bodies derived from human embryonic stem cells. J. Stem Cells *4*, 29–45.

Surjit, M., Ganti, K.P., Mukherji, A., Ye, T., Hua, G., Metzger, D., Li, M., and Chambon, P. (2011). Widespread negative response elements mediate direct repression by agonist-liganded glucocorticoid receptor. Cell *145*, 224–241.

Takao, K., and Miyakawa, T. (2014). Genomic responses in mouse models greatly mimic human inflammatory diseases. Proc. Natl. Acad. Sci. 1–6.

Talbert, P.B., and Henikoff, S. (2010). Histone variants--ancient wrap artists of the epigenome. Nat. Rev. Mol. Cell Biol. *11*, 264–275.

Taylor, G.C.A., Eskeland, R., Hekimoglu-Balkan, B., Pradeepa, M.M., and Bickmore, W.A. (2013). H4K16 acetylation marks active genes and enhancers of embryonic stem cells, but does not alter chromatin compaction. Genome Res. *23*, 2053–2065.

Tchen, C.R., Martins, J.R.S., Paktiawal, N., Perelli, R., Saklatvala, J., and Clark, A.R. (2010). Glucocorticoid regulation of mouse and human dual specificity

phosphatase 1 (DUSP1) genes: unusual cis-acting elements and unexpected evolutionary divergence. J. Biol. Chem. *285*, 2642–2652.

The Wellcome Trust Case Control Consortium (2007). Genome-wide association study of 14,000 cases of seven common diseases and 3,000 shared controls. Nature *447*, 661–678.

Theocharidis, A., van Dongen, S., Enright, A.J., and Freeman, T.C. (2009). Network visualization and analysis of gene expression data using BioLayout Express(3D). Nat. Protoc. *4*, 1535–1550.

Therizols, P., Illingworth, R.S., Courilleau, C., Boyle, S., Wood, A.J., and Bickmore, W. a (2014). Chromatin decondensation is sufficient to alter nuclear organization in embryonic stem cells. Science *346*, 1238–1242.

Thurman, R.E., Rynes, E., Humbert, R., Vierstra, J., Maurano, M.T., Haugen, E., Sheffield, N.C., Stergachis, A.B., Wang, H., Vernot, B., et al. (2012). The accessible chromatin landscape of the human genome. Nature *489*, 75–82.

Trotter, K.W., and Archer, T.K. (2007). Nuclear receptors and chromatin remodeling machinery. Mol. Cell. Endocrinol. *265-266*, 162–167.

Tsai, K.-L., Tomomori-Sato, C., Sato, S., Conaway, R.C., Conaway, J.W., and Asturias, F.J. (2014). Subunit architecture and functional modular rearrangements of the transcriptional mediator complex. Cell *157*, 1430–1444.

Uhlenhaut, N.H., Barish, G.D., Yu, R.T., Downes, M., Karunasiri, M., Liddle, C., Schwalie, P., Hübner, N., and Evans, R.M. (2013). Insights into Negative Regulation by the Glucocorticoid Receptor from Genome-wide Profiling of Inflammatory Cistromes. Mol. Cell *49*, 158–171.

Vandevyver, S., Dejager, L., and Libert, C. (2012). On the trail of the glucocorticoid receptor: into the nucleus and back. Traffic *13*, 364–374.

Varga, G., Ehrchen, J., Tsianakas, A., Tenbrock, K., Rattenholl, A., Seeliger, S., Mack, M., Roth, J., and Sunderkoetter, C. (2008). Glucocorticoids induce an activated, anti-inflammatory monocyte subset in mice that resembles myeloid-derived suppressor cells. J. Leukoc. Biol. *84*, 644–650.

Vierstra, J., Rynes, E., Sandstrom, R., Zhang, M., Canfield, T., Hansen, R.S., Stehling-Sun, S., Sabo, P.J., Byron, R., Humbert, R., et al. (2014). Mouse regulatory DNA landscapes reveal global principles of cis-regulatory evolution. Science (80-.). *346*, 1007–1012.

Villar, D., Flicek, P., and Odom, D.T. (2014). Evolution of transcription factor binding in metazoans - mechanisms and functional implications. Nat. Rev. Genet. *15*, 221–233.

Villeponteau, B., and Martinson, H.G. (1987). Gamma Rays and Bleomycin Nick DNA and Reverse the DNase I Sensitivity of 3-Globin Gene Chromatin In Vivo. Mol. Cell. Biol. *7*, 1917–1924.

Villeponteau, B., Lundell, M., and Martinson, H.G. (1984). Torsional Stress Promotes the DNAase I Sensitivity of Active Genes. Cell *39*, 469–478.

Visel, A., Blow, M.J., Li, Z., Zhang, T., Akiyama, J. a, Holt, A., Plajzer-Frick, I., Shoukry, M., Wright, C., Chen, F., et al. (2009). ChIP-seq accurately predicts tissue-specific activity of enhancers. Nature *457*, 854–858.

Voss, T.C., Schiltz, R.L., Sung, M.-H., Yen, P.M., Stamatoyannopoulos, J. a, Biddie, S.C., Johnson, T. a, Miranda, T.B., John, S., and Hager, G.L. (2011). Dynamic exchange at regulatory elements during chromatin remodeling underlies assisted loading mechanism. Cell *146*, 544–554.

Wang, K.C., Yang, Y.W., Liu, B., Sanyal, A., Corces-Zimmerman, R., Chen, Y., Lajoie, B.R., Protacio, A., Flynn, R. a, Gupta, R. a, et al. (2011). A long noncoding RNA maintains active chromatin to coordinate homeotic gene expression. Nature *472*, 120–124.

Wang, Q., Carroll, J.S., and Brown, M. (2005). Spatial and temporal recruitment of androgen receptor and its coactivators involves chromosomal looping and polymerase tracking. Mol. Cell *19*, 631–642.

Wang, W., Guo, C., Li, W., Li, J., Wang, W., Myatt, L., and Sun, K. (2012). Involvement of GR and p300 in the Induction of H6PD by Cortisol in Human Amnion Fibroblasts. Endocrinology *153*, 5993–6002.

Watson, L.C., Kuchenbecker, K.M., Schiller, B.J., Gross, J.D., Pufall, M. a, and Yamamoto, K.R. (2013). The glucocorticoid receptor dimer interface allosterically transmits sequence-specific DNA signals. Nat. Struct. Mol. Biol. *20*, 876–883.

Wells, C. a, Ravasi, T., Faulkner, G.J., Carninci, P., Okazaki, Y., Hayashizaki, Y., Sweet, M., Wainwright, B.J., and Hume, D. a (2003). Genetic control of the innate immune response. BMC Immunol. *4*, 5.

Williamson, I., Eskeland, R., Lettice, L. a, Hill, A.E., Boyle, S., Grimes, G.R., Hill, R.E., and Bickmore, W. a (2012). Anterior-posterior differences in HoxD chromatin topology in limb development. Development *139*, 3157–3167.

Williamson, I., Berlivet, S., Eskeland, R., Boyle, S., Illingworth, R.S., Paquette, D., Dostie, J., and Bickmore, W.A. (2014). Spatial genome organization: contrasting views from chromosome conformation capture and fluorescence in situ hybridization. Genes Dev. *28*, 2778–2791.

Wochnik, G.M., Rüegg, J., Abel, G.A., Schmidt, U., Holsboer, F., and Rein, T. (2005). FK506-binding proteins 51 and 52 differentially regulate dynein interaction and nuclear translocation of the glucocorticoid receptor in mammalian cells. J. Biol. Chem. *280*, 4609–4616.

Wu, C., Orozco, C., Boyer, J., Leglise, M., Goodale, J., Batalov, S., Hodge, C.L., Haase, J., Janes, J., Huss, J.W., et al. (2009). BioGPS: an extensible and customizable portal for querying and organizing gene annotation resources. Genome Biol. *10*, R130.

Wynn, T. a, Chawla, A., and Pollard, J.W. (2013). Macrophage biology in development, homeostasis and disease. Nature *496*, 445–455.

Xue, J., Schmidt, S. V, Sander, J., Draffehn, A., Krebs, W., Quester, I., De Nardo, D., Gohel, T.D., Emde, M., Schmidleithner, L., et al. (2014). Transcriptome-based network analysis reveals a spectrum model of human macrophage activation. Immunity *40*, 274–288.

Yokota, H., van den Engh, G., Hearst, J., Sachs, R., and Trask, B. (1995). The Journal of Cell Biology. J. Cell Biol. *130*, 1239–1249.

Yokota, H., Singer, M.J., Engh, G.J. Van Den, and Trask, B.J. (1997). Regional differences in the compaction of chromatin in human G 0 /G 1 interphase nuclei H. Chromosom. Res. *5*, 157–166.

Yue, F., Cheng, Y., Breschi, A., Vierstra, J., Wu, W., Ryba, T., Sandstrom, R., Ma, Z., Davis, C., Pope, B.D., et al. (2014). A comparative encyclopedia of DNA elements in the mouse genome. Nature *515*, 355–364.

Zaret, K.S., and Yamamoto, K.R. (1984). Reversible and persistent changes in chromatin structure accompany activation of a glucocorticoid-dependent enhancer element. Cell *38*, 29–38.

Zhang, F., Cong, L., Lodato, S., Kosuri, S., Church, G.M., and Arlotta, P. (2011). Efficient construction of sequence-specific TAL effectors for modulating mammalian transcription. Nat. Biotechnol. *29*, 149–154.

Appendix 1

This contains one entry for each gene regulated by dexamethasone 100nM in mBMDM
logFC = log2 fold change, adj.p.val = adjusted p value (Benjamini-Hochberg)
Time represents the point where the gene has its maximal change from baseline by lfc.

Official Gene Symbol	logFC	adj.p.val	Time
F13a1	5.435155836	1.87E-16	24
Hp	4.599651578	2.06E-12	24
Pik3ip1	4.371279103	1.41E-12	10
Sult1a1	4.129464854	4.59E-12	10
Fkbp5	4.002554804	8.07E-13	10
Ddit4	3.979811626	2.94E-10	4
NA	3.954736843	1.34E-14	4
Ms4a6b	3.909149922	2.15E-11	24
Ms4a4b	3.856029719	5.25E-11	24
Lifr	3.647042737	1.20E-10	24
Zbtb16	3.49437474	1.38E-09	4
6030422H21Rik	3.485671443	7.59E-10	2
Prss16	3.477071823	1.24E-11	10
Dusp1	3.363805076	5.11E-11	1
Saa3	3.281105596	1.63E-13	24
Lyve1	3.204087271	7.58E-11	10
Cd55	3.022962191	1.46E-07	24
Ms4a4c	3.010537516	1.26E-07	24
Abhd15	2.962026041	7.41E-10	4
Rab15	2.854500771	3.98E-09	10
Sla	2.794717076	5.19E-13	4
Klf9	2.666514357	5.25E-11	24
Serpine2	2.664846017	1.00E-06	24
Filip1l	2.639129969	2.06E-12	24
Cbr2	2.623414223	7.49E-10	24
Tsc22d3	2.577505081	4.29E-15	4
Cd163	2.545715246	8.78E-11	24
Per1	2.540304193	4.41E-13	2
Thbs1	2.516264494	4.67E-08	24
Map3k6	2.444695128	6.36E-12	10
Marco	2.351556829	1.18E-08	24
Il15ra	2.32209633	1.71E-07	2
Gda	2.259680848	8.57E-10	24
Apoc2	2.240905265	7.39E-12	24

Jdp2	2.235236381	1.92E-12	24
Sell	2.224631268	2.96E-08	24
Klhl6	2.212938786	1.67E-12	4
Mertk	2.124716056	2.08E-11	10
Ms4a6c	2.117456202	3.08E-10	24
Fam40b	2.112916033	2.94E-09	10
Cytip	2.094188592	2.38E-12	4
Fpr2	2.083019014	4.37E-06	24
Chi3l3	2.05894013	1.21E-07	24
Thbd	2.039018148	3.61E-10	4
B3gnt5	2.032204922	2.51E-06	4
Jag1	1.975272171	2.57E-05	4
Klf4	1.965627121	1.37E-09	2
Tlr8	1.948153802	3.62E-08	10
Gpr126	1.942767667	2.53E-07	4
Pex13	1.935376652	2.93E-12	4
Pla2g7	1.929061629	4.59E-09	24
AA409587	1.868530059	7.94E-08	2
Rnf169	1.863025622	2.38E-12	4
Lcn2	1.79704023	0.00017732	24
Lama3	1.792991339	2.43E-06	10
Ankrd29	1.786062972	1.83E-07	10
Fmnl2	1.779092813	2.40E-07	4
Ttc39c	1.770587156	1.32E-11	10
Pyhin1	1.765530256	4.56E-05	24
Nrg4	1.763219155	4.45E-08	24
Frmd4b	1.761710281	9.43E-09	24
P2ry12	1.758403183	1.52E-05	24
Maf	1.737816627	0.002025068	2
AA467197	1.690083178	2.12E-10	10
Stk17b	1.675291862	2.86E-11	24
Tmem37	1.668657246	9.63E-09	10
Ttpal	1.654378982	2.08E-07	4
Rffl	1.650638261	1.73E-06	4
4930523C07Rik	1.650597073	2.60E-07	24
Tns1	1.615814627	1.21E-09	10
A130040M12Rik	1.599548188	9.68E-08	4
Gpx3	1.599393721	3.66E-08	24
N4bp1	1.598411372	1.17E-08	10
Mmp8	1.588032995	3.58E-06	24
Samhd1	1.580359967	2.25E-05	2
Fpr1	1.575637582	1.99E-08	24
Chka	1.569628632	9.07E-07	2

Pstpip2	1.567613225	2.12E-05	10
Fhit	1.558985961	3.95E-06	24
Id1	1.549897704	0.000248871	24
Frat2	1.529601207	4.57E-05	4
Mgst2	1.527710059	1.53E-07	10
A130012E19Rik	1.516499445	0.017609868	2
Ogfrl1	1.515574597	1.71E-09	24
Ssh2	1.507675005	3.97E-09	4
Sik1	1.503465608	5.89E-07	2
Ccny	1.502090911	0.00070203	1
Rhoj	1.500088766	1.41E-06	10
Fabp4	1.496777089	0.031978093	2
Ap1s2	1.452176988	4.12E-05	2
Tlr7	1.451090517	2.28E-09	24
Foxred2	1.441950879	2.16E-09	10
Tigd2	1.409222107	9.89E-12	4
Glul	1.408643445	1.06E-09	10
Clec10a	1.398280949	2.15E-05	10
Fos	1.394439826	4.71E-05	4
Eps8	1.386235464	3.12E-11	10
Tmod1	1.38463195	4.98E-11	10
Dyrk3	1.383148147	8.70E-06	4
Sh3kbp1	1.372681511	3.21E-08	10
Klhl24	1.367227231	0.000157838	2
Ncoa5	1.356570992	7.28E-07	4
Acvr2a	1.345260941	1.44E-05	4
Ldlrad3	1.344645041	7.12E-06	24
Trp53inp1	1.341104072	1.82E-10	4
Ang	1.326696645	4.93E-09	24
Tcp11l2	1.326217601	1.28E-07	10
Mmp19	1.323751093	2.06E-07	10
Ptger2	1.300083043	1.63E-06	4
Aoah	1.28636391	0.001261189	24
Mlxip	1.280511165	8.81E-07	2
D930015E06Rik	1.278204166	8.01E-10	4
Rcsd1	1.275227282	1.53E-08	4
Gpr65	1.272778101	1.02E-08	4
Hivep2	1.254292168	4.55E-06	4
Wee1	1.24729766	1.50E-07	4
Il18rap	1.244413916	1.78E-05	10
Wnk1	1.242159407	0.011964331	4
Serinc3	1.224856774	9.78E-07	24
Cxcr4	1.223466803	3.37E-08	24

Mxd4	1.208626211	1.15E-07	10
Acss1	1.199777961	4.37E-08	4
Lyzl4	1.193382929	1.89E-06	24
Smurf2	1.191627743	8.09E-06	4
Ms4a6d	1.182134359	7.14E-10	24
Sgms1	1.180922805	4.82E-07	4
2210406H18Rik	1.165669127	2.01E-06	24
Tcf7l2	1.163752257	2.69E-07	4
Stxbp5	1.153607813	6.01E-05	24
Gab3	1.152348717	1.33E-07	4
Nedd9	1.144872474	1.53E-07	4
Ly6a	1.139359276	0.00943417	24
Bst1	1.11917443	9.46E-08	24
Gprc5b	1.107162284	3.46E-08	10
Tnks	1.099065979	0.000183217	4
Sgk1	1.0980162	3.61E-10	4
Tgfbi	1.091692315	1.85E-05	10
Peli2	1.074942073	7.67E-05	10
Rin3	1.073034378	7.26E-06	10
Adrb2	1.069024412	1.95E-07	4
Sqrdl	1.068701137	1.72E-08	10
P2ry13	1.066512991	1.47E-05	24
Fcna	1.066467547	4.92E-07	24
B3galnt1	1.045185998	5.72E-08	24
Stab1	1.045067906	2.21E-06	24
Usp2	1.044129785	0.000137044	4
Rnase4	1.042613479	2.93E-08	24
Phf15	1.034347654	7.76E-09	4
Dock10	1.025276734	2.74E-08	10
St14	1.02370349	0.001419124	24
Elmo2	1.023666512	0.001786397	10
Ypel5	1.020942933	8.14E-10	4
Glrx	1.02045127	4.50E-07	10
Man2a1	1.009025741	9.70E-09	24
Gng2	1.009019709	9.48E-06	24
Zc3h12c	1.008496066	3.00E-06	2
Mbnl3	1.008263897	0.010913661	24
Ckap4	1.005866077	0.00097655	4
Myo10	1.002623811	3.06E-07	10
Slc24a3	1.000212899	0.000102883	10
Nr1d2	-1.000532259	4.62E-09	10
Atp6v0a1	-1.01119555	3.58E-05	10
Gpr162	-1.014609578	0.000341237	10

Cdkn1c	-1.019055366	0.03008497	10
Tmem158	-1.019588632	0.014093005	24
Ckb	-1.027224432	4.76E-09	24
Clec2i	-1.034643358	2.11E-05	10
Dio2	-1.049316288	0.009913706	24
Fam46c	-1.049442686	1.84E-06	10
Ednrb	-1.056092767	0.000396377	4
Ndrg4	-1.056118654	3.33E-06	24
Plk2	-1.058527911	0.006192991	2
Ccr5	-1.060748452	0.004550396	4
Pdgfa	-1.068793081	6.72E-06	10
Enc1	-1.093687562	3.53E-06	4
Dusp4	-1.095287466	1.89E-06	24
Rapgef3	-1.095604435	3.89E-05	4
Ptchd1	-1.09680213	0.002138765	24
Pdlim4	-1.103989253	5.19E-07	10
Rgs2	-1.122039369	2.75E-05	10
Slc15a3	-1.123357517	5.58E-08	10
Mamdc2	-1.133274664	3.08E-06	24
Akap2	-1.141301103	1.20E-05	10
Olfm1	-1.146380321	1.07E-07	24
Ifit2	-1.146391556	0.006600447	10
Afp	-1.152571716	9.44E-06	24
Cyp2s1	-1.155119822	0.017933157	24
Gpr176	-1.155999008	2.11E-05	10
Zranb3	-1.208161284	1.62E-06	24
Lat	-1.235195696	2.27E-05	24
Tox2	-1.235564976	4.76E-08	24
Procr	-1.247325483	1.48E-08	24
Ifit3	-1.254771345	0.012863893	10
Cd72	-1.286467411	4.22E-07	24
Kit	-1.319484026	1.95E-05	24
Mmp13	-1.320981799	4.89E-05	24
Il1rn	-1.327997128	0.00181262	24
Rsad2	-1.338134934	0.000880947	10
Ifit1	-1.353409644	0.002107779	10
H2-Aa	-1.354965441	6.93E-05	24
Irg1	-1.479734796	5.43E-07	24
Plau	-1.500286492	9.81E-05	10
Itgb3	-1.524604535	8.08E-05	24
Fcrls	-1.529191421	8.35E-08	24
Pcp4l1	-1.540628793	4.12E-07	24
Clec7a	-1.620584758	7.90E-07	10

Tubb2b	-1.704978219	2.66E-07	10
Egr2	-1.914428385	0.000423715	10
Serpinb9b	-1.990919488	1.36E-07	24
Mmp12	-2.379516911	9.17E-10	24

Appendix 2

This contains one entry for each gene regulated by dexamethasone 100nM in hMDM
logFC = log2 fold change, adj.p.val = adjusted p value (Benjamini-Hochberg)
Time represents the point where the gene has its maximal change from baseline by lfc.

Official Gene Symbol	logFC	adj.p.val	Time
THBS1	6.011209305	2.90E-10	10
NA	5.860788311	2.47E-13	4
PDK4	5.576900738	1.42E-05	4
ZBTB16	5.520246906	7.97E-11	4
ADAMTS2	4.836201777	4.52E-09	24
ALOX15B	4.487971798	5.04E-08	10
CSGALNACT1	4.456692393	2.21E-10	10
PKP2	4.25952153	1.23E-09	4
SPRY1	3.876521772	8.65E-08	4
FBLN5	3.865219421	8.70E-07	10
LHFP	3.846029032	3.92E-11	10
FKBP5	3.810817922	2.99E-08	4
SLC16A10	3.618428074	6.98E-05	10
SRPX	3.580319696	0.002451263	24
RGS1	3.530196157	0.000595165	1
TPST1	3.407762656	2.65E-09	10
TFCP2L1	3.375479259	1.54E-05	10
CAMP	3.33652724	6.72E-07	24
TFPI	3.214769973	1.35E-06	10
DAAM2	3.204361515	2.25E-10	24
TSC22D3	3.170353709	1.09E-11	2
PER1	3.15474706	1.25E-13	2
DUSP1	3.137911717	1.09E-11	2
NHSL1	3.097129116	1.11E-10	4
DDIT4	2.999764261	7.51E-13	10
ST6GALNAC3	2.964764017	2.65E-09	10
GRB10	2.925126431	7.30E-11	10
PRKCH	2.901474641	2.68E-10	4
RHOBTB3	2.897045146	1.51E-07	4
TBC1D16	2.869961149	2.65E-09	10
EBI3	2.828475078	6.67E-06	24
IL1R2	2.816837527	2.62E-06	24
FLT3	2.812254981	3.20E-07	24
SAP30	2.797419166	4.08E-09	10

SGMS2	2.772752397	1.16E-07	4
TBC1D1	2.761206378	2.29E-10	4
MT2A	2.722036611	0.000238207	10
RBMS3	2.708370442	3.89E-08	10
FRAT1	2.627753621	2.72E-10	4
SH3PXD2B	2.590721293	4.70E-12	4
NUDT16	2.553557391	4.03E-09	10
USP53	2.539109483	5.01E-06	4
KLF9	2.537338629	5.97E-11	4
ADORA3	2.53459692	0.003175306	24
GRAMD3	2.50856061	1.03E-07	10
MDM2	2.500403017	3.76E-10	4
PLEKHA7	2.497428525	3.20E-07	4
CNIH4	2.462674729	3.02E-08	4
CD163	2.428398187	3.48E-07	10
CRISPLD2	2.415055036	0.004001197	24
TMCC3	2.399492446	7.85E-05	2
MTMR11	2.38161627	6.05E-06	4
PKIB	2.380442458	3.03E-06	10
FOS	2.373397158	2.42E-10	4
PTX3	2.369402551	8.59E-05	10
PHF17	2.365408241	1.09E-11	2
LDLRAD3	2.36402155	3.34E-06	10
PCYOX1L	2.350852707	0.000204655	10
DUSP4	2.337580771	0.000628178	4
SESN1	2.329288415	1.15E-11	10
MAN1A1	2.327313791	9.19E-10	24
FAM117B	2.313578863	4.47E-06	4
FMN1	2.289455077	9.77E-06	4
CYFIP2	2.287260459	0.000339764	10
GADD45B	2.22349637	9.83E-08	2
PRKCE	2.195454054	2.39E-10	10
GLDN	2.192955986	0.008999155	24
SLC16A6	2.16605694	0.001349284	10
SRGAP1	2.165082352	8.70E-07	4
RBP7	2.165050126	1.17E-05	10
MEGF9	2.143498887	2.12E-07	4
CPM	2.137981203	3.83E-10	10
MT1X	2.127942411	0.001502375	10
MERTK	2.118218316	3.42E-12	4
C5orf62	2.101832849	6.11E-14	4
MT1P2	2.10148216	0.004874976	10
C19orf59	2.096129218	5.20E-07	24

CCNA1	2.063152723	0.004439186	4
GPR126	2.061674601	0.000416505	10
ISG20	2.060295238	4.12E-05	10
PAPOLG	2.057912252	7.94E-09	4
ZCCHC6	2.035393876	3.15E-10	10
THRB	2.033081186	0.000273633	10
P2RY13	2.022155736	0.000702702	4
BLM	2.019030261	0.000110565	10
CYTIP	2.014133687	2.26E-08	2
KCNE1	2.013014064	0.048004236	10
GLUL	1.990465351	4.73E-05	10
SHOX2	1.970106234	1.38E-05	4
KLF4	1.954949187	1.05E-05	4
SLAMF1	1.925165676	0.003449345	4
SLITRK4	1.924140704	0.004077529	4
APCDD1	1.91586443	7.96E-08	10
PALD1	1.908224705	0.000784953	10
MMP19	1.907484294	0.001507136	10
NFIL3	1.890152977	2.50E-09	2
IL1R1	1.887164105	7.01E-06	10
KCNJ2	1.886561006	8.66E-06	4
P2RY12	1.868120995	0.005509819	24
KIAA0146	1.865449078	5.22E-07	1
LONRF1	1.855378347	1.41E-07	2
LOC285812	1.846725377	2.06E-05	4
SLC25A15	1.846167577	0.000128556	4
PGRMC2	1.844929779	8.88E-05	10
LRRC16A	1.844048532	0.000172003	10
FILIP1L	1.841723799	9.73E-05	4
PPARGC1A	1.829195341	0.003071635	24
RNF144B	1.821808551	4.26E-05	2
NAV2	1.820198826	0.019163574	10
VCAN	1.816167791	1.45E-06	10
CEBPD	1.805750432	1.72E-05	1
CTTNBP2	1.803414835	0.001972932	10
GAB1	1.798258614	6.26E-08	4
TSPAN2	1.790855265	0.037854712	10
FAM59A	1.788293916	7.51E-06	4
B3GNT5	1.779217192	5.80E-11	4
SEMA3C	1.772648955	0.00033442	10
FPR1	1.771500198	5.51E-05	10
SLC22A16	1.771090196	0.030365095	10
CLEC4E	1.769994058	0.001593079	10

SHMT1	1.753889709	2.22E-07	10
VSIG4	1.752602984	0.000310521	24
C10orf54	1.749834302	1.48E-06	10
LINC00341	1.74795307	1.02E-06	4
FCAR	1.734375837	1.10E-05	4
MYC	1.727880154	5.70E-10	1
GPR82	1.722568696	3.20E-05	10
ITPKC	1.720594744	9.83E-08	2
SLC25A37	1.71190505	1.76E-05	4
CDKN1C	1.711525375	0.000683609	24
S100A8	1.710557418	0.005682313	24
ATAD2	1.705410863	1.64E-06	4
IRAK3	1.699302777	1.08E-08	10
GADD45A	1.686298253	0.046881195	2
SLC38A1	1.683268886	0.001249891	10
TNFRSF21	1.683089982	4.37E-08	10
TNFRSF11A	1.676791939	6.63E-05	10
KIF13B	1.675137688	4.61E-11	4
ZNF189	1.666159052	3.11E-05	2
ADM	1.664014379	2.10E-06	1
PIK3IP1	1.663919989	3.15E-08	10
KLF7	1.663855874	1.56E-05	2
SSH2	1.652178798	5.45E-09	4
MT1F	1.626635757	0.001439376	10
OLIG1	1.625107843	0.005615405	24
LOC729680	1.622592474	0.000319066	10
RCAN1	1.618555922	0.000690268	10
TNFAIP3	1.613243138	1.17E-05	1
GFOD1	1.594779062	3.84E-05	4
MET	1.590858534	1.19E-06	10
TMEM17	1.590565717	2.81E-06	4
CALCRL	1.5890609	0.000126495	10
WDR63	1.587050056	3.24E-05	4
MS4A6A	1.584745269	0.002329683	4
ORMDL1	1.583163967	1.21E-05	10
TMEM198B	1.57384955	2.63E-07	10
GCLC	1.573170983	9.62E-05	4
RUNX2	1.571783948	0.030626315	4
SLC15A2	1.568017019	0.005617312	10
ERLIN1	1.565093068	0.000345688	4
SRGAP2C	1.563863929	1.47E-07	4
GNB5	1.559097321	1.64E-05	10
ARRDC3	1.55556886	7.21E-08	1

SOCS1	1.549099457	1.85E-05	4
ALCAM	1.549028576	3.23E-05	10
YPEL2	1.548345991	3.19E-05	4
OGFRL1	1.542016732	8.45E-08	4
PSTPIP2	1.540792943	1.57E-05	4
PPM1L	1.535734209	0.000145678	10
CD72	1.530468303	5.56E-05	10
IRS2	1.527573415	9.42E-11	10
TXNIP	1.525897445	0.000171486	10
INSR	1.521014859	0.000186497	10
ABLIM3	1.51504739	0.001582473	10
SLC19A2	1.514207595	1.39E-05	2
TBC1D8	1.511054435	4.08E-05	10
ALDH1L2	1.500985653	2.99E-05	10
PSME4	1.500335467	7.58E-05	4
METTL7A	1.48689094	2.36E-07	24
EZR	1.46212862	0.000454978	10
SRGAP2	1.43487271	7.10E-08	4
MS4A4A	1.432577545	9.00E-05	10
ECHDC3	1.42583698	1.90E-08	10
ELK1	1.417121679	6.07E-06	4
SLC11A1	1.401803322	0.001963584	10
ACSL1	1.371622812	1.28E-07	4
MTMR4	1.363521359	3.46E-07	4
C5	1.352097478	0.000501407	24
FOXO1	1.340757809	6.67E-05	4
IL13RA1	1.331423726	1.96E-07	10
SLA	1.329050898	7.07E-09	4
GRAMD1B	1.327926444	0.0001498	10
C1QB	1.312287499	0.000138508	24
SLC31A2	1.307859569	5.42E-09	4
PTEN	1.292599145	4.21E-08	10
FAM100B	1.279235041	1.15E-08	4
HMGB2	1.273309156	6.18E-09	10
SPTLC2	1.26879127	2.90E-08	4
PHC2	1.253422701	7.43E-10	4
PMS1	1.252198464	6.17E-07	10
MAP3K6	1.236628026	0.00178247	10
HIPK2	1.225602838	4.03E-07	10
ZBTB8A	1.215650994	0.004564297	10
MCL1	1.210648563	5.69E-07	4
SH3BP5	1.207415905	0.000501368	4
FRMD4A	1.175251398	0.002002282	4

SMAP2	1.165033849	6.38E-08	4
CLN8	1.150329348	0.002706623	4
KLHL8	1.14380126	2.12E-07	4
GPR34	1.143705519	5.97E-07	10
ENOX2	1.119867864	0.000229518	10
TMEM39A	1.113677954	0.000697014	4
SDC4	1.109329708	2.25E-05	10
FAR2	1.108694009	1.82E-06	10
TP53BP2	1.09455046	9.73E-09	2
MTSS1	1.09037403	0.003286841	10
FGD4	1.073698059	1.93E-06	4
TOP1	1.060702469	8.50E-08	4
DISP1	1.058189086	0.002695905	10
FOXN2	1.057143584	2.70E-06	4
TLR2	1.054146997	6.21E-06	4
SETMAR	1.038860033	1.59E-05	4
FOXO3	1.019263123	3.07E-08	4
JDP2	1.014392814	1.79E-08	10
TCF4	-1.003287912	1.38E-06	4
FMNL3	-1.003908606	0.008225375	24
MYO9B	-1.005273326	1.23E-07	10
ICAM1	-1.007942338	2.60E-06	10
BLNK	-1.009990976	8.15E-08	4
KCTD7	-1.010382907	3.12E-05	4
TMC8	-1.010420379	7.49E-05	4
TRERF1	-1.011372912	0.000122778	10
IL16	-1.013127963	7.19E-05	4
ATF5	-1.013870994	3.83E-05	4
NMT2	-1.014215506	0.001554975	24
RTN4R	-1.017192114	0.022422163	24
FCGR1B	-1.01776657	9.86E-05	10
FAS	-1.017846845	0.024787432	10
NFKBIE	-1.017892315	0.029224105	24
TOR3A	-1.022607872	0.003286262	24
BTG2	-1.026655332	0.016581842	1
GBP1	-1.028267937	0.027490786	10
ZCCHC24	-1.030188956	0.000104053	10
RELB	-1.03157367	3.19E-05	4
RNF125	-1.032123363	0.000301167	4
ATP2B1	-1.03788801	7.85E-06	10
LOC344887	-1.044946425	0.010789359	4
ACVR2A	-1.047285611	0.000103929	10
ZFYVE16	-1.048569713	1.76E-05	10

NLN	-1.050774899	0.017119733	4
SAMD4A	-1.051568149	0.034402011	10
SGTB	-1.0517475	1.93E-06	10
ARHGAP25	-1.052237902	2.56E-08	10
JAKMIP2	-1.052761271	0.027454672	24
PDE4DIP	-1.054055285	0.010477912	10
TRAF3IP3	-1.062143523	0.000653719	10
DPCD	-1.068060663	0.000175423	10
TLE3	-1.070497058	0.004627151	10
CA2	-1.076757213	0.009864512	10
PAK1	-1.081943684	0.000333389	10
PEA15	-1.082703192	1.15E-05	24
HIVEP1	-1.086939011	0.002246749	2
PTGIR	-1.08992229	0.042090685	10
CD48	-1.094235707	0.030002029	24
SLC29A3	-1.094682184	0.042617616	4
MXD1	-1.116551626	3.67E-05	4
SLC7A11	-1.117384188	0.014800316	10
C16orf54	-1.118173159	0.000322366	24
P2RY6	-1.119387416	0.020219996	4
SLC46A3	-1.122498284	5.05E-09	10
TAGAP	-1.129273443	0.001658482	1
SPATA12	-1.129284362	0.004178064	10
PLAU	-1.130136268	0.001348149	24
HEG1	-1.131821171	0.021987704	4
PTGS1	-1.137497504	2.89E-06	24
RAB7B	-1.137743652	0.038250294	24
HPSE	-1.147787511	0.001487404	24
GNG2	-1.15435356	0.002410116	10
P2RX7	-1.172723665	0.000770697	24
CYTL1	-1.189717129	0.004155805	24
NQO1	-1.193597707	2.10E-06	10
NUMA1	-1.201777113	0.002706623	4
MRPS6	-1.219032494	0.016432575	4
TESC	-1.219914851	6.63E-05	10
EHD1	-1.22292058	0.000621808	4
LOC285628	-1.239516984	0.029861865	1
VASH1	-1.248801459	0.000457018	10
NOD2	-1.251705045	0.000483132	2
MFSD2A	-1.256450115	0.006737917	2
KLRG1	-1.260079361	0.000341258	10
GPR84	-1.262407904	0.014653574	24
ITGAL	-1.268328785	0.01606464	24

TNFSF15	-1.293479624	0.046565506	4
SLC2A6	-1.293754364	0.004188819	24
TJP2	-1.296670922	0.000115947	10
TNFSF10	-1.297876733	0.04091709	4
BIRC3	-1.319683571	0.00779449	24
TLR7	-1.342508265	8.06E-06	4
TMEM138	-1.348565008	1.07E-05	10
ZBTB46	-1.361634124	0.000683609	24
PIR	-1.368139348	1.35E-08	10
ME1	-1.371401015	5.44E-07	10
TNF	-1.374692547	0.000640579	24
CLEC4A	-1.377369856	3.42E-06	10
LXN	-1.399281292	8.20E-07	24
GPR68	-1.408268429	0.004238373	4
CXCL2	-1.44052364	0.024392458	24
SLC9A9	-1.460726595	0.000612964	10
BCL11A	-1.464786737	0.009231081	10
BCL3	-1.519292419	1.37E-06	4
NBPF1	-1.523916536	0.001502375	10
ASRGL1	-1.525060449	2.28E-06	10
TNFSF13B	-1.535665252	1.92E-07	24
SLC5A3	-1.535959823	0.002751118	4
CRHBP	-1.553849975	0.000587068	10
FBLIM1	-1.557861642	0.007220932	24
TMEM71	-1.569118286	6.59E-06	10
ARG2	-1.571531914	0.002834606	10
BCAR3	-1.607185286	0.004912547	24
TEF	-1.612090312	2.36E-07	24
CHST2	-1.63740843	0.02910728	10
MTHFD1L	-1.637651226	1.30E-05	24
SRGAP3	-1.644134234	0.001061038	10
CD200R1	-1.671368919	0.001485256	10
CD83	-1.682680879	0.022906236	2
RGS16	-1.692132553	0.020132944	10
KLHL13	-1.708937978	0.009483796	24
SLAMF7	-1.718616152	0.023951314	24
C1orf21	-1.72919737	0.000937542	10
CD274	-1.74042145	0.004800619	4
CD163L1	-1.777604388	0.000181387	24
KITLG	-1.815871583	0.001017396	4
HS3ST1	-1.843946079	0.014803361	2
PTGFRN	-1.861862967	0.0004685	10
PER3	-1.933565648	2.78E-08	24

SGPP2	-1.941393962	0.014440102	24
IRF1	-1.981440311	2.94E-05	2
HIVEP3	-1.996685266	0.000571742	24
LOC440934	-2.022652508	0.045735038	4
CIITA	-2.076825979	1.08E-05	24
GPRC5B	-2.109931988	0.030962304	10
C5orf20	-2.129351761	0.011652281	10
NR1D2	-2.14768144	9.74E-13	10
IFIT1	-2.192912361	0.042143443	10
CCL4	-2.299143199	0.006910067	10
TIFAB	-2.387018307	0.007353268	10
IL8	-2.442276848	0.01981637	4
PER2	-2.450384507	4.37E-08	24
MRC2	-2.589341666	0.003636145	24
CXCL1	-2.606922466	0.03566627	2